BIOMECHANICS OF THE LENS CAPSULE FROM NATIVE TO AFTER CATARACT SURGERY

A Dissertation

by

RYAN MICHAEL PEDRIGI

Submitted to the Office of Graduate Studies of
Texas A&M University
in partial fulfillment of the requirements for the degree of

DOCTOR OF PHILOSOPHY

August 2008

Major Subject: Biomedical Engineering

BIOMECHANICS OF THE LENS CAPSULE FROM NATIVE TO AFTER CATARACT SURGERY

A Dissertation

by

RYAN MICHAEL PEDRIGI

Submitted to the Office of Graduate Studies of
Texas A&M University
in partial fulfillment of the requirements for the degree of

DOCTOR OF PHILOSOPHY

Approved by:

Chair of Committee,	Jay D. Humphrey
Committee Members,	Joan Dziezyc
	James E. Moore, Jr.
	Alvin T. Yeh
Head of Department,	Gerard L. Cote

August 2008

Major Subject: Biomedical Engineering

ABSTRACT

Biomechanics of the Lens Capsule from Native

to After Cataract Surgery. (August 2008)

Ryan Michael Pedrigi, B.S., Kansas State University

Chair of Advisory Committee: Dr. Jay D. Humphrey

The primary function of the lens capsule of the eye unfolds during the process of accommodation; wherein, tension imposed onto its equator is released, allowing the elastic capsule to mold the underlying lens nucleus and cortex into a more quasi-spherical morphology to change focus from distant to near objects. Given its highly mechanical nature, it is prudent to study the native lens capsule from the perspective of biomechanics for such applications as understanding the mechanism of accommodation. Further, cataract surgery introduces alterations to the geometry of the lens capsule that lead to changes in resident cell behavior from quiescent to contractile and synthetic. Though resultant changes in capsule histology are well documented little has been done to quantify the corresponding altered mechanics, which is important for elucidating related post-surgical pathologies and improving prosthetic lens design.

In this study we present the first data on the in situ multiaxial mechanical behavior of the native and hyperglycemic anterior lens capsule in both the porcine and human models. From these data, native stresses in the lens capsule are calculated using a finite element analysis, and alterations in the corresponding strain field are calculated

after the introduction of a continuous circular capsulorhexis, which is imposed during cataract surgery. Finally, we quantify both the altered mechanical behavior and contractile loads imposed onto the lens capsule after cataract surgery.

ACKNOWLEDGEMENTS

I would like to thank the following members of my committee: my mentor, Jay Humphrey, who is an endless source of knowledge, inspiration, and compassion, who provided continual guidance, support, and demonstrated a true passion for this field of study; Joan Dzieyzc, for donating countless hours of her time over the past several years towards aiding in preparation and execution of many of the experiments described within, as well as providing guidance for this project; Alvin Yeh, for answering all of my silly questions concerning optics; and finally, James Moore, for not only providing guidance, but also access to his pool and barbecue for me and other overworked graduate students.

I would like to thank several of my Texas A&M University collaborators on this project: Mark Heistand, Guido David, Leah Moeller, Emily Staff, and Harrison Kaladimos. I am also thankful for the assistance of Adam Larson, Jason Hirshburg, and Art Valentin. Thanks also to my collaborators at Alcon Laboratories: Drs. Mutlu Karakelle, Mike Simpson, and Quin Peng.

Finally, thanks to my parents, Cindy and Steve Goodrich, and Mike and Anne Pedrigi for their endless encouragement and support during my ten years of higher education.

TABLE OF CONTENTS

CHAPTER Page

LIST OF FIGURES

FIGURE Page

CHAPTER I

INTRODUCTION: THE IMPORTANCE OF LENS CAPSULE BIOMECHANICS

The anterior segment of the eye is principally responsible for focusing light onto the retina; wherein, the curvature of the cornea provides the majority of the refractive power and the lens then fine-tunes the focus of incoming light. In order for the lens, which is composed of a nucleus, cortex, and capsule, to be able to focus light at different focal distances, it is capable of undergoing a morphological adjustment called accommodation (see Figure 1.1 for basic anatomy and schematic illustration). Specifically, the resting lens has a traction imposed onto its equator by attached zonules (that act as tension cables) and during accommodation this traction is released by the inward contraction of the surrounding ciliary muscle that frees the lens. This allows the elastic capsule to increase the curvature of the underlying lens nucleus and cortex, and, thus, change focus from distant to near objects. The intrinsic mechanical nature of the lens has prompted some studies of its mechanical behavior and properties, as well as computational modeling to quantify tractions and altered geometry at rest and during accommodation. The motivation to understand better the mechanism of accommodation is to identify the underlying etiology of its degeneration with age, called presbyopia, and to provide a theoretical framework that can be used as the basis for design implementation of an accommodative feature into prosthetic intraocular lenses (IOLs).

This dissertation follows the style of Biomechanics and Modeling in Mechanobiology.

An effective accommodative IOL (AIOL) design promises to improve the visual capabilities of those who have undergone cataract surgery and to treat presbyopia.

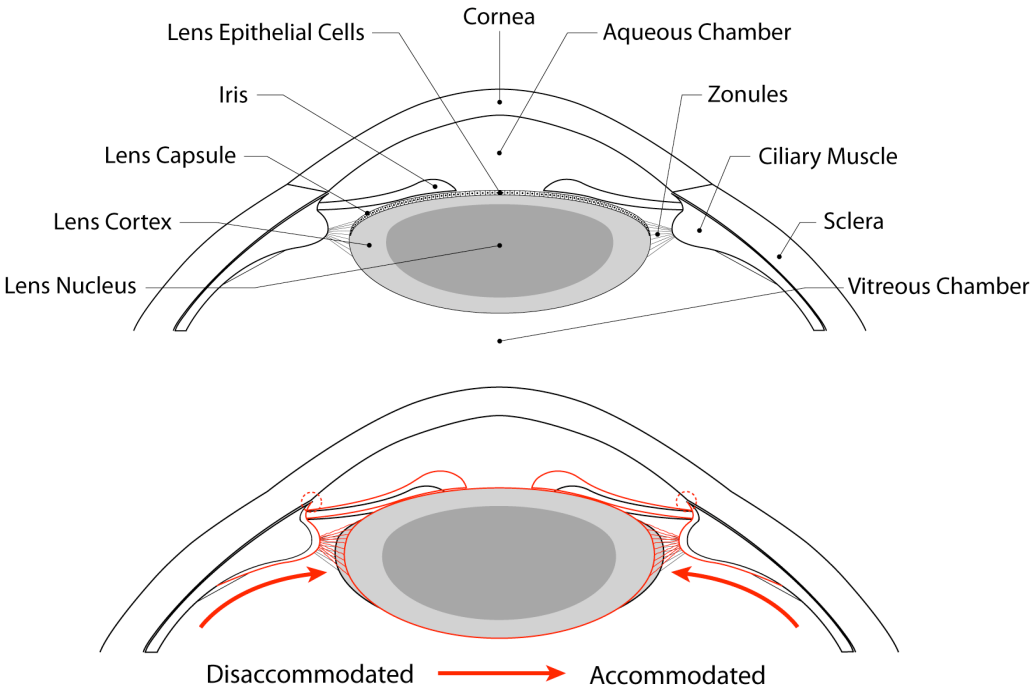

Figure 1.1. Illustration of the anterior segment of the eye. (top) Anatomy and (bottom) changes in the geometry of various ocular constituents undergone during accommodation.

A cataract is a partial or total opacity of the lens, and it is the most common cause of blindness in the world. Cataracts are nearly inevitable with age, and cataract surgery is the most commonly performed surgical procedure in the United States with around three-million annually (Leaming, 2004). During this procedure a hole is placed into the anterior portion of the lens capsule, through which the lens nucleus and cortex is broken up and aspirated, and an IOL is placed into the empty remnant capsular bag. The lens capsule, therefore, plays a paramount role during and after this procedure as it

contains the surgical work area and permanently houses the implanted IOL. Current IOL designs are flat with two arms (called haptics) that extend from the optic to the equator where they press against the capsule to hold the implant centered about the optical axis of the eye. The dramatic geometrical differences between the implant and the native lens perturbs the native mechanical environment of the post-surgical lens capsule and is likely an underlying modulator of the biological response to surgery carried out by the inhabiting lens epithelial cells (LECs). This response includes transdifferentiation into a wound-healing phenotype that promotes a more contractile and synthetic behavior (compared to a nearly quiescent behavior natively), ultimately leading to altered matrix and geometry of the capsule (Figure 1.2).

Because of the principle role that the lens capsule plays in accommodation and cataract surgery, both of which are highly mechanical processes, understanding the associated mechanics is important for modeling of accommodation, elucidating the etiology of presbyopia, designing implants, and understanding the cell mechanobiological response to cataract surgery that leads to capsule remodeling and often post-surgical complications of the patient. Though some studies have quantified the mechanics of the native lens capsule, they are limited by the use of a 1-D approach; therefore, no one has considered the possible anisotropy and regional variations in properties that may exist within the tissue. Additionally, native stresses of the lens capsule have not been quantified, which are important for understanding the mechanical perturbation introduced to the lens capsule during cataract surgery.

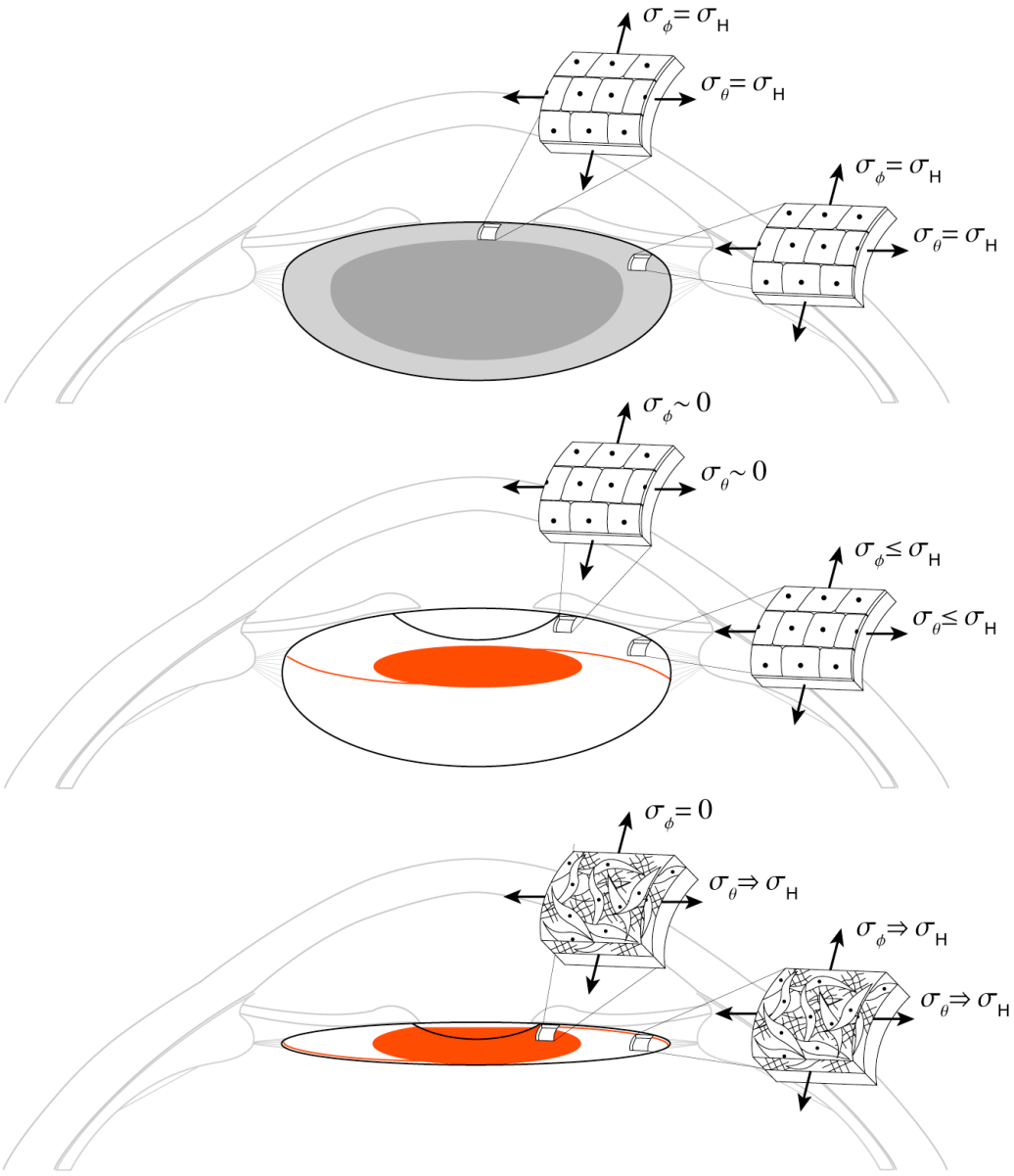

Figure 1.2. Evolution of the lens capsule from native to after cataract surgery. (top - native) The inhabiting LECs are quiescent and display a cobblestone morphology under the homeostatic stress (σ_H) due to the pressure from the underlying lens nucleus and cortex; (center – immediately after cataract surgery) the stresses of the capsule are close to zero because of the geometrical differences between the native lens and implant; (bottom – months after the procedure) the transdifferentiated LECs (spindle-shaped morphology) have contracted the capsule around the implant and are depositing matrix proteins not seen in the native capsule.

Finally, remodeling of the lens capsule after cataract surgery is well documented; however, very little has been done to quantify the associated post-surgical mechanics.

The purpose of this dissertation is to address some of these deficiencies in the understanding of lens capsule mechanics through biomechanical testing and some computational analyses performed on the native, diabetic, and post-surgical lens capsule. Foremost, we introduce a novel experimental mechanical test of the native in situ anterior porcine lens capsule that allows for assessment of behavior in different regions of the capsule from the pole to the equator. We report the first biaxial mechanical data showing regional variations in anterior lens capsule behavior. Using this same setup, alterations in the behavior of porcine lens capsules cultured in high-glucose (simulating hyperglycemia), as well as native and diabetic human anterior lens capsules are studied. From the human data, quantification of mechanical properties and the native stress field is obtained via finite element analysis. These experiments represent the first thrust of the dissertation, understanding the native biaxial mechanics of the lens capsule and possible changes with diabetes. The second thrust is geared towards quantifying altered capsular mechanical behavior during and after cataract surgery. Towards this end, we show the first data on redistribution of the anterior porcine lens capsule strain field with the introduction of a continuous circular capsulorhexis. Moreover, we quantify changes in the mechanical behavior in both the short- and long-term of the post-surgical anterior lens capsule. Finally, a novel culture device is introduced to quantify the degree of contractile loading of the porcine lens capsule by the LECs as a function of time after cataract surgery. Collectively, these studies quantify for the first time the native biaxial

mechanical properties and stresses of the anterior capsule and significant changes that are undergone in these mechanics after cataract surgery.

CHAPTER II

ROLES OF MECHANICS IN THE BIOLOGY OF CHANGING LENS GEOMETRY AND FUNCTION THROUGHOUT LIFE

Overview

Vision arises through two distinct physiological processes: convergence of light onto the retina via tissues having optical properties derived from both intrinsic refractive capabilities of the underlying ultrastructure and overall geometry, and conversion of this refracted light into an electrical signal. With regards to the former, the lens entails a central role through a complex physiological mechanism (termed accommodation) that alters tractions acting on the lens, and thereby its curvature and refractive power, ultimately allowing for precise focusing of light onto the retina. Considered from this simplified perspective, vision depends strongly on biomechanical interactions and thus motivates study of the biomechanics of the lens.

Biomechanics can be defined as the development, extension, and application of mechanics to answer questions of importance in biology and medicine. The purpose of this review is to illustrate the influence of biomechanics on the workings of the lens through an exploration of its changes throughout human life, with specific attention to: development, accommodative function, age-related degeneration of both accommodative function and lens transparency in the formation of presbyopia and cataract, respectively, and altered structure and function following surgical intervention. Additionally, the

continued necessity of biomechanics in overcoming current limitations of prosthetic lenses will be considered.

Development, Anatomy, and Physiology

Formation of the lens during embryonic development has been characterized as a multi-stage process that is initiated from a precursor basal lamina, secreted by specific ectoderm cells of the head. This precursor tissue is composed primarily of the glycoproteins laminin and fibronectin, and arises for purposes of adherence between the ectoderm cells and optic vesicle during the lens placode stage (Haloui et al. 1988). The subsequent lens pit stage is characterized by the invagination of these cells into the lens placode to form the optic cup, with added deposition of laminin, fibronectin, and, shortly thereafter, type-IV collagen; this marks the beginning of an increased thickening of the original basal lamina to form the lens capsule (Parmigiani and McAvoy, 1991). This initial thickening of the lens capsule is most evident in the posterior portion of the lens vesicle, likely due to accumulating extracellular matrix (ECM) proteins and growth factors associated with the formation of a precursor vitreous body, synthesized by the proximal optic cup (specifically, the presumptive neural retina – Coulombre and Coulombre, 1963; Smith et al. 1976; Parmigiani and McAvoy, 1984). As the lens vesicle matures, these exogenous stimuli additionally cause the posterior cells to elongate, forming the embryonic lens nucleus (Lovicu and McAvoy, 2005). Because all mature lens fiber cells degrade most of their organelles, and correspondingly their ability to synthesize ECM proteins, the foremost thickening of the posterior lens capsule is critical

structurally for this portion remains acellular during normalcy (Parmigiani and McAvoy, 1989). Anterior to the primary lens fiber cells is an epithelium formed of the cells of the lens vesicle. At later stages of embryonic and subsequently fetal development, this anterior lens epithelium deposits successive layers of laminae (mainly type-IV collagen and laminin) along the maturing anterior lens capsule. Additionally, the lens epithelial cells (LECs) actively proliferate, the progeny of which differentiate into secondary lens fiber cells that form successive layers on the rapidly developing lens (Parmigiani and McAvoy, 1989; Parmigiani and McAvoy, 1991). At birth, the adult lens nucleus is considered formed, thus continued deposition of lens fiber cells appends to a second region termed the cortex (Dubbelman et al. 2003). The adult human lens can, therefore, be divided into three regions: nucleus, cortex, and capsule.

Although lifelong growth of the human lens cortex is accomplished through continual deposition of secondary lens fiber cells, only cells from a specialized region of the epithelium, termed the germinative zone, are actively proliferating; thus, continued growth of the lens occurs at a significantly slower rate than during prenatal development (Bhat, 2001). Differentiation of precursor secondary lens fiber cells occurs subsequent to their migration from the germinative zone to just below the equator, wherein this process is marked by elongation of their apical and basal ends to the anterior and posterior poles of the lens and accumulation of the intracellular protein crystallin. Crystallin allows for the relatively high refractive index of the lens, and, upon degradation of all membrane-bound organelles that occurs immediately prior to terminal differentiation, it is the primary constituent of the lens fiber cells (40% by wet weight – Fagerholm et al. 1981;

Bloemendal et al. 2004). Expression of the fiber phenotype by the progeny of the lens epithelium has been attributed primarily to biological factors in the surrounding ocular media, with particular emphasis on fibroblast growth factor (FGF – see Chamberlain and McAvoy, 1989; Chow et al. 1995; Robinson et al. 1995). McAvoy et al. (1999) suggest that this role of FGF is physiologically sensible because the relative position of the germinative zone to the subequatorial region of fiber differentiation coincides with the immediately adjacent transition of the aqueous to vitreous humor. Since the vitreous humor contains larger concentrations of FGF, it is likely that an increasing gradient of this growth factor exists along this transitive zone of ocular media, which correlates spatially with the stages of lens fiber differentiation. Indeed, McAvoy et al. (1999) describe an experiment whereby increasing concentrations of FGF imposed onto in vitro cultured LECs caused proliferation, migratory behavior, and differentiation into fiber-like cells (see also the review by Lovicu and McAvoy, 2005).

As the volume of the lens cortex increases there is an associated increase in both the surface area and thickness of the surrounding lens capsule, the latter of which may emerge as a consequence of LECs attempting to maintain a homeostatic stress field that is perturbed by the radially expanding lens. In an excellent study, Fisher and Pettet (1972) documented changes in human capsular thickness as a function of both age and radial position. For example, their results for the pole, mid-periphery, and equator of the anterior capsule from representative neonatal, 37, and 77 year-old donors were: 8, 9, 11; 13, 20, 24; and 15, 31, 19 μm, respectively. The apparent change in region of most prominent thickening, from equator to mid-periphery, may not only correlate with

changes in lens volume but also local stresses induced during disaccommodation via the zonules, whose attachment to the capsule is initially centered about the equator but has been shown to shift anteriorly with age (Farnesworth and Shyne, 1979; Glasser and Campbell, 1998). In contrast to the anterior portion of the capsule, thickness of the posterior portion remains nearly constant at 4 μm (at the pole) throughout life, which may be attributed to the absence of epithelial cells. More recently, Krag et al. (1997b) and Krag and Andreassen (2003a and 2003b) demonstrated quantitatively similar measurements of thickness in the human anterior and posterior capsule through a comparable range of donor age; however, no alterations of thickness with radial position were considered.

Similar to most basal lamina, the structural components of the postnatal lens capsule include type-IV collagen (approximately 65% by dry weight) and laminin, with smaller amounts of entactin and proteoglycans (Barnard et al. 1992). Although fibronectin is an important component of the embryonic lens capsule, likely promoting lens cell attachment and migration during morphogenesis, it is absent in the postnatal capsule presumably due to its lack of function within healthy mature tissue (Parmigiani and McAvoy, 1991). The ultrastructure of isolated human lens capsules consists of a multilayered, three-dimensional meshwork of interconnected fibrils that form a pentagonal pattern with 40 nanometers between connection points (Barnard et al. 1992). Each collagen fiber within the network has an approximate diameter of 50-70 nanometers, with microfibrils being as small as 1.5 nanometers (Farnsworth et al. 1976; Barnard et al. 1992). Ultimately this structure facilitates its function as both a filtering

membrane for potentially diffusive molecules, which is impermeable to proteins and therefore microorganisms (i.e., bacteria), and as a deformable support for the alteration of lens shape during accommodation (Seland, 1992).

Accommodation is a mechanistic process that focuses near objects onto the retina by altering the geometry and corresponding refractive power of the lens. This process occurs via interactions between the lens capsule and ciliary body, whereby the latter provides the driving force. The ciliary body consists of the zonulae, ciliary muscle, ciliary processes, and ciliary epithelium that lie along the inner sclera from the scleral spur in the anterior chamber (proximal to the iris) to the anterior choroid (proximal to the ora serrata of the retina) in the posterior chamber (Kaufman and Alm, 2003). These tissues form a ring about the lens (often termed the ciliary ring) that attach to the lens capsule via the zonules, which originate at the posterior-most portion of the ciliary body (termed pars plana) as a flat, dense meshwork of interconnected fiber bundles of approximately 25 to 60 μm in diameter that directly extend to the epithelium of the ciliary processes (Streetan, 1977). The ciliary processes may act similar to a fulcrum, redirecting zonular fibers towards the peripheral anterior, equator, or peripheral posterior lens capsule, the first two of which form a nearly continuous band of attachment (Glasser and Campbell, 1998). As the zonules approach the capsular surface, the bundles separate gradually into individually diverging fibrils that interlace with capsular fibrils of an approximately equivalent diameter, between 35 and 55 nanometers (Streetan, 1977). These fibrils only penetrate the capsule superficially, however, with a maximum insertion depth between 0.5 and 1 micron (Farnsworth et al. 1976; Seland, 1992).

The mechanical interaction of the aforementioned tissues composing the accommodative apparatus, which leads to an altered refractive power of the lens, is generally accepted to be qualitative described by the Helmholtz theory of accommodation. Specifically, the disaccommodated lens (i.e., 'resting' state) is proposed to place the zonules in tension, which in turn imposes an equatorial traction on the capsule that is transferred to the surface of the lens, thereby applying a pressure that leads to an elliptical shape. Not intuitively, accommodation results from the release of zonular tension through contraction of the ciliary muscle, which is a type of smooth muscle that attaches to the anterior of the scleral spur and the posterior of the anterior choroid, spanning the distance adjacent to the sclera where it is loosely attached. The scleral spur acts as an anchor during contraction, pulling the ciliary body and anterior choroid forward along the inner surface of the sclera whose curvature causes a narrowing of the ciliary ring and ultimately release of the resting zonular tension on the capsule and corresponding pressure on the lens (Kaufman and Alm, 2003). In this fully accommodated state with minimal zonular tension, the lens assumes a quasi-spherical shape, mostly due to the strain energy stored in the elastic capsule versus that of the lens (Fisher, 1971; 1973). Using a scanning partial coherence interferometer, Drexler et al. (1997) showed that accommodation of healthy, pre-presbyopic human lenses results in a nominal translation of the anterior pole 185 μm forward (i.e., towards the cornea), whereas the posterior pole shifts backwards (i.e., towards the retina) 69 μm. Further studies by Dubbelman et al. (2003; 2005) using Scheimpflug imaging showed a comparable anterior polar shift of 320 μm, but additionally they demonstrated that the

nucleus accounts for most of lens thickening during accommodation while thickness of the cortex remains nearly constant.

Despite a basic understanding of interactions between constituents of the accommodative apparatus during accommodation and disaccommodation, precise quantification of individual mechanical contributions by these constituents remains limited. For this reason, analytical and computational mechanical modeling has been undertaken by several researchers, based mostly on geometric measurements of Brown (1973), elastic constants determined by Fisher (1971) for the human lens, and elastic constants determined by Krag and colleagues for the human lens capsule (Krag et al. 1997b; Krag and Andreassen, 2003a,b). An early model by Koretz and Handleman (1982) sought to determine relative force alterations (in this case dimensionless) that occur with accommodation given prescribed material properties and geometrical displacements. Assuming the lens to be a linearly elastic, homogeneous, isotropic solid whose curvature can be described by a spherical surface, they found that near incompressibility (Poisson ratio of 0.46) allowed force distributions that agreed qualitatively with the Helmholtz theory of accommodation. A similar analytical model was developed by Wyatt (1988), who represented the accommodative apparatus as a two-dimensional triangular connection between the ora serrata, scleral spur, and ciliary processes that acted as a "suspension point" of the lens. The model was solved as a simple statics problem and predicted an equatorial force of 1215 mN for the disaccommodated lens, which was almost completely released during accommodation. More recently, Burd et al. (2002) employed a commercial finite element analysis (FEA)

package (ABAQUS) to predict numerically the deformation of the lens (altered anterior/posterior curvature and polar displacement) and its corresponding change in optical power due to a physiologically relevant (based on cited literature) outward displacement of the ciliary body (represented in the model as a single point of connection for the anterior, posterior, and equatorial zonules). Assuming a stress-free reference configuration (including negation of pre-strain in the lens capsule) and a linearly elastic behavior for all constituents, they predicted a 49% and 13% reduction in anterior and posterior curvature, respectively, with a corresponding polar shift of only two-fold that observed by Drexler et al. (1997) (see above). This decreased curvature for the maximally disaccommodated lens resulted in a decreased optical power of about 9 D due to a calculated ("total") zonular force of 80 to 100 mN, which is about 7 fold higher than that reported by Wyatt (1988).

Modeling results of the aforementioned investigators align well with the Helmholtz theory of accommodation, yet this theory has been contested and finite element models have been used to investigate alternative mechanisms. For example, Coleman and Fish (2001) suggest that the lens, zonules, and anterior vitreous body form a diaphragm between the aqueous and vitreous chambers, whose differential pressure determines lens shape. This concept was motivated by measurements of differences in intraocular pressure in primate eyes during electrical stimulation of the ciliary muscle (Coleman, 1986). To investigate this hypothesis further, Martin et al. (2005) used a finite element model similar to that of Burd et al. (2002) to examine the effects of differential pressures on accommodation in the pre-presbyopic human lens. Their results show that a

homogeneous pressure of 225 Pa on the posterior chamber (based on measurements by Coleman, 1986) reduces the accommodative amplitude of the lens below that observed physiologically, in comparison to the model with no applied pressure (i.e., the model corresponding to the Helmholtz theory). Although these results question the function of the vitreous during accommodation, as suggested by Coleman, limitations of the model leave open the possibility of at least a supportive role. Another prominent theory of accommodation, by Schachar and Bax (2001), proposes that increases in curvature of the central lens (i.e., accommodation) is achieved through an outward displacement of the ciliary body that releases anterior and posterior zonular tension, while simultaneously increasing equatorial zonular tension, the overall result of which is an increase in equatorial diameter. To illustrate the consequences of this theory, Schachar and Bax (2001) developed a finite element model similar to that of Burd et al. (1999; 2002), but with the important distinction that the they used the disaccommodated lens as the reference configuration and predicted altered tractions and geometry associated with accommodation. They found that an equatorial tension of 150 mN was required for maximal accommodation with an associated outward equatorial displacement of 100 μm. Interestingly the thickening of the central lens, which is associated with an increased lens curvature and thus accommodative power, was only present within this model for outward ciliary displacements less than 100 μm; greater displacements decreased the central lens thickness, as predicted by the Helmholtz theory. This point is emphasized in a critical discussion of these results by Judge and Burd (2002).

Further studies of accommodation in the human lens have employed various in vivo imaging modalities (i.e., ultrasound, magnetic resonance imaging, and Scheimpflug – Schachar et al. 1996; Strenk et al. 1999; Dubbelman et al. 2005), topographical measurements of the isolated lens (Schachar 2004a; 2004b), and optical measurements of the isolated lens (Glasser and Campbell, 1998; 1999). Nevertheless, uncertainties remain as to the mechanism of accommodation, though most studies support the Helmholtz theory. It is apparent, however, that mechanical analyses based on quantified geometries and mechanical properties of the lens will continue to play an important role in physiologic studies.

Age-Related Dysfunction: Presbyopia and Cataract

Beyond fundamental comprehension of a unique physiological process, studies of the accommodative mechanism are also clinically applicable for understanding its gradual degeneration in the development of presbyopia. Although technically characterized as a disease, presbyopia is an inevitability that appears to develop naturally with the aging accommodative apparatus, and it completely inhibits adjustment of lens curvature and corresponding dioptric power by 50 years of age (Koretz et al. 1989). Since accommodation is a process that unfolds through the mechanical interactions of several constituents, most theories of presbyopia are based on alterations of constituent geometry and/or mechanical properties. Among these theories, the geometric theory and lenticular sclerosis are often cited, and may ultimately result from malignant growth of the lens.

Although a more exact definition may exist, here the geometric theory of presbyopia will encompass any age-related changes in geometry and/or orientation of the accommodative apparatus that may adversely affect accommodative function. As discussed previously, accommodation appears to arise from contraction of the ciliary muscle, narrowing of the ciliary body as it is pulled forward along the inner sclera, release of zonular tension, and relaxation of the lens from a radius of curvature of (for example) 12 to 7 mm anteriorly and 6.5 to 5 mm posteriorly (for 7 D accommodation of a 29 year-old lens – Dubbelman et al. 2005). Logically, changes in lens curvature during accommodation must decrease with age as presbyopia develops, but Brown (1974) showed further, using slit-image photography (Scheimpflug imaging), that the disaccommodated in vivo human lens (N=100; ages: 3-82 years) also undergoes a significant decrease in anterior radius of curvature with age from a mean 15.98 to 8.26 mm (posterior curvature was shown to undergo only minor changes). More recently, quantitatively similar results were obtained by Koretz et al. (2004) with both Scheimpflug and magnetic resonance imaging (MRI), thereby collectively demonstrating the interesting phenomenon (called "Brown's lens paradox") that despite curvature of the disaccommodated lens increasing with age, falsely suggesting a myopic shift, presbyopia causes hyperopia. To resolve this illogical observation the lens must also undergo a corresponding decrease in refractive index (and corresponding power) with age, which has yet to be proven quantitatively (Moffat et al. 2002; Jones et al. 2005). Nevertheless, these demonstrated changes in resting lens curvature towards an

accommodative form independently illustrate a basis for presbyopia, as this occurrence drastically reduces the potential for curvature changes with ciliary muscle contraction.

The underlying mechanism modulating convergence of the disaccommodated and accommodated lens curvatures with age may be linked to lens growth. Using Scheimpflug imaging, Dubbelman et al. (2001) showed that the sagittal thickness of the in vivo disaccommodated human lens increases with age (N=102; ages: 16-65) from a mean 3.3 to 4.6 mm, which has been corroborated by several other investigators (Koretz et al. 1989; Cook et al. 1994; Strenk et al. 1999). Furthermore, Strenk et al. (1999) showed that the equatorial diameter of the lens (disaccommodated) remains nearly constant with age, suggesting that lens growth primarily occurs in the sagittal direction. Intuitively, these anteroposterior increases in lens thickness decrease the anterior chamber (distance from cornea to anterior lens surface), which is exacerbated by the fact that thickening of the lens occurs predominantly in the anterior portion (Koretz et al. 1989; Cook et al. 1994; Strenk et al. 2004). Collectively, these measurements indicate that the center of mass of the lens moves anteriorly, possibly leading to a corresponding anterior movement of the zonule-connected ciliary body. Similar to accommodation, this anterior displacement would cause a narrowing of the ciliary ring about the lens (due to curvature of the sclera) and decrease resting zonular tension. Consequently, the disaccommodated lens would have a decreased radius of curvature whose alterations with ciliary muscle contraction would be significantly attenuated or inhibited altogether (Strenk et al. 2005).

Another theory of presbyopia is based on lenticular sclerosis, which is defined by Kaufman and Alm (2003) as a progressive hardening of the lens throughout life that leads to its inability to accommodate. This theory was proposed by Helmholtz in 1855 (Strenk et al. 2005), yet it was over 100 years later that quantitative mechanical testing was used to determine the resistance of the human lens to an elastic deformation (note: if elastic, then determination of relationships between stress and strain are more appropriate than hardness, a measure of plastic deformation), particularly as a function of age. Of the few mechanical tests that have been performed, the most often cited are the lens spinning experiments of Fisher (1971) due, in part, to its creative simulation of an in vivo disaccommodative loading. The experimental device spun human lenses (N=40; ages: 1-65 years) on a rotor at 1000 to 1500 revolutions per minute about the optical axis, which was predicted to allow both a nearly elastic deformation and a centripetal force that mimics the in vivo zonular pull applied to the capsule. Using equatorial and polar strains and centripetal forces, all calculated from experimental data, Fisher determined the Young's Modulus (for linear elasticity), E, for the lens in both of these directions, showing them to be nearly constant until 40 years of age when they become progressively greater (e.g., E=0.8 kPa at birth and 3 kPa at 60 years of age for both equatorial and polar directions, suggesting isotropy of the lens at the extremities of life). Furthermore, a theoretical model of the lens was constructed to estimate the separate elastic moduli for the lens cortex and nucleus, whereby it was found that the cortex stiffens throughout life while the nucleus maintains a similar mechanical behavior until age 40 years. This latter result is particularly provocative when considering that the

lens nucleus undergoes the majority of deformation during accommodation (Dubbelman et al. 2003), for this discounts lenticular sclerosis as a factor in the pathogenesis of presbyopia, a disease that begins developing early in life. These findings are not supported directly by the experiments, however, as deformation of the nucleus was not delineated directly from that of the overlying cortex. More recently, Heys et al. (2004) used a 0.4 mm diameter probe to perform indentation testing in 1 mm increments along the entire diameter of an equatorial section 'cored' from the center of human lenses (N=18; ages: 14 to 76 years). Their results, reported in terms of a linear shear modulus as a function of age and radial position, suggest that both the nucleus and the cortex undergo progressive stiffening, particularly from 20 to 60 years of age. Comparisons between the nucleus and cortex, however, showed that the nucleus underwent a nearly 450-fold increase in its shear modulus (0.04 to 17.40 kPa); whereas the cortex had a mere 20-fold increase (0.10 to 2.04 kPa). Similar results were obtained by Pau and Kranz (1991), which collectively suggest that, in contrast to the indirect findings of Fisher (1971), the lens nucleus progressively stiffens through an age range that correlates well with the development of presbyopia.

In addition to the nucleus and cortex, the tertiary structure of the lens that provides its primary molding pressure during accommodation is the lens capsule (Glasser and Campbell, 1999); this suggests that mechanical alterations of this membrane could also contribute to the development of presbyopia. Fisher (1969) first tested the isolated human anterior lens capsule (denuded of its epithelial lining) by pressurizing it with a saline solution and measuring changes in volume; thus, despite

introducing a biaxial load, only one-dimensional mechanical data were obtained. Data (N=30; ages: 1-80 years) showed a nonlinear material behavior over finite strains that was approximated to be linear (i.e., described by a Young's modulus) by considering only the upper portion of the curve. Results showed a decrease in the elastic modulus (6 to 2 MPa) and also ultimate stress (2.3 to 0.7 MPa) with age, despite measured increases in capsule thickness, which supports his theory that decreases in stiffness of the capsule cause its gradual inability to mold the lens (note that these results were shown to vary nearly linearly with age, beginning at infancy). More recent studies by Krag and colleagues (Krag et al. 1997b; Krag and Andreassen, 2003a, 2003b) provide additional insight into Fisher's result of decreased capsule stiffening with age. Based on uniaxial extension tests on circumferential rings excised from both the anterior and posterior human lens capsule (N=92; ages: 1-98 years), they showed a nonlinear elastic behavior similar to that reported by Fisher, but they approximated it as bilinear versus simply ignoring the first region of the curve. Their results for the anterior lens capsule in the "low modulus" region of the stress-strain curve (0-10% strain), which has more physiological and clinical relevance, showed the expected increase in Young's modulus with age (0.4 to 1.5 MPa – primarily occurring in the first 35 years of life). Conversely, the "high modulus" region (based on ultimate strain), which likely holds little relevance due to much larger strains than those seen physiologically, qualitatively agreed with the results of Fisher, showing a linear decrease with age (~33 to 5 MPa). With regards to presbyopia, a stiffer lens capsule could inhibit the effects of ciliary muscle contraction on attaining a disaccommodated lens curvature; this may not be an issue, however, for

the majority of presbyopes suffer from hyperopia, not myopia. As expected, Krag and colleagues demonstrated very similar mechanical behavior of the posterior capsule, but with a lower tolerance for loading due to its smaller thickness.

Further evidence for stiffening of the lens capsule with age comes indirectly from Bailey et al. (1993) who reported uniaxial stress-strain data as a function of the degree of glycosylation cross-links of the type-IV collagen, formed by incubating porcine lens capsules for 8 to 12 weeks in a high-glucose media (133 mM). Their results showed that increasing cross-links progressively stiffened the lens capsule and also decreased its ultimate stress and strain. Using a culture protocol similar to that of Bailey for porcine lens capsules, Pedrigi et al. (2007b) corroborated these results qualitatively with biaxial mechanical testing, and additionally showed that regional material symmetries were maintained in the presence of glucose exposure. Another study by Pedrigi et al. (2007a), comparing the biaxial mechanical behavior of human anterior lens capsules from both normal and diabetic donors, showed a stiffer behavior for the diabetic capsule, which is also in accordance with the results of Bailey et al. (1993) due to glycosylation of type-IV collagen in diabetes. It has also been shown that advanced glycation end products (AGEs – glucose cross-links matured through oxidation) progressively increase in the crystalline proteins of the human lens with aging (Ahmed et al. 2003). Therefore, age-related AGE accumulation within the crystalline lens may be a significant contributor to the stiffening of all of its constituents due to long half-lives of both type-IV collagen and crystalline proteins that compose the capsule and nucleus/cortex, respectively, which may ultimately contribute to the development of presbyopia. In addition to this disease,

AGE formations within the lens are hypothesized to have a considerable role in the pathogenesis of senile nuclear cataract (Boscia et al. 2000; Pokupec et al. 2003).

A cataract is a partial or total opacity of the lens that causes light absorption or scattering; it is the foremost cause of visual impairment worldwide (Parsons et al. 2005). Although many types of cataracts exist, the most common is senile nuclear cataract, which accounts for at least 60% of all cataract surgeries (Kaufman and Alm, 2003). Several hypotheses have been proposed for the etiology of nuclear cataract, among which oxidative stress induced damage of the lens crystalline proteins is a leading candidate (Spector, 1995; Giblin 2000; Truscott, 2000; Luo, 2003). Oxidative stress results from development of reactive oxygen species (ROS), a term encompassing a variety of compounds (e.g., singlet oxygen, superoxide, and hydrogen peroxide) having an enhanced energy state of oxygen that damages cellular lipids, proteins, and DNA, ultimately leading to cell necrosis (Lou, 2003). These pro-oxidants (ROS) can be eliminated through the production of antioxidants, the most pivotal of which to the protection of lens fiber cells is the tripeptide glutathione (Giblin, 2000). Due to lack of membrane-bound organelles within mature lens fiber cells, glutathione or precursor substrates (i.e., cysteine) for glutathione biosynthesis must be produced by epithelial and undifferentiated peripheral fiber cells of the superficial layers of the lens and diffuse inwards. Once glutathione becomes oxidized by surrounding ROS it must then diffuse back outwards where it can be regenerated into a reduced, antioxidant functional molecule by the same cells of its origin. Studies have illustrated a significant nonlinear decline in the diffusion of this antioxidant with age (Truscott, 2005), which suggests

increases in oxidative stress, particularly of the lens fiber cells in the nucleus, that can lead to cellular damage through multiple mechanisms, including formation of nuclear cataract-correlated AGEs.

AGEs form through a progression of the Maillard reaction, which is a non-enzymatic reaction between sugars and proteins (i.e., glycation) initially forming Schiff base adducts that rearrange into more stable Amadori products. These initial products are relatively harmless due to their reversible nature; however, maturation of the Amadori products, which often occurs through oxidation (i.e., glycoxidation), leads to the formation of harmful AGEs characterized by protein cross-linking, browning, and fluorescence (Zarina, 2000; Stitt, 2001). In the fiber cells of the human lens, crystalline proteins are particularly vulnerable to AGE accumulation because they do not turnover and insulin is not required for glucose uptake; thus, un-modulated concentrations of this sugar are constantly present (Pokupec et al. 2003). Amadori products form through a reaction between crystalline proteins and surrounding glucose, and become oxidized as the lens ages due to the decline in antioxidants. These oxidized Amadori products lead to AGE cross-linking of the crystalline proteins, causing aggregation, formation of high molecular weight clusters, and ultimately development of a light-scattering cataract (Boscia et al. 2000; Pokupec et al. 2003). Indeed, several studies have demonstrated, through analysis of non-diabetic human cadaver and patient lenses obtained during cataract surgery, that AGE concentrations increase in those with cataract (Nagaraj et al. 1999; Zarina et al. 2000; Ahmed et al. 2003; Franke et al. 2003; Pokupec et al. 2003). These results were shown to be exacerbated in lenses from diabetic donors, which

correlate with many epidemiological studies that have shown an increased prevalence of cataract in diabetic persons (Klein et al. 1985; Delcourt et al. 2000, and CDC, 2004).

The incidence and temporal relationship between presbyopia and cataract suggest an intertwined pathogenesis, and that their developments are symptoms of a natural breakdown of the lens, leading to its diminished functionality. Although little has been done to link the two pathologies directly, McGinty and Truscott (2006) propose lenticular sclerosis observed in presbyopia as the cause of the reduction in lens diffusivity, leading to the development of cataract. However, no conclusive evidence is presented to explain the development of lenticular sclerosis. Furthermore, Sweeney and Truscott (1998) show that an impediment to glutathione diffusion begins in the first decade of life, whereas their study of lens stiffening demonstrated the most dramatic changes beginning at the end of the second decade (Heys et al. 2004). Together these results appear to suggest that, contrary to the aforementioned proposal, breakdown of lens diffusivity begins first leading to lenticular sclerosis and eventually nuclear cataract. What then underlies the loss of lens diffusivity? Ironically, the one change that all lenses undergo throughout life is growth, which results in geometrical changes of a structure whose spatial relationships between constituents is pivotal to its functionality. Therefore, growth of the lens may create a barrier between the lens nucleus and aqueous humor, progressively suppressing nutrient diffusivity as additional layers of fiber cells are added with age and resulting in progressive damage to the crystalline proteins via AGE formation, which Stitt (2001) states can reduce the deformability of the lens, irrespective of cataract formation, leading to presbyopia. Additionally, growth of the lens may alter

its geometrical relationship with the ciliary muscle, rendering the latter incapable of inducing lens curvature changes upon contraction, which may imply that both lenticular sclerosis and geometric alterations of the accommodative apparatus are mechanisms of presbyopia. Finally, lens size may reach a point in later life that results in complete inhibition of nutrient transport to the center-most layers (i.e., nucleus), leading to a highly oxidized environment that causes additional formation of AGEs, crystalline protein aggregation, and ultimately a light-scattering cataract.

Cataract Surgery Induced Remodeling of the Lens Capsule

As the lens ages it appears to inevitably succumb to presbyopia and eventually cataract, the latter of which is estimated to be prevalent in 50% of persons over 60 years of age and nearly 100% over 80 years of age (Hammond, 2001). This inevitability of cataract in the older population suggests the corrective surgical procedure (more than 3 million procedures performed annually in the United States alone; Leaming, 2004), as a final stage of human lens 'development.' Cataract surgery (extracapsular) involves three basic steps once access to the aqueous chamber has been achieved: approximately a quarter of the anterior lens capsule is removed via the introduction of a continuous circular capsulorhexis (CCC); the lens is broken up, most often with ultrasound (phacoemulsification), and suctioned out; and a prosthetic intraocular lens (IOL) is placed in the remnant empty capsular bag. This surgical procedure dramatically alters both the biological and mechanical environment of the native lens, leading to a significant remodeling of the capsular bag that can cause complications. The two

primary aspects of this remodeling are gross structural and LEC induced constituent alterations.

In contrast to the quasi-spherical native lens, the IOL is a nearly flat, essentially two-dimensional circular plate (similar to a contact lens) whose position is initially maintained only by two small haptics that press against the equator of the capsular bag. Hayashi et al. (2002) describe this initial placement of the IOL to be only "weakly supported by the IOL haptics," which leaves it open to translations (i.e., decentration) that can cause visual disturbances (second leading complication of cataract surgery – Tehrani et al. 2003). Their study of human patients immediately following cataract surgery (N=70) showed, via a Scheimpflug videophotography system, that the anterior and posterior portions of the lens capsule contract down and enclose the IOL within approximately 6 and 11 days, respectively, which they hypothesize as the mechanism that allows for true initial stabilization. A further study by Tehrani et al. (2003) quantified contraction of the lens capsule in patients following cataract surgery (N=55) based on measurements of both the cross-sectional (equator-to-equator) and capsulorhexis diameters using a Koch capsule measuring ring implanted along with the IOL. Their results at 6 months post-operatively showed significant reduction in both capsule and capsulorhexis diameters on the order of about 15% (from a mean 10.53 to 9.01 mm and 5.24 to 4.47 mm, respectively), with the majority of this contraction occurring within the first month (see also Kurz et al. 2005). Although no explanation for these results is offered by either group, we hypothesize that structural changes result from a wound-healing type response by LECs transdifferentiated into a myofibroblast-

like phenotype, which is corroborated by several histopathology studies describing constituent alterations of the capsule subsequent to cataract surgery.

As mentioned previously, LECs form a monolayer along the inner anterior lens capsule, and two of their important functions are constituent maintenance, through secretion of primarily type IV collagen and laminin, and proliferation (limited to the germinative zone) to form pre-differentiated lens fiber cells to be added to the cortex. Cataract surgery causes the surviving LECs to undergo a function-altering, transdifferentiation into a myofibroblast (i.e., wound-healing) phenotype that is characterized by a heightened proliferation (throughout the remaining monolayer), altered protein expression, increased contractility leading to altered capsule morphology and wrinkling, ECM deposition, and migration to normally acellular regions of the capsule. This errant behavior exhibited by the LECs can result in various capsule opacifications (e.g., anterior capsule opacification, posterior capsule opacification, Soemmering's ring, and Elschnig's pearls) that significantly reduce visual acuity, symptomatically similar to the original cataract. Werner et al. (2000) cite that LEC proliferation and matrix deposition along the remnant anterior capsule is initiated shortly after cataract surgery, potentially leading to clinically significant anterior capsule opacification (ACO) as rapidly as 1 month post-operatively. Shigemitsu et al. (1999) examined the matrix constituents of human anterior capsule specimens (N=6) obtained during invasive corrective surgery for ACO, and showed that they contain fibroblast growth factor (FGF), transforming growth factor-beta (TGF-β), fibronectin, collagen types I, III, IV, V, VI, alpha-smooth muscle actin (α-SMA), and LECs. Marcantonio et

al. (2000) further reported an accumulation of multilayered LECs, particularly near the capsulorhexis edge, having an elongated, spindle morphology and expressing the intracellular contractile protein α-SMA. Similar to ACO, posterior capsule opacification (PCO) occurs through the accumulation of nearly identical matrix proteins (Shigemitsu et al. 1999; Marcantonio et al. 2000; Wormstone, 2002; Saika et al. 2003a) and contraction (resulting in wrinkling) of the posterior capsule by migrating LECs. Most studies place emphasis on PCO, however, due to the fact that it develops along the optical axis of the intact posterior lens capsule, and therefore is most visually debilitating.

Since transdifferentiated LECs appear to underlie the constituent alterations of the lens capsule following cataract surgery, characterization of the exact regulatory proteins and signaling pathways involved may be critical to clinical prevention. Of the inflammatory proteins present in the post-surgical lens, most studies have implicated TGF-β as a primary modulator of errant LEC behavior. During normalcy, the majority of TGF-β within the eye is heavily regulated through latency-associated peptides, but still functions as an immunosuppressor within the aqueous humor and as a regulator of both LEC proliferation and lens fiber differentiation (De Iongh et al. 2005). The association between TGF-β and PCO may stem from its known role in wound healing as a stimulus to fibroblast proliferation and as a mediator of ECM deposition, which are similar to those seen in PCO. Furthermore, studies including primary LEC cultures, in vitro capsular bag models, and in vivo animal experimentation have found that TGF-β likely induces epithelial-mesenchymal transition (EMT); a phenotypic change of the LECs that

causes a fibroblast-like morphology, increased motility, and secretion of various ECM proteins as found in PCO. The specific molecular markers associated with this change in phenotype are most often the intracellular contractile protein α-SMA and ECM proteins collagen types I and III, fibronectin, and tenascin. These molecular changes induce LEC migration, further ECM synthesis and deposition, and wrinkling (i.e., cell contraction) of the posterior capsule resulting in opacification (Wormstone, 2002; Saika et al. 2003b; Sponer et al. 2005).

Despite numerous studies showing that TGF-β is a primary mediator of the pathological wound healing type of response seen in LECs after cataract surgery, many researchers question its independent efficacy and cite the necessary, complementary roles of additional stimuli. Although there are many examples of this, perhaps the most prevailing argument is that cataract surgery initially induces a dramatic increase in proteins associated with a disrupted blood-aqueous barrier and inflammatory response, yet these return to basal levels within a relatively short period compared to that required for the development of PCO (Wormstone, 2002). Since TGF-β is among the proteins briefly up-regulated, the question remains: what continues to stimulate the LECs in the months and often years that lead up to a clinically significant inhibition of vision? Interestingly, De Jong-Hesse et al. (2005) showed that, in comparison to controls, LECs cultured on fibronectin and type-I collagen increased both proliferation and, more importantly, their expression of α-SMA, a primary marker for EMT. Corroborating many of these results, Oharazawa et al. (1999) hypothesized that “fibronectin may be one of the key components which lead to epithelial-mesenchymal transition resulting in

PCO." Since signaling between the cell and ECM can be mediated through integrins, several studies have shown that these transmembrane proteins play a fundamental role in the induction of EMT through either integrin-specific signal transduction pathways (Zuk and Hay, 1994; Bhowmick et al. 2001; Lee et al. 2004) or direct modulation of endogenously expressed TGF-β by the LECs (De Iongh et al. 2005).

The above discussion suggests a complementary role of TGF-β and integrin-ECM derived signals in the modulation of LEC transdifferentiation and corresponding errant behavior subsequent to cataract surgery. In addition to constituent changes, another type of ECM-derived signal that may influence cellular behavior is an altered mechanical stimulus. Since cataract surgery involves removal of the quasi-spherical lens nucleus and cortex, which is replaced with a flat IOL, the tractions (e.g., pressure) imposed onto the capsule (placing this tissue under stress) by these native structures must also be removed. This dramatic alteration in the mechanical environment of the resident LECs, which initially leads to a nearly stress-free capsule, is likely experienced through integrin-mediated pathways (Huang et al. 2004; Millward-Sadler and Salter, 2004) that results in a contractile response to restore their native mechanical environment. This hypothesis is consistent with studies by Brown et al. (1998) suggesting that fibroblasts seeded in an initially stress-free collagen matrix tend to compact the matrix to induce an "endogenous tension." Subsequent relief of this tension induces further compactions, which appears to restore the tension back near the original endogenous level. They termed this cellular behavior a "tensional homeostasis," meaning that the cells appear to seek to maintain constant their local mechanical

environment. Interestingly, a recent study by Annes et al. (2004) concludes that latent TGF-β may require force generation by local cells, through integrin attachments to the ECM, to physically disrupt its binding to the large latent complex (containing both latent TGF-β binding protein, LTBP, and latency-associated protein, LAP), and thereby activate the molecule (see also Keski-Oja et al. 2004). Given that Saika et al. (2001) showed that LTBP and LAP are up-regulated in post-surgical capsular opacification, these diverse studies collectively suggest that mechanical perturbations causing LEC transdifferentiation can induce secretion of latent and active TGF-β, which in turn promotes ECM synthesis. Finally, we have shown that the presence of a continuous circular capsulorhexis (CCC) in the anterior capsule maintains a traction-free (meridional stress) condition at the edge of the capsulorhexis (Heistand et al. 2006), which may prevent the contractile LECs from restoring their tensional homeostasis. Thus, unlike surgery-induced increases in cytokines and growth factors that return to baseline concentrations within months, the CCC indefinitely prevents the cells from restoring a normal mechanobiological environment, which could very well be the persistent stimulus for continued matrix remodeling that results in such long term (i.e., over years) complications as PCO.

The Role of Mechanics in the Development of Future AIOLs

The need for continued improvements in IOL technology has been motivated by the need to reduce post-surgical opacifications, particularly PCO, the most frequent complication of cataract surgery and second leading cause of visual impairment

worldwide. Pandey et al. (2004) cite three factors pivotal to the decline in incidence of PCO from 50% in the 1980's and early 1990's to less than 10% today: material biocompatibility (i.e., acrylic rather than polymethylmethacrylate, PMMA), adhesiveness of the IOL to the posterior capsule, and, most importantly, a square- versus rounded-edged optic (see also Nishi et al. 2000; Oner et al. 2000). These three advances appear to work collectively to form a tight, static barrier with the overlapping capsular bag that physically inhibits LEC migration and corresponding matrix deposition along the optical axis. Although these novel IOL designs have successfully decreased PCO, they continue to lack the important capability of accommodation, therefore, putting into question the capacity of future IOL designs, which will likely be dynamic structures, to prevent PCO through a technology that requires static adhesion of the capsule. Consequently, there remains a pressing need for continued characterization of the underlying mechanisms inducing errant LEC behavior that leads to capsule opacification. Particular emphasis should be placed on quantifying the effects (e.g., altered protein expression) of mechanical perturbations to the remnant LECs, such as loss of their homeostatic or quiescent stress state.

It is hoped that advances in IOL technology to enable accommodation will not only improve visual function after cataract surgery, but also provide a corrective procedure for presbyopia. Notwithstanding the technical difficulty involved, accommodative IOLs (AIOLs) have been developed by numerous research groups (e.g., Nishi and Nishi, 1998; Koopmans et al. 2003; 2006, Ben-Nun, 2006; Dick and Dell, 2006), the refractive changes of which are all initiated through ciliary muscle contraction

and corresponding alterations in capsular compressive forces. Specific mechanistic processes in these new AIOLs allow characterization into one of three groups: passive-shift AIOLs simply utilize altered haptics of normal IOLs to amplify the concept of pseudo-accommodation, which is the observed anterior-shift of the IOL optic with ciliary muscle contraction; dual optic AIOLs are composed of two lenses, connected at the periphery with springs, whose change in relative position alters their combined refractive power; and finally, capsular refilling AIOLs utilize an injected elastic material to mimic closely the structure, mechanical behavior, and refractive power of the native lens for a given accommodative stimulus (Menapace et al. 2006). Aside from the passive-shift AIOLs, which are commercially available, animal experimentation has been the primary mode of in vivo assessment. Although some results are encouraging, maximum accommodative amplitude, even with polymer refilling materials, has only been a fraction (~30%) of that measured prior to implantation in the pre-presbyopic animals (Koopmans et al. 2006). A contributing factor for this reduced accommodative amplitude is the difficulty of predicting performance of these AIOLs within a surgically treated capsular bag that undergoes post-surgical remodeling through contraction and fibrotic deposition by the LECs. Additionally, fibrosis of the remnant capsule is particularly severe with all current AIOL designs, making PCO one of the largest obstacles confronting future implementation (Nishi and Nishi, 1998; Menapace et al. 2006).

One aspect of the current AIOL design process, which is significantly impeding its advancement, is modeling of the mechanical interaction between the remodeled

capsular bag and the implant as a function of imposed tractions for a given zonular tension (i.e., accommodative stimulus); related to this, of course, is the need to predict better any alterations of stress-field values from homeostatic. The majority of mechanical modeling has focused on physiological accommodation of the native lens (section II), and almost nothing has been done to computationally predict its post-surgical behavior (particularly with an implanted IOL or AIOL). The only studies addressing this issue have been performed by Spalton and colleagues (Boyce et al. 2002; Heatley et al. 2004), who employed a mathematical model that utilized geometrical changes of the lens capsule after cataract surgery (Tehrani et al. 2003), thickness and Young's modulus of elasticity measurements in fresh senile human anterior and posterior lens capsules (Krag et al. 1997b; Krag and Andreassen, 2003a,b), vitreous pressure changes with accommodation (Coleman, 1986), and (passive-shift) AIOL dimensions to predict anterior displacement and corresponding accommodative amplitude of the AIOL. One limitation of this work, in addition to limitations common to many prior models based on linearly elastic, homogeneous, isotropic material behaviors (e.g., Schachar and Bax, 2001; Burd et al. 2002), is the use of capsular material parameters derived from uniaxial extension tests on pre-surgical capsules – primarily those performed by Krag and colleagues. Although these experiments found important relationships between changes in mechanical behavior and specimen age (i.e., a decrease in mechanical strength and distensibility with age), material parameters for analytical or computational modeling of the lens capsule should be derived from

mechanical tests that reflect the multiaxial stresses it experiences in vivo and account for post-surgical remodeling.

Toward this end, we developed a new technique whereby the lens capsule can be isolated in situ from the underlying cortex, loaded by a pressure that induces in-plane biaxial stresses, and yet maintained in nearly a native geometry with natural boundary conditions around the periphery. Consistent with uniaxial findings in both human and porcine lens capsules, we observed a nonlinear material behavior over finite strains. In addition, we found that the lens capsule exhibits a complex, regionally-dependent anisotropic behavior (properties are different in different directions) that is characterized by a progressively stiffer circumferential compared to meridional behavior as one moves from the pole to the equator along any meridian (Heistand et al. 2005; Pedrigi et al. 2007a). Modeling the capsule as a nonlinear, anisotropic, hyperelastic membrane, a custom sub-domain inverse finite element approach (Seshaiyer and Humphrey, 2002) was used to calculate values of the material parameters for a Fung exponential strain energy-based constitutive relation (David et al. 2007), from which we developed a finite element model of the lens capsule (David and Humphrey, 2007; Pedrigi et al. 2007a). Using this model, we have begun to predict capsular deformations during accommodation for purposes of assessing the interaction of the capsule with an IOL or AIOL; yet, a continuing lack of information on material parameters derived from post-surgical specimens limits the potential power of its predictions. That is, despite having a general theoretical framework for data analysis, there is a pressing need to measure material behavior of post-surgical specimens as a function of time since surgery to

account for the perhaps continued remodeling that occurs subsequent to this corrective procedure (see section IV). Although investigators of AIOLs have recognized this point and hinted at its need (refs), no study has been performed to address this deficit in knowledge of capsular behavior.

Overall, therefore, two impediments to the development of an AIOL that will have an accommodative amplitude similar to that seen in the young human lens are the acute onset of capsule opacifications, particularly PCO, and the limited work that has been done to develop mechanical models with the capability of assessing the interaction between prototype AIOL designs, and the remodeling capsule. With regards to the latter, future models will need to incorporate the kinetics of growth and remodeling (cf. Humphrey and Rajagopal, 2003) derived from mechanical testing of post-surgical capsule specimens. Ultimately, this will improve computational predictive capabilities and allow for a more expedient progression of AIOL technology.

Conclusion

The lens is a mechanical structure whose primary function is to alter its curvature and corresponding refractive power for purposes of the precise focusing of light onto the retina (i.e., accommodation). Consistent with this function, biomechanics has been utilized through a multitude of studies to illustrate the mechanism of accommodation and geometrical changes of the lens with age that likely lead to dysfunction of both the accommodative apparatus and ultimately its transparency in the development of presbyopia and cataract, respectively. The near inevitability of cataract opens up yet

another frontier of biomechanics exploration within the lens: progression of IOL technology, including introduction of accommodation into these prosthetics (i.e., AIOLs), and also study of mechanobiological mechanisms underlying LEC behavior within the post-surgical capsule. A common thread between these two study ventures is the necessity for quantification of alterations in both constituent matrix proteins and mechanical properties of the post-surgical capsule to fully understand the implications of its altered mechanical environment.

CHAPTER III

REGIONAL MULTIAXIAL MECHANICAL BEHAVIOR OF THE PORCINE ANTERIOR LENS CAPSULE

Overview

The lens capsule of the eye plays fundamental roles in both physiologic processes such as accommodation and clinical treatments such as cataract surgery; wherein, the highly mechanical nature of these processes motivates study from the perspective of biomechanics. Although this tissue experiences multiaxial stresses in vivo, no measurement of possible regional variations in its material symmetry has been made. Rather all prior mechanical data have implicitly assumed isotropy and regional homogeneity through either pressure-volume or uniaxial force-length mechanical tests. Here, we report a new experimental approach to study in situ the regional, multiaxial mechanical behavior of the lens capsule. Moreover, we report multiaxial data illustrating that the porcine anterior lens capsule exhibits a typical nonlinear pseudoelastic behavior over finite strains, that the in situ state is pre-stressed, and that the meridional and circumferential directions are principal directions of strain. This strain field is nearly equibiaxial at the pole, but increasingly non-equibiaxial towards the equator. Such data are fundamental towards developing more appropriate constitutive formulations.

Introduction

The lens capsule consists primarily of type IV collagen (65% by dry weight) and laminin, and contains a monolayer of epithelial cells on the underside of the anterior portion that act to maintain the capsule and append to the lens throughout life. Mechanically, the capsule is well approximated as a membrane due to its ratio of diameter to thickness of around 200 to 1. The primary function of the capsule is to mediate tractions imposed by the ciliary muscle to the underlying lens nucleus and cortex for purposes of molding this portion of the lens into a more flattened morphology; thus, disaccommodating the lens and changing ones focus from near to distant objects.

In addition to this fundamental role in normalcy, the lens capsule plays a central role in cataract surgery. A cataract is an opacity of the lens that results in impaired vision or blindness. Cataracts affect 50% of persons over 60 years of age and nearly 100% over 80 years of age (Hammond, 2001), and the corrective procedure is the most frequently performed in the United States with over 3 million annually (Leaming, 2004). Briefly, in cataract surgery, a portion of the anterior lens capsule is removed, through which the opacified lens nucleus and cortex is replaced with a prosthetic intraocular lens (IOL). Despite advances in surgical technique, the post-surgical complication of capsular opacities, such as posterior capsule opacification (PCO), has occurred in up to 50% of all patients within 2-5 years following cataract surgery (Emery, 1999; Spalton, 1999). These opacities, often referred to as secondary cataracts, result from epithelial cells migrating from the anterior portion of the lens capsule to the posterior where they transdifferentiate, proliferate, synthesize matrix proteins (collagens I, III, etc.), cytokines

and matrix metalloproteinases, and contract as in a wound healing response (Marcantonio and Vrensen, 1999; Wormstone, 2002; Saika et al. 2003a). These symptoms often require surgical (via laser) removal of a portion of the posterior lens capsule.

Fortuitously, a new IOL design by Alcon Laboratories, Inc. (the AcrySof lens) has been reported to reduce PCO from 50% to ~10% (Spalton, 1999) likely due to the "sharp rectangular edge design" and possibly "increased adhesiveness" of the IOL optic to the lens capsule (Linnola, 1997; Nagata et al. 1998; Nishi et al. 2000). Indeed, these apparent mechanical advantages of the AcrySof lens have promoted other mechanically-motivated devices. For example, Nishi et al. (1997) increased the tension in the lens capsule, following cataract surgery, by implanting an inflatable endocapsular balloon. Alternatively, Nishi et al. (2001) reduced post-surgical shrinkage of the lens capsule by implanting a square-edged capsular tension ring. Both interventions reduced PCO, although not to the extent achieved with the AcrySof lens, demonstrating that mechanical factors play a substantial role in the etiology of this disease and, thus, motivating quantification of lens capsule mechanics.

Based on a multitude of studies that have demonstrated the mechano-sensitivity of most all cell types, we hypothesize that the errant epithelial cell response resulting in capsular opacifications is, at least partially, modulated by perturbations of the native lens capsule stress and strain fields. Testing this hypothesis will require, first, quantification of these mechanical quantities and then measure of their alterations with various surgical interventions and implant designs. Toward this end, we must know the associated

geometry, mechanical properties, and applied loads. In this paper, we present the first data on the in situ regional, multiaxial, pseudoelastic behavior of the porcine anterior lens capsule obtained using a novel experimental approach. We submit that this is an important step towards understanding better the design of implants used during cataract surgery and the underlying mechanotransduction mechanisms in the etiology of PCO.

Methods

Upon receipt of fresh porcine eyes via overnight shipment in iced saline from SiouxPreme, Inc. (Sioux City, Iowa), the cornea and iris were removed and 40 um diameter polystyrene microspheres (Bangs Laboratories, Fishers, IN) were then placed on the exposed anterior capsule. They were arranged in seven overlapping sets of five (labeled A to G) extending from the pole (determined by the position of the y-suture) towards the equator along two orthogonal axes (Figure 3.1). Due to their hydrophobic nature, these microspheres demonstrated a natural adhesion to the capsule surface after an hour of air-drying. Next, a precision micro-manipulator was used to insert a 25-gauge needle just beneath the lens capsule, opposite the quadrant containing markers. Cyanoacrylate adhesive was applied around the needle to seal the insertion site, and a physiologic saline solution was injected slowly into the lens.

Once the lens capsule was successfully separated from the underlying lens nucleus and cortex, the eye was immersed in saline solution warmed to 35°C (within 10 minutes) and specimens were rehydrated for one hour (equivalent to the dehydration time) to eliminate any adverse effects of the dehydration. The specimen chamber was

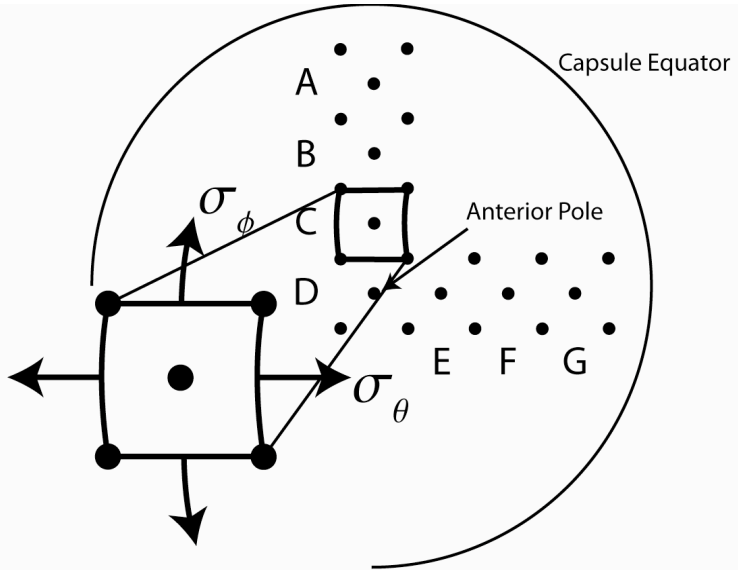

Figure 3.1. Schematic of the anterior lens capsule with markers. Marker arrangements consisted of seven overlapping sets of five (sets are denoted A to G) along two orthogonal axes extending from the pole towards the equator. Shown in the enlarged view of set C are the two principle directions meridional (ϕ) and circumferential (θ), with respect to which strains are calculated and averaged over the four marker triplets within each set.

then positioned for testing so that the microspheres on the surface of the anterior lens capsule could be imaged at different distention pressures with two cameras; one positioned directly above the capsule and the other placed in-plane, oriented 45° from the first (Figure 3.2). This arrangement allows each microsphere to be related to a global 3D coordinate system, constructed from the two 2D views of each camera. Further details of our custom bi-plane video system can be found in Heistand et al. (2005).

Experimental Protocol. The lens capsule was loaded via pressurization, which was accomplished by raising a saline reservoir via a pulley system that was connected to a pressure transducer and the inserted needle. Inflation was introduced through five consecutive cycles in increments of 5 mmHg (1-2 minutes per increment) from 5 to 40

and back down to 5 mmHg. The first four cycles were performed to precondition or "stress-soften" the tissue, which minimizes any viscous (time-dependent) effects and thereby allows the lens capsule to be modeled as a hyperelastic material. Data acquisition was then performed on the fifth cycle and images were obtained at every increment of pressure. Upon completion of the fifth cycle the lens capsule was imaged in its unloaded configuration by removing the pressurization needle and its stress-free configuration by cutting around its equator and allowing it to rest freely atop the lens nucleus and cortex.

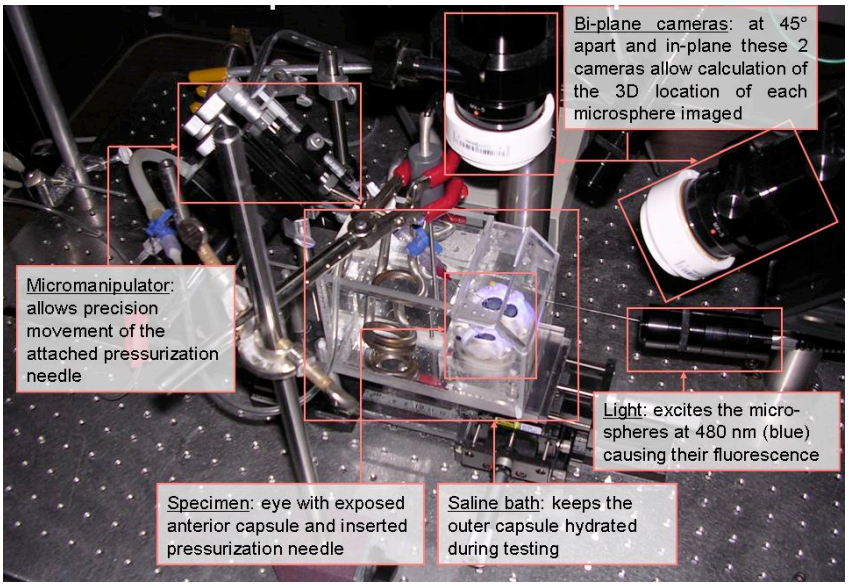

Figure 3.2. Image showing some components of our novel biaxial mechanical system. Most importantly notice that the eye sits in a temperature-controlled saline bath and is imaged by the two cameras, one of which is directly overhead while the other is 45 degrees off axis from the first.

Calculation of Strain. Following Humphrey (2002), in-plane finite Green strains, **E**, were computed regionally by dividing each marker set of 5 into triplets, computing

the deformation gradient, $\mathbf{F}$, and then using the equation $\mathbf{E} = (\mathbf{F}^T\mathbf{F}-\mathbf{I})/2$. Green strains are computed with respect to two directions shown previously to be principal (Heistand et al., 2005); these are meridional, which is tangent to the marker triplet centroid and always points towards the anterior capsule pole, and circumferential, which is perpendicular to the meridional component and likewise tangent to the triplet centroid. The deformation gradient can be calculated directly for each marker triplet by quantifying the deformation of position vectors from a reference configuration ($\Delta\mathbf{X}^{(1)} = \mathbf{X}^{\mathbf{B}}-\mathbf{X}^{\mathbf{A}}$ and $\Delta\mathbf{X}^{(2)} = \mathbf{X}^{\mathbf{C}}-\mathbf{X}^{\mathbf{A}}$) to configurations defined by subsequent loadings at various distension pressures ($\Delta\mathbf{x}^{(1)} = \mathbf{x}^{\mathbf{b}}-\mathbf{x}^{\mathbf{a}}$ and $\Delta\mathbf{x}^{(2)} = \mathbf{x}^{\mathbf{c}}-\mathbf{x}^{\mathbf{a}}$). Due to the proximity of the markers within a triplet, we assumed a homogeneous deformation within each area bounded by the triplet. Thus, $\Delta\mathbf{x} \approx \mathbf{F}(\Delta\mathbf{X})$ and the in-plane components of $\mathbf{F}$ can be determined for each pressure state using the matrix equation

$$\begin{bmatrix} \Delta x_1^{(1)} & \Delta x_1^{(2)} \\ \Delta x_2^{(1)} & \Delta x_2^{(2)} \end{bmatrix} = \begin{bmatrix} F_{11} & F_{12} \\ F_{21} & F_{22} \end{bmatrix} \begin{bmatrix} \Delta X_1^{(1)} & \Delta X_1^{(2)} \\ \Delta X_2^{(1)} & \Delta X_2^{(2)} \end{bmatrix}. \tag{3.1}$$

Additionally, Heistand et al. (2005) demonstrated that the deformation within each marker set is well approximated as homogeneous; therefore, mechanical behavior curves given below will illustrate the mean behavior of the four marker triplets within each set.

Results

To concisely illustrate the mechanical behavior that we found for the porcine anterior lens capsule, mean pressure-strain curves with respect to the stress-free reference configuration over five experiments are given for sets D (positioned at the

anterior pole) and G (nearest the equator) in Figure 3.3. It appears from the data that the mechanical behavior is nearly identical between the two principle directions at set D, but that at set G the stiffness in the meridional direction decreases while that in the circumferential direction increases. A qualitative comparison of set D to all other data sets (data not shown) demonstrated a similar trend, but to an incrementally larger degree as one moves from the pole towards the equator of the capsule; the difference being largest at the equator.

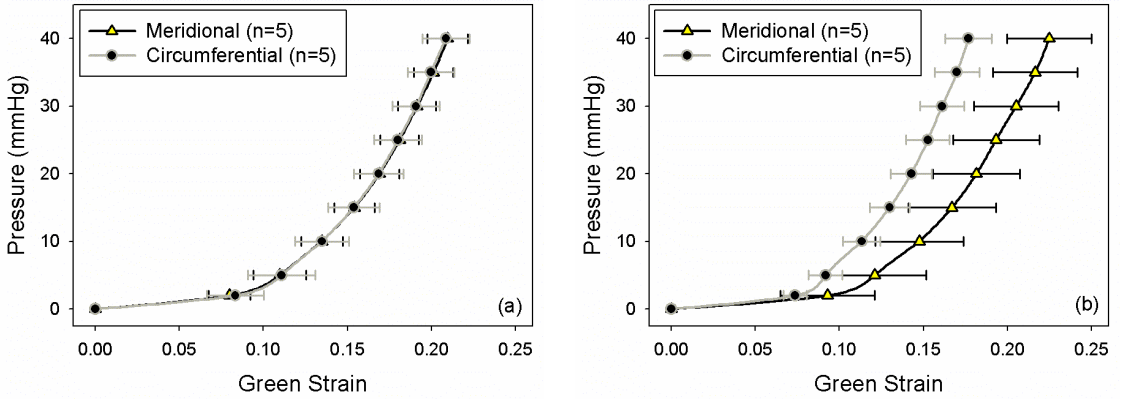

Figure 3.3. Mechanical behavior of the porcine anterior lens capsule at sets **(a)** D and **(b)** G with respect to the stress-free configuration. Notice the increase in stiffness in the circumferential direction and its decrease in the meridional at set G compared to D. Each curve represents the mean of five experiments and error bars represent ± standard error.

A second important finding of this study came forth due to our ability to obtain a stress-free configuration of the capsule and use it as the reference for measures of strain at each pressure state. Comparison between the stress-free reference point (at zero strain) and the second point (representing strain in the unloaded configuration of the capsule) within Figure 3.3 illustrates a significant pre-strain experienced by the lens capsule;

wherein, we found a nearly homogeneous (i.e., across all marker sets) value of 0.072 ± 0.004 (mean ± standard error). Pre-strain within the lens capsule is the result of pressure exerted onto it by the underlying lens nucleus and cortex. We estimated this pressure by fitting an exponential model to the raw pressure-strain data and calculating its value given the previously found value of pre-strain; overall, the mean across all data sets and experiments was 2.70 ± 0.11 mmHg.

Discussion

The lens capsule plays a fundamental role in both the physiologic process of accommodation and the clinical intervention of cataract surgery, both of which are highly mechanical in nature. Yet despite this fact, our understanding of the biomechanics of the lens capsule remains basic and incomplete. Early work by Fisher (1969) suggested that the ultimate tensile stress of the human anterior lens capsule decreases with age (from 2.3 to 0.7 MPa), consistent with the clinical experience that older capsules are more fragile. Yet these results are limited by the fact that pressure-volume tests were employed, which implicitly assume the material to be homogeneous and isotropic; essentially reducing the biaxial data into a 1D analysis. Further, despite finite deformations and a nonlinear material behavior, data were fitted using linear elasticity.

More recently, Krag and colleagues reported many important findings on the uniaxial mechanical behavior of circumferential rings excised from both the porcine and human lens capsule (Krag and Andreassen 1996; Krag et al. 1997a, 1997b; Krag and Andreassen, 1998, 2003a, 2003b). Similar to Fisher (1969), data revealed a nonlinear

mechanical behavior with stresses on the order of 3 to 4 MPa at stretches of 60-80% (1st Piola-Kirchhoff stress versus linearized strain). Moreover, they illustrated important changes in the human lens capsule with age; wherein, it was found that mechanical strength decreases while stiffness and thickness increase. It was also shown that the anterior and posterior lens capsules exhibit a nearly identical mechanical behavior, but that the posterior is less stiff due to its lesser thickness. Finally, they explored the viscoelastic nature of the capsule by showing both differences between the loading and unloading curves during a mechanical test and also performing stress-relaxation tests, the latter of which found capsule behavior to reach steady state within one minute of loading. These are important findings. Bailey et al. (1993) similarly reported uniaxial mechanical behavior, though as a function of the degree of glycosylation cross-linking within porcine lens capsules incubated in a high-glucose (133 mM) solution. As expected, data revealed increased stiffening of the capsule with increased cross-links, likely reflecting that which would occur in a diabetic or older individual.

Overall, 1D data provide important insights into some characteristics of the behavior of a material, but they are not sufficient for delineating the multiaxial behavior that exists in vivo; thereby, motivating the need for multiaxial mechanical testing. Further, it is preferable to test biological tissues in situ (i.e., while maintaining their native geometry and natural boundary conditions); however, most specimens are excised due to difficulties arising from the presence of adherent tissue. We developed a new technique whereby the lens capsule can be tested in situ via inflation, which separates the capsule from the underlying lens nucleus and cortex. Consistent with uniaxial

findings, we observed a nonlinear material behavior over finite strains. Moreover, the strain in the anterior lens capsule appears to vary with region and direction; wherein again, the meridional compared to circumferential strain appeared to incrementally increase from the pole to the equator. These results are not unexpected; indeed, they are qualitatively similar to results obtained for other nonlinear biological membranes such as intracranial saccular aneurysms (Humphrey, 2002). Finally, as reported in Heistand et al. (2005), we found that the capsule exhibited some hysteresis during mechanical testing, though minimized through preconditioning, and that there was very little creep over a period of 30 minutes at a constant pressure of 45 mmHg; consistent with the viscoelastic nature described by Krag and Andreassen (2003).

We emphasize that this experiment focuses on the quantification of mechanical properties, not the study of a particular in vivo situation. Because of the inherent geometric and material complexities, analysis of in vivo conditions will require finite element or comparable numerical studies.

In conclusion, we recall that there are five primary steps to formulate a constitutive relation: delineate general characteristic behaviors, establish an appropriate theoretical framework, identify the specific functional form, calculate the values of the material parameters, and evaluate the predictive capability (Humphrey, 2002). Based on the present findings, it appears that a nonlinear hyperelastic membrane theory may be useful to quantify the material behavior of the anterior lens capsule with possible regional variations in the mechanical properties (i.e., regional anisotropy). Having now

established a novel method to collect the requisite multiaxial data, there is a need to formulate a constitutive descriptor appropriate for nonlinear finite element analysis.

CHAPTER IV

ALTERED MULTIAXIAL MECHANICAL PROPERTIES OF THE PORCINE ANTERIOR LENS CAPSULE CULTURED IN HIGH GLUCOSE*

Overview

Hyperglycemia is a metabolic disorder that can alter the mechanical properties of tissues whose protein constituents have long half-lives through the formation of advanced glycation end products (AGEs). Recently, we developed a novel experimental approach to study the regional, multiaxial mechanical properties of the lens capsule of the eye. In this paper, we use this experimental system to quantify the alteration in mechanical properties of the porcine lens capsule when cultured for 8-14 weeks in high glucose versus control media. Specifically, the lens capsule is significantly stiffer in both the circumferential and meridional directions (considered principal directions). An inverse finite element method shows further that the material symmetries of the lens capsule are maintained despite glucose induced alterations of the type-IV collagen, the primary structural constituent of the lens capsule.

Introduction

Hyperglycemia is a metabolic disorder that manifests itself as high glucose levels in the blood, resulting from impaired action of insulin and leading to diabetes mellitus.

*Reprinted from Journal of Biomechanical Engineering, Vol. 129, R.M. Pedrigi, E. Staff, G. David, S. Glenn, J.D. Humphrey, Altered multiaxial mechanical properties of the porcine anterior lens capsule cultured in high glucose, pp. 121-125, 2007 with permission from ASME.

Additional consequences of long-term hyperglycemia include nephropathy, neuropathy, retinopathy, cataractogenesis, and cardiovascular disease. Many studies strongly support the hypothesis that each of these diseases develops, at least in part, due to the formation of advanced glycation end products (AGEs); see Swamy-Mruthinti et al. (1999), Candido et al. (2003), Vasan et al. (2003), Layton and Sastry (2004), and Ahmed (2005). AGEs begin to accumulate on proteins to a degree that depends on the concentration of glucose present. Most proteins in the body have a high turnover rate; therefore, the adverse effects seen on the tissue by this process are negligible. Certain proteins, an important example of which is collagen, have long half-lives, however, and it is in collagenous tissues (for example) where AGEs can play a particularly devastating role (Aronson, 2003).

In this study the lens capsule was of particular interest, being a thick basement membrane that consists primarily of type-IV collagen (65% by dry weight), with admixed adhesion molecules and proteoglycans. The ultrastructure reveals a three-dimensional meshwork of interconnected collagen fibrils, which form a pentagonal pattern (Barnard et al., 1992). These multilayered networks of fibers ultimately enable the primary functions of the lens capsule: a deformable support, through which lens shape can be altered or maintained, and a filtering membrane for potentially diffusive molecules (Seland, 1992). The thickness of the lens capsule in the porcine eye varies with arc length, but on average is 60 and 40 μm in the anterior and posterior portions, respectively.

We recently developed a new approach to quantify in situ the mechanical properties of the anterior lens capsule. Briefly, we insert a pressurization needle just underneath the capsule, which is distended with a saline solution while simultaneously tracking microspheres affixed to its surface. By tracking separate sets of five microspheres, we can infer possible regional differences in the biaxial material behavior. Indeed, we have shown that the anterior lens capsule exhibits a regional anisotropy wherein the ratio of circumferential-to-meridional stiffness increases as one moves from the pole towards the equator (Heistand et al. 2005). The purpose of the current study is to use this novel approach to compare the properties of porcine lens capsules cultured in vitro in either a high glucose or a control media. Adverse effects of hyperglycemia on the mechanical properties of the lens capsule may have important implications to areas of ophthalmology ranging from cataract surgery to understanding the etiological foundations of presbyopia in diabetic patients.

Methods

Tissue Culture Protocol. Whole porcine globes (n=40) were harvested from seven month old pigs at SiouxPreme Pork Products (Sioux Center, Iowa) and included in the study. Globes were shipped on ice and received within 24 h of death. Upon arrival, the tissue was stored near 4°C for 4-6 hours until dissection. The complete lens capsules were then removed from the globes and placed in a 10% antibiotic-antimycotic (Invitrogen) media for 3 hours, with solution changed at ½ hour, 1 hour, and 2 hours. Capsules were then divided equally into a low glucose group (control) and a high

glucose group, and transferred to vented dishes containing the corresponding media. Both groups were maintained at a 7.4 pH in DMEM (Dulbecco's Modified Eagle Medium), which has a nominal glucose concentration of 5.56 mM, with 2% FBS (Fetal Bovine Serum, Invitrogen) and 1% antibiotic-antimycotic. The high glucose group received a further media supplement of 128 mM D-Glucose, for a total of 133 mM glucose versus 5.56 mM in the control group. The capsules were cultured in an incubator at 37°C with 5% CO_2 for 8-14 weeks. Media was replaced every third day, and cultures were monitored closely for signs of contamination. Immediately following a biomechanical test, remnant tissue was placed for 5 hours at 37°C in a 3-(4,5-dimethylthiazol-2-yl)-2,5-diphenyltetrazolium bromide (MTT) solution (5 mg/mL) prepared in DMEM (Sigma, St. Louis, MO), to determine lens epithelial cell viability, which reflects tissue viability. The ability of MTT to determine the condition of cells in culture is based on its enzymatic reaction with the mitochondria. When exposed to MTT, a mitochondrial dehydrogenase from viable cells cleaves to the tetrazolium rings of the pale yellow MTT and forms dark blue formazan crystals (Mosmann, 1983).

Biomechanical Testing. Prior to mechanical testing, each cultured capsule was placed in a conical-shaped acrylic holder, and 40 μm diameter fluorescent microspheres were affixed to the dried capsule through their hydrophobic nature. Overall, 11 microspheres were positioned as three overlapping groups of five markers on the anterior surface of the capsule (see Page 59). The center set was placed at the pole of the capsule (as revealed by the y-suture), whereas the other two sets were positioned along the major and minor axis, respectively. This arrangement allowed slight regional

anisotropies, as reported by Heistand et al. (2005), to be studied in the cultured capsules. The capsule was then placed in a fluid-filled chamber at 37°C, and loading was accomplished by pressurization with the same physiologic saline solution. Specifically, a precision micro-manipulator was used to insert a 25-gauge needle just beneath the lens capsule, along the major axis opposite the side containing markers. A cyanoacrylate adhesive was then applied around the needle to seal the insertion site. This needle was attached to both a height-adjustable fluid reservoir and a pressure-transducer, which allowed accurate control of intra-capsular pressure. To eliminate any effects of the dehydration process mentioned above, the capsule was rehydrated for one hour (equivalent to dehydration time) prior to mechanical testing.

The custom data acquisition system and corresponding methods of data analysis are described in detail in Heistand et al. (2005). Briefly, a bi-plane video system (current resolution of ~7 μm), allowed the 3-D position of each marker to be determined from two 2-D views. The marker arrangement described above permits each set of five microspheres to be divided into four sub-sets of triplets, which are convenient for measuring local multiaxial strains. A local coordinate system was defined at the centroid of each triplet, and the associated circumferential and meridional directions were identified. Relative to these directions, in-plane Green strains (which are exact for finite deformations; Humphrey, 2002) associated with each marker triplet were computed at every pressure state from the change in 3-D position of each marker in the triplet relative to a stress-free reference configuration. This calculation assumes a homogeneous

deformation within each triplet (area typically ~0.25 mm squared), which was verified previously.

The specific experimental protocol involved three steps: pre-conditioning, testing, and determination of a suitable stress-free reference configuration. Toward this end, each capsule was loaded through five consecutive cycles of step changes in pressure, in 5 mmHg increments for 1-2 minutes each, from 5 to 35 (or 30 in the case of preconditioning) to 5 mmHg. The first four cycles were performed to precondition or "stress-soften" the tissue, which minimizes any viscous (time-dependent) effects and thereby allows the lens capsule to be modeled as a hyperelastic material. Data acquisition was performed on the fifth cycle and images were obtained at every increment of pressure. The unloaded configuration was obtained separately, subsequent to the fifth cycle of pressurization, outside of the bath to ensure that all pressurization fluid was extracted (some fluid can be trapped at very low pressures, that is, less than 5 mmHg). Finally, the stress-free configuration was obtained by cutting around the equator of the capsule and imaging the microspheres as the capsule rested free atop the lens. This configuration served as the reference in all strain calculations (the only exception is that subsequent comparison of circumferential and meridional strains is given with respect to the unloaded configuration because differences between them can equal the error innate with obtaining the stress-free configuration).

Estimation of Material Parameters. Knowing the deformation of a material and the corresponding loading, the mechanical properties of that material can be determined through an inverse approach (the forward problem being determination of deformations

given the properties and loads). We also developed a sub-domain inverse finite element method to determine material properties of distended biomembranes from measured pressures and 3-D locations of markers arranged in sets of five (Seshaiyer and Humphrey, 2003). Briefly, we combined a nonlinear regression method (Marquardt-Levenberg) with a custom finite element code for nonlinear membranes (solved using a Newton-Raphson method). We prescribe the 3-D locations of the outer four markers of each set of five (Figure 4.1) as displacement boundary conditions and then minimize differences between finite element predicted and experimentally measured positions of the central marker (*x,y,z* coordinates) at multiple pressures. Extensive numerical simulations reveal that the method is robust as long as the associated state of strain is not equibiaxial. Note, therefore, that the virtual work statement for an inflated nonlinear membrane is

$$\int_{\Omega} \delta w dA = \int_{\Omega} Pn \cdot \delta x da \tag{4.1}$$

where dA is an undeformed surface area, P the distending pressure, **n** an outward unit normal vector to the membrane, and **x** the location of material particles in a deformed configuration, having deformed area da. We assumed the lens capsule behaves as a hyperelastic material and employed a Fung exponential strain energy function, w, which has been shown to describe well the behavior of diverse biomembranes such as mesentery, pericardium, pleura, saccular aneurysms, and skin (Humphrey, 2002). The Fung model is given as:

$$w = c\left(e^{Q} - 1\right) \qquad Q = c_1 E_{11}^2 + c_2 E_{22}^2 + 2c_3 E_{11} E_{22} \tag{4.2}$$

where c, c_1, c_2, and c_3 are material parameters to be determined from the sub-domain method and E_{11} and E_{22} are circumferential and meridional (i.e., principal, as revealed by the pressure-strain data) components of the Green strain tensor, respectively. Theoretical arguments restrict the possible values of the material parameters, namely $c>0$, $c_1>0$, $c_2>0$, and $c_1c_2>(c_3)^2$. This helps to limit the parameter search space in the Marquardt-Levenberg regression, which aids in determining meaningful best-fit values.

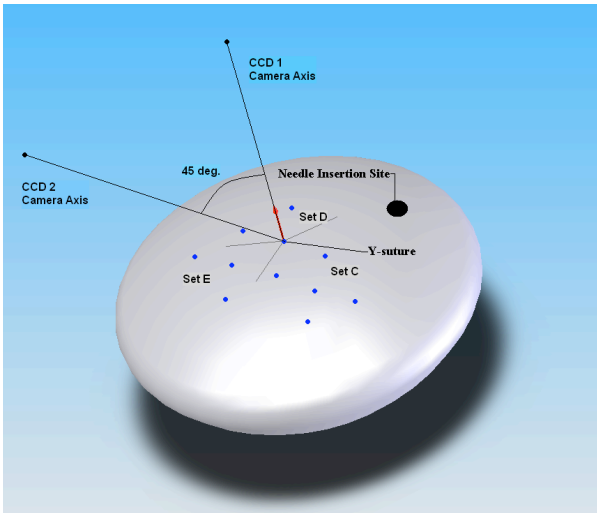

Figure 4.1. CAD drawing of the lens capsule. Shown are the needle insertion site (to distend the capsule at multiple pressures from 5 to 35 mmHg), the overlapping sets of 5 microspheres needed for both the strain calculation and inverse finite element estimation of the material properties, the y-suture on which Set D is centered, and two axis representing that of the CCD video cameras used to obtain the three-dimensional coordinates of each marker at a given pressure state.

Results

Figure 4.2 presents mean mechanical data, averaged at every pressure state from 2 to 35 mmHg, for Set D (centered at the pole) along the meridional direction of the anterior lens capsule for 8- and 14-week high glucose and control cultured, freshly

isolated, and fresh in situ tested lens capsules. All data are presented with respect to the stress-free configuration of the lens capsule. Qualitatively, it can be clearly seen that both the 8- and 14-week high glucose cultured lens capsules exhibited significant stiffening at all pressure states in comparison to the controls. Statistically significant differences between the high glucose and control capsules was determined by a t-test ($p<0.05$) and the error bars represent standard error. Finally, the mean freshly isolated and in situ mechanical data show both the effect of isolating the lens capsule from surrounding ocular constituents, which is seen to be statistically insignificant, and illustrate the degree of stiffening that is innate with long periods of tissue culture.

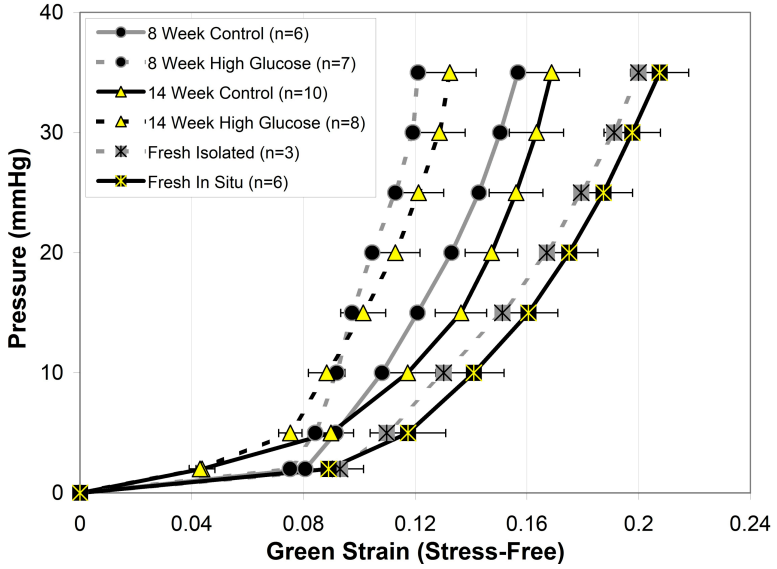

Figure 4.2. Summary of pressure-distension data for Set D in the meridional direction of all 40 lens capsules (note that circumferential data is very similar for Set D and therefore not shown). Data are shown as mean ± standard error, except for 8-week cultured capsules and freshly isolated (for clarity), which had similar standard errors. A t-test reveals that high-glucose responses are significantly stiffer ($p< 0.05$) than corresponding controls for the 14 week cultured lens capsules; which are not statistically different from the 8 week culture period in either the high glucose or control groups. Strains are relative to the cut, stress-free configuration.

Another important aspect of this study is to investigate potential alterations of material symmetries known to be in the normal porcine capsule, due to high glucose. Figure 4.3a shows mean data from Set C of the 14 week, high glucose cultured lens capsules in both the circumferential and meridional directions, while Figure 4.3b similarly shows mean data from Set D for these same lens capsules. These two figures reveal that while the circumferential direction exhibits nearly the same response to an applied load as the meridional direction in Set D, as one moves away from the pole and towards the equator (as in moving from Set D to Set C), the circumferential direction becomes stiffer than the meridional.

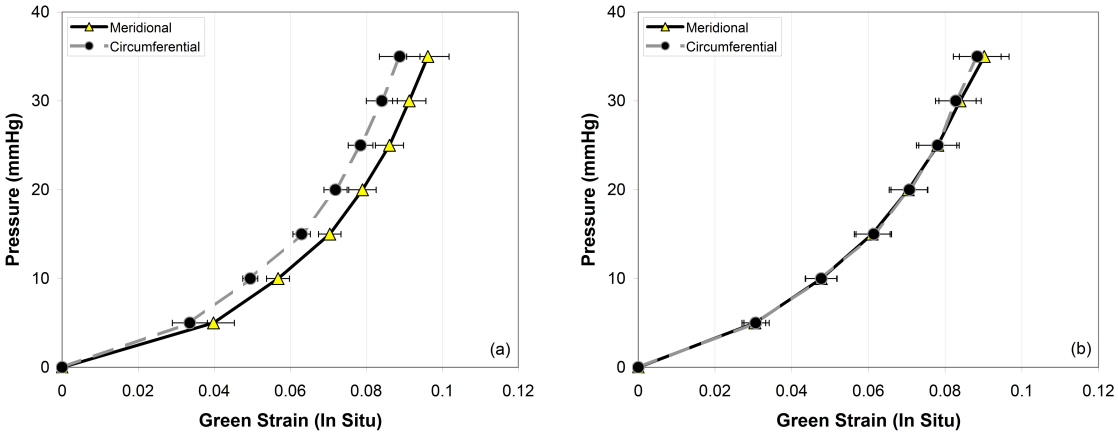

Figure 4.3. Mechanical behavior data for **(a)** Sets C and **(b)** D for the 14 week high-glucose cultured lens capsules in both principle directions. Note that, consistent with Heistand et al. (2005), the circumferential direction becomes "stiffer" than the meridional as one moves towards the equator from the pole (Set D), indicating that the lens capsule is a regionally non-homogeneous material. Strains are relative to the intact, unloaded configuration. Error bars represent standard error.

This data aligns well with that shown by Heistand et al. (2005) for the fresh, in situ tested lens capsule, which implies that material anisotropy exhibited by the normal

lens capsule is maintained in the presence of hyperglycemia. Indeed, Figure 4.4a shows results from the inverse FEM in terms of the ratio of the circumferential to the meridional stiffness parameters (c_1/c_2) for all three regions: Set C, Set D, and Set E. This illustrates further this stiffening of the circumferential direction with position towards the equator, implying a regional material anisotropy. Finally, Figure 4.4b shows best fit values of c (N/m) from the Fung strain energy function. Consistent with Figure 4.2, the increased stiffness due to the high glucose is reflected in higher values of c.

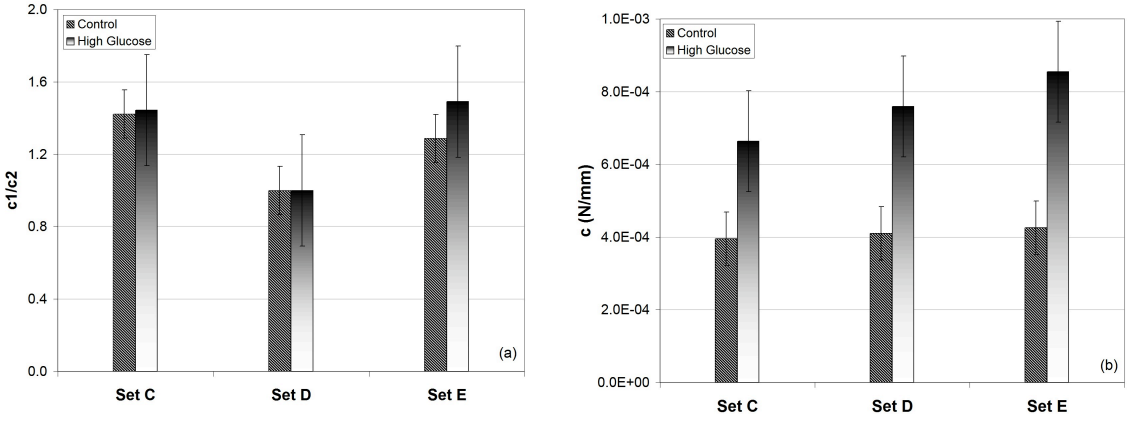

Figure 4.4. Subdomain inverse finite element estimation of the best-fit parameters in the Fung strain energy function for the 14 week control and high glucose cultured lens capsules. Panel **(a)** shows the ratio of c_1 to c_2 and panel **(b)** shows c (N/m). The change in c_1/c_2 from the pole (Set D) to the periphery (Sets C and E) indicates a regional anisotropy. In a comparison of the control versus high glucose lens capsules, this regional anisotropy does not appear to be affected by the process of glycation/glycoxidation, as does the overall stiffness of the capsule indicated by the statistically larger c-value (Figure 4.4b) in the high glucose cultured capsules. Error bars represent standard error.

Discussion

Diabetes Mellitus is reaching epidemic proportions worldwide, with rates expected to increase dramatically in the years to come. In the United States, 6% of the

population is currently affected with the disease and up to 16% of the population is estimated to have the so-called metabolic syndrome (pre-diabetes), which is a range of metabolic disorders that places the patient at risk for developing type-2 diabetes, and is characterized by, among other things, hyperglycemia (Rizvi, 2004; Stumvoll et al. 2005). The primary concern related to hyperglycemia is protein glycation, which can lead to AGE formation and cause changes in the mechanical properties of proteins and the corresponding tissue in which those proteins reside.

The purpose of this study was to quantify the effects of hyperglycemia on the regional mechanical properties of the lens capsule of the eye. To our knowledge the only related study (Bailey et al. 1993) used in vitro uniaxial extension tests on rectangular strips excised from porcine lens capsules cultured for 8-12 weeks in a 133 mM high-glucose media. Their study showed that due to increased glucose cross-linking (glycation) of the high glucose cultured lens capsule, the ultimate stress (failure property) and strain (i.e., extensibility) were reduced in comparison to control. Although this finding is important qualitatively, this research is limited by the uniaxial testing device. Because the lens capsule experiences multiaxial stresses in vivo, imposed by the lens and perhaps additional ocular components (i.e., ciliary body, aqueous humor, etc.), it is essential to determine how modifications in the mechanical properties due to protein glycation effect the overall stiffness and material symmetries that are present in normalcy. In this study, the mechanical properties of the cultured tissue were evaluated in their native geometry by distending intact capsules with known pressures. Qualitatively similar to Bailey et al. our results revealed a nominal 20% reduction in

distension of the high glucose cultured lens capsules relative to the controls, for a given pressure state. Nevertheless, the material anisotropy that exists as a function of meridional position in the porcine lens capsule (Heistand et al. 2005) was demonstrated here to be maintained after glucose cross-linking. Interestingly, the 8- and 14-week high glucose cultured lens capsules were not statistically different; this suggested that glycation of the type-IV collagen protein may have reached steady state at 133 mM at or before the 8-week mark. This finding is in contrast to that of Bailey et al. who stated that the 12 week cultured lens capsules were stiffer than the 8 week (data not shown).

Hyperglycemia increases glucose concentrations of the aqueous humor (Sato and Roy, 2002), which can initiate disease processes such as cataract formation (Swamy-Mruthinti, 1999). Cataract surgery involves removal of the anterior pole of the lens capsule, extraction of the clouded lens, and implantation of an artificial intraocular lens (IOL). Because this procedure imposes a severe mechanical insult, and because the lens capsule plays a central role in holding the IOL, there is a need to understand completely the mechanics of the native lens capsule. Only in this way can we quantify mechanical alterations imposed by surgery, mimic better the native mechanical environment with an implanted device, understand physiological processes such as accommodation, and prevent post-operative complications such as posterior capsule opacification (PCO or secondary cataracts). Alterations in the mechanical properties of the lens capsule due to hyperglycemia prior to cataract surgery may impact the behavior of the tissue post-operatively and should be considered in IOL design. Furthermore, future IOLs may have the capacity to allow accommodation, which results via changes in lens capsule (and

ultimately lens) morphology, imposed by tensions derived from the ciliary body. If future accommodating IOLs are to operate through a similar mechanism, the underlying mechanics of the lens capsule, the conduit through which these forces are transmitted, will need to be clearly elucidated. Obviously if the lens capsule is stiffer, there will need to be more force imposed on this tissue to achieve an accommodative displacement. Correspondingly, hyperglycemia-induced stiffening of the lens capsule may also lead to a premature development of presbyopia, which is a loss of accommodative function that occurs naturally with age. There is clearly a need for a better understanding of the lens capsule.

In conclusion, the results of this study correlate well with those reported by others on hyperglycemia-induced alterations of the mechanical properties of collagenous tissues – the porcine lens capsule stiffens when cultured in a high glucose versus control media. In addition, however, it appears that the local material symmetry is maintained and stiffening occurs homogeneously. These results should be considered when evaluating IOL design, clinical procedures for cataract surgery, and in studying the etiology of presbyopia in hyperglycemic or diabetic patients.

CHAPTER V

REGIONAL MECHANICAL PROPERTIES AND STRESS ANALYSIS OF THE HUMAN ANTERIOR LENS CAPSULE*

Overview

The lens capsule of the eye functions, in part, as a deformable support through which the ciliary body applies tractions that can alter lens curvature and corresponding refractive index during the process of accommodation. Although it has long been recognized that characterization of the mechanical properties of the lens capsule is fundamental to understanding this physiologic process as well as diverse clinical interventions, prior data have been limited by one-dimensional testing of excised specimens despite the existence of multiaxial loading in vivo,. In this paper, we employ a novel experimental approach to study in situ the regional, multiaxial mechanical behavior of both normal and diabetic human anterior lens capsules. Furthermore, we use these data to calculate material parameters in a nonlinear stress-strain relation via a custom sub-domain inverse finite element method (FEM). These parameters are then used to predict capsular stresses in response to imposed loads using a forward FEM model. Our results for both normal and diabetic human eyes show that the anterior lens capsule exhibits a nonlinear pseudoelastic behavior over finite strains that are typical of soft tissues, and that strains are principal relative to meridional and circumferential

*This article was published in Vision Research, Vol. 47, R.M. Pedrigi, G. David, J. Dziezyc, and J.D. Humphrey, Regional mechanical properties and stress analysis of the human anterior lens capsule, pp. 1781-1789, Copyright Elsevier, 2007.

directions. Experimental data and parameter estimation suggest further that the capsule is regionally anisotropic, with the circumferential direction becoming increasingly stiffer than the meridional direction towards the equator. Although both normal and diabetic lens capsules exhibited these general characteristic behaviors, diabetic capsules were significantly stiffer for a given distension. Finally, the forward FEM model predicted a nearly uniform, equibiaxial stress field during normalcy that is perturbed by cataract surgery. Such mechanical perturbations may be an underlying modulator of the sustained errant epithelial cell behavior that is observed well after cataract surgery, which may ultimately contribute to opacification of the posterior lens capsule.

Introduction

The primary function of the lens of the eye, termed accommodation, is to precisely focus images onto the retina by changing curvature and corresponding refractive index. Investigators have long sought to understand the mechanism of accommodation in terms of interactions of the constituent tissues, which recently has been aided by biomechanical modeling. Such models depend heavily on accurate measurements of tissue mechanical properties and seek to predict stresses and strains. A critical component of the accommodative apparatus is the lens capsule, a bag-like membrane that encapsulates the lens and mediates tractions imposed onto the lens nucleus and cortex by the ciliary body.

Beyond the need to understand the physiological process of accommodation, there is also a pressing need to understand the gradual development of presbyopia that is

nearly inevitable with aging and to find improved clinical procedures for correction. Finally, further motivation to understand the mechanics of the lens capsule stems from another age related disease, cataract, which is a partial or total opacity of the lens that is the foremost cause of visual impairment and blindness worldwide (Parsons et al. 2005). Greater than one-half of all Americans over age 60 and nearly all over age 80 years develop a cataract (Hammond, 2001), and cataract surgery has become one of the most frequently performed surgical procedures in the United States with approximately 3 million annually (Learning, 2004). Surgery involves three basic steps once access to the aqueous chamber has been achieved: approximately a quarter of the anterior lens capsule is removed via the introduction of a continuous circular capsulorhexis (CCC); the lens is broken up, most often with ultrasound (phacoemulsification), and suctioned out; and finally an artificial intraocular lens (IOL) is placed in the remnants of the empty capsular bag. Although improved surgical technique and, perhaps more importantly, novel IOL designs have decreased post-surgical complications, current IOL designs lack the important feature of accommodation.

Research into this deficit in IOL design has been undertaken by numerous groups (e.g., Nishi and Nishi, 1998; Koopmans et al. 2003, 2006; Ben-Nun, 2006; Dick and Dell, 2006), and has led to several accommodative IOLs (AIOLs) that function by utilizing original components of the accommodative apparatus. Some AIOLs are becoming available commercially, yet in vivo assessments in animal models, particularly pre-presbyopic rhesus monkeys, reveal a lack of return to pre-surgical accommodative function (Norrby et al. 2006). One possible hindrance to the design of an effective AIOL

is the nearly complete lack of biomechanical modeling of the post-surgical lens capsule and its mechanical interaction with an implanted AIOL.

We emphasize that cataract surgery dramatically alters both the biological and the mechanical environment of the native lens capsule, which may contribute to complications such as posterior capsule opacification (PCO). Such opacities of the remnant capsule appear to originate from the transdifferentiation of lens epithelial cells (LECs) into a wound-healing, fibroblast-like phenotype that promotes their proliferation, secretion of various extracellular matrix proteins, migration, and contraction of the capsule, all of which can cause visual disturbances (Marcantonio and Vrensen, 1999; Marcantonio et al. 2000; Wormstone et al. 2002). Although PCO has recently been lessened in older patients, primarily through improved IOL designs that physically inhibit the migration of LECs to the central posterior capsule, younger patients continue to have significant occurrences (Kock and Kohnen, 1997; Raina et al. 2004). Moreover, it is doubtful that AIOLs will be able to utilize similar methods to prevent the migration of LECs since these prosthetics will likely be dynamic structures, not static like current IOLs. Hence, there also remains a pressing need to understand more fundamentally the mechanisms that induce the pathological transdifferentiation and errant behavior of LECs subsequent to cataract surgery. We hypothesize that the surgical procedure and/or design of the IOL (or AIOL) induce persistent regional changes in capsular mechanical stress or strain from normal values, which via mechanotransduction mechanisms stimulate, in part, the epithelial cells to alter their gene expression in a way that causes capsular opacification. Testing this hypothesis will require a better understanding of the

biomechanical properties of the normal lens capsule, which in turn would allow quantification of the native mechanical environment experienced by LECs as well as possible alterations that result from surgery or the implantation of a prosthesis.

In summary, therefore, increased understanding of the biomechanics of the lens capsule could contribute to an improved understanding of the physiological accommodative mechanism, the development and treatment of presbyopia, and the possible improvement of interventions to treat cataracts or complications resulting from such interventions. Toward this end, we report the first data on the regional multiaxial mechanical properties of the human anterior lens capsule in health and diabetes, and use this information to compute biaxial stress fields in both the native capsule and that immediately following a CCC. We show, for example, that the normal lens capsule exhibits a strong, regionally varying anisotropy, which together with regional variations in capsular thickness yields a nearly uniform and equibiaxial stress field during normalcy. Moreover, this stress field differs markedly following the introduction of a CCC, as revealed primarily by increases in circumferential and decreases in meridional stresses, particularly near the edge of the capsulorhexis. Although removal of the lens and implantation of an IOL or AIOL will perturb the stress and strain fields further, the traction-free edge resulting from the CCC may play a dominant role.

Methods

The lens capsule consists primarily of type IV collagen (65% by dry weight) with admixed adhesion molecules and proteoglycans. The thickness of the human anterior

lens capsule varies regionally from pole to equator and increases with age, but it is approximately 15-22 μm (Fisher and Pettet, 1972; Krag et al. 1997b). Given its thinness, its radius of curvature on the order of 10 mm (based on measurements of the lens; Manns et al. 2004), and its low bending stiffness (Heistand et al. 2005), the lens capsule can be treated mechanically as a membrane. This observation, in turn, dictates appropriate theoretical, experimental, and computational methods for quantifying the associated biomechanics.

Theoretical Framework. Similar to many other soft tissues, the human lens capsule exhibits a highly nonlinear response over finite strains (Krag et al. 1997b). The capsule stress relaxes under large, fixed extensions (Krag and Andreassen 2003a), but the hysteresis associated with losses in stored energy during slow cyclic loading can be minimized by preconditioning (Heistand et al. 2005). Moreover, although not investigated in the human capsule, we recently showed that the porcine anterior lens capsule exhibits a strong regionally dependent anisotropy (Heistand et al. 2005). Given these observations, it is prudent to employ a general membrane constitutive theory to admit a nonlinear, possibly anisotropic pseudoelastic behavior. Toward this end, we used a "stress-strain" relation of the form (Humphrey, 1998)

$$\mathbf{T} = \frac{1}{\det \mathbf{F}} \mathbf{F} \cdot \frac{\partial w}{\partial \mathbf{E}} \cdot \mathbf{F}^T \leftrightarrow T_{\alpha\beta} = \frac{1}{\det \mathbf{F}} F_{\alpha\Gamma} F_{\beta\Delta} \frac{\partial w}{\partial E_{\Gamma\Delta}}, \alpha, \beta, \Gamma, \Delta = 1,2 \qquad (5.1)$$

wherein **T** is the Cauchy stress resultant (force per deformed length), **F** is the 2D deformation gradient tensor, **E** is the 2D Green strain tensor $\mathbf{E}=\frac{1}{2}(\mathbf{F}^T\mathbf{F}-\mathbf{I})$, and w is a

scalar strain-energy function (defined per unit undeformed surface area) that describes isothermal material behavior.

Experimental Procedures and Device. Enucleated human eyes were obtained from eye banks via overnight shipment in cold saline. In total, 12 eyes were tested: 6 from normal subjects aged 29 to 81 years old (67 ± 19, mean ± SD) and 6 from diabetic patients aged 44 to 77 years old (65 ± 13). The ages were not statistically different between healthy and diabetic as determined by a t-test ($p < 0.05$).

We used a custom bi-plane video based system to study the regional multiaxial mechanical properties of the lens capsule (Figure 5.1; Heistand et al. 2005). Briefly, enucleated eyes were secured in a moldable wax fixture, and the cornea and iris were removed to expose the anterior lens capsule. To investigate possible regional variations in capsular behavior, 23 fluorescent microspheres (40-micron diameter) were arranged on the exposed capsular surface in 7 overlapping sets of 5 that extended along two orthogonal axes from near the equator (labeled sets A and G) to their intersection at the pole (set D). The total arc length spanned by these 23 video tracking markers along either axis was about 4 mm from the pole. Based on images from Glasser and Campbell (1998) of the accommodative apparatus and geometric measurements compiled by Burd et al. (2002) for FEM modeling of the lens, this placement of markers appears to have avoided possible complexities due to the anterior-most zonular insertions and similarly the steep increases in curvature near the equator. In other words, local changes in curvature of the capsule within the regions defined by the markers should not introduce significant errors in our data analysis. Once all 23 markers adhered naturally to the

surface of the capsule, the specimen was placed in an acrylic chamber. Next, a 25 G needle, attached to a 1 cc syringe and a precision micromanipulator, was inserted at an angle just beneath the capsule, and into the lens, along the major axis opposite the side containing markers. The insertion site was sealed with a small amount of cyanoacrylate, and the specimen chamber was gently filled with a physiologic solution (Alcon BSS) and warmed to 37°C.

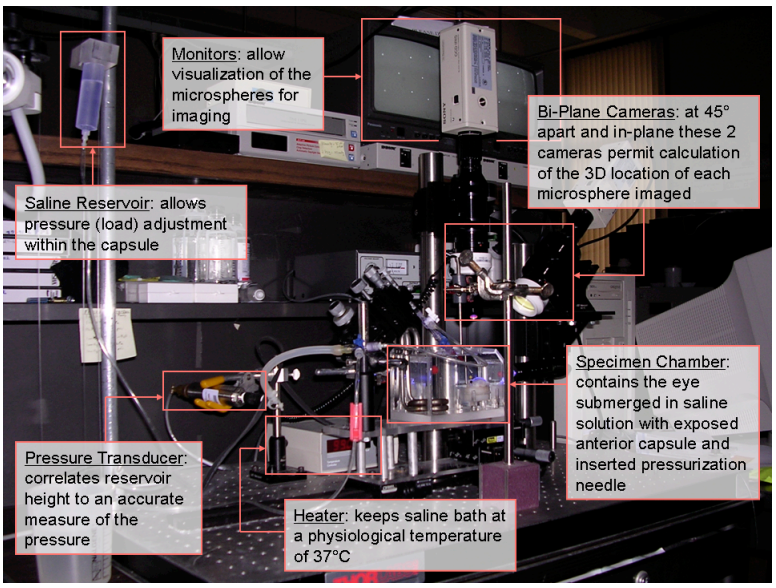

Figure 5.1. Image of the primary components of the experimental system. These include: a temperature-controlled specimen chamber, a distension system consisting of a needle, micromanipulator, and pressure transducer, and finally a bi-plane video system for tracking the motion of microspheres that are affixed to the surface of the capsule. One component that is not highlighted within the image is the 480 nm (blue) light that excites the microspheres, causing their fluorescence.

The anterior lens capsule was pressure-loaded via the inserted needle, which allowed injected BSS to separate the capsule from the lens (except at the equator were the capsule remained attached, as confirmed via histology (Heistand et al. 2005), and

thereby preserved natural boundary conditions); this permitted the capsule to be distended at various pressures in situ. The bi-plane video set-up allowed the 3D location of each marker to be determined from two captured 2D views, from which regional in-plane strains were calculated from the marker histories. Specifically, each individual set of five microspheres was divided into four sub-sets of three, and a local coordinate system was defined at the centroid of each of these triplets. This coordinate system was based on identified circumferential and meridional directions. Strains were computed relative to these directions by assuming a homogeneous deformation within each triplet (area typically ~0.25 mm squared) and the deformation gradient, **F**, was calculated via $\Delta\mathbf{x} \sim \mathbf{F} \cdot \Delta\mathbf{X}$ where $\Delta\mathbf{x}$ and ΔX denote finite but small distances between pairs of markers. Components of the Green strain were then computed from **F**. We emphasize that in contrast to the often used definition of strain (change in length per original length), which is only valid for infinitesimal strains and rotations, Green strain is exact for large strains and is properly insensitive to rigid body motions (Humphrey, 2002). Given our current optics and video resolution (~7 microns), our error in strain measurement was no more than 1%.

The specific experimental protocol involved three steps: preconditioning, testing, and determination of a suitable stress-free reference configuration. It is well known that the behavior of most soft tissues depends, in part, on the prior strain history. The process of isolating and handling a tissue prior to testing necessarily subjects it to non-physiologic strains that are often not reproducible from experiment to experiment. Thus, it is best to subject each specimen to the same well controlled strain history prior to data

collection (Fung, 1990). Toward this end, we subjected each specimen to five consecutive cycles of step changes in pressure, in 5 mmHg increments for 1-2 minutes each, from 0 to 35 to 0 mmHg. Comparison of pressure-strain results across these five cycles revealed a slight preconditioning, that is a softening, similar to that for most collagenous tissues. Moreover, pilot studies on multiple specimens revealed a steady state response over cycles 3 to 5, hence data were subsequently collected for cycles 1 and 5 only, with data from cycle 5 used for analysis. Finally, after the completion of pressure-strain testing, the anterior lens capsule was cut free (around the equator) from the posterior capsule to alleviate in situ stresses, while remaining on the anterior lens. This provided a natural stress-free reference configuration (i.e., 3D locations for the 23 tracking markers) for strain calculation.

Estimation of Material Parameters. We used a custom sub-domain inverse finite element method (Seshaiyer and Humphrey, 2003) to determine material properties of the distended capsules from measured pressures and 3D locations of markers arranged in sets of five. Numerical patch tests revealed that the method is robust as long as the associated state of strain is not exactly equibiaxial. Briefly, we prescribed the 3D locations of the outer four markers of each set of five as displacement boundary conditions and then minimized via nonlinear regression (Marquardt-Levenberg) the residual between numerically calculated (via a forward finite element solution) and experimentally measured positions of the central marker at multiple pressures. The forward portion of the algorithm is accomplished by balancing the energy stored in the material and the work done by the applied forces, i.e. the virtual work principle:

$$\int_{\Omega_o} \delta w dA = \int_{\Omega} P\mathbf{n} \cdot \delta\mathbf{x} da + \int_{\Sigma} \mathbf{T}^{(n)} \cdot \delta\mathbf{x} da \tag{5.2}$$

where P is the distending pressure, $\boldsymbol{n}$ an outward unit normal vector, $\delta\boldsymbol{x}$ a virtual displacement, Ωo the undeformed surface, Ω the deformed surface, and Σ a subset of the deformed surface subject to traction forces (the tractions $\mathbf{T}^{(n)}$ are zero for purposes of estimating parameters). We considered two forms of w, but for brevity we focus here on the Fung exponential model, which has been shown to describe well the behavior of diverse biomembranes such as mesentery, pericardium, pleura, saccular aneurysms and skin (Fung, 1990). It is,

$$w = c\left(e^{Q} - 1\right) \qquad Q = c_1 E_{11}^2 + c_2 E_{22}^2 + 2c_3 E_{11} E_{22} \tag{5.3}$$

where c, c_1, c_2, and c_3 are material parameters, and E_{11} and E_{22} are circumferential and meridional (i.e., principal, as revealed by the pressure-strain data) components of the Green strain tensor, respectively. Theoretical arguments restrict the possible values of the material parameters, namely $c>0$, $c_1>c_3$, $c_2>c_3$, $c_3>0$ (refer to David et al. 2007 for details).

Finite Element Stress Analysis. Albeit consistent with our sub-domain inverse finite element method, we used a more general, nonlinear finite element procedure to simulate the lens capsule under various loading conditions by enforcing the virtual work principle (equation 5.3) for each element of the domain. We used quadrilateral elements with isoparametric shape functions and a 2-point Gaussian quadrature. Assuming axisymmetry, we modeled the quarter-surface in the first quadrant. The boundaries along the *yz* and *xz* planes were kept in-plane by enforcing rolling boundary conditions and the *xy* plane (i.e., equator) was similarly subjected to a rolling boundary condition.

Comparative models with a fixed boundary equator showed that the two boundary conditions did not yield noticeable differences in stresses and strains away from the equator (closer to the pole). Along the edge of a CCC, when present, we enforced a traction-free boundary condition, thus $\mathbf{T}^{(n)}=0$. As shown in David and Humphrey (2007), increasing the mesh density showed a nearly quadratic convergence; the mesh size (~210 elements) used in this paper provided reasonable estimates of the regional stresses and strains.

Results

Pressure-Strain Behavior. Results for both normal and diabetic human eyes showed that, similar to porcine eyes (Heistand et al. 2005), the anterior lens capsule exhibits a nonlinear pseudoelastic behavior over finite strains (typical of most soft tissues) with negligible hysteresis between the loading and unloading curves (data not shown); this justifies the assumption of a hyperelastic response and, thus, use of a strain-energy function, w, for quantification. The shear strain relative to the circumferential and meridional directions was nearly zero in all regions, thus implying that these are principal directions. Moreover, the circumferential and meridional strains were nearly equibiaxial at the pole, but became increasingly non-equibiaxial toward the equator with meridional strain greater than circumferential (Figure 5.2 – compare panels *a* and *b*). Although both the normal and diabetic lens capsules exhibited these general characteristic behaviors, the latter was significantly stiffer at each pressure state in both the circumferential and meridional directions (i.e., the material symmetries were

maintained, but the stiffness differed - Figure 5.2). The pre-strain (i.e., difference between the stress-free and in situ unloaded configurations) in the anterior capsule was approximately 3% (data not shown), though this value may vary slightly depending on the degree of post-mortem accommodation for a given lens. Figure 5.2 is plotted with respect to the in situ unloaded configuration due to the sensitivity of the statistical comparisons and the small degree of error associated with obtaining the stress-free configuration.

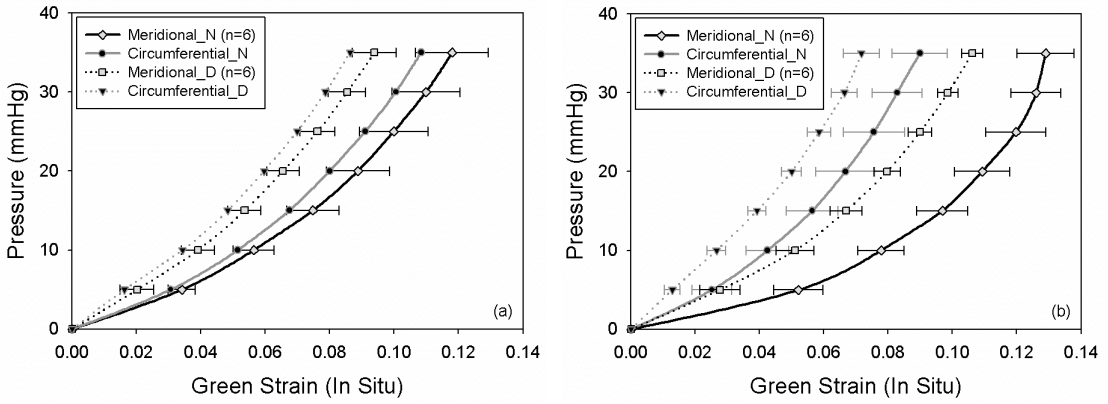

Figure 5.2. Comparison of diabetic (mean age 65 years) and non-diabetic (67 years) anterior lens capsule behavior. Plots show pressure versus Green strain data, with respect to the in situ unloaded configuration, averaged from six experiments each in the meridional and circumferential directions at both **(a)** set D (centered at the pole) and **(b)** set F (near the equator). Although hard to see, meridional and circumferential diabetic strains at each pressure state are statistically less (ANOVA, $p < 0.05$) than non-diabetic strains in both directions for both sets D and F (note: circumferential error bars were removed from (a) for clarity). Material symmetries are also shown to be maintained in the diabetic lens capsules. Error bars represent ± standard error.

Material Properties. Best-fit values of the four material parameters revealed that the anterior lens capsule exhibited a regionally varying anisotropy (Figure 5.3). In particular, whereas the value of the overall stiffness parameter, c (N/m), did not vary

statistically from region-to-region (ANOVA, $p<0.05$), the ratio c_1/c_2, which reflects the ratio of circumferential to meridional stiffness, varied nonlinearly from the innermost to the outermost regions. In other words, the anterior lens capsule was nearly isotropic at the pole, but increasingly stiffer circumferentially towards the equator. This finding was consistent for both the normal and diabetic capsules (not shown).

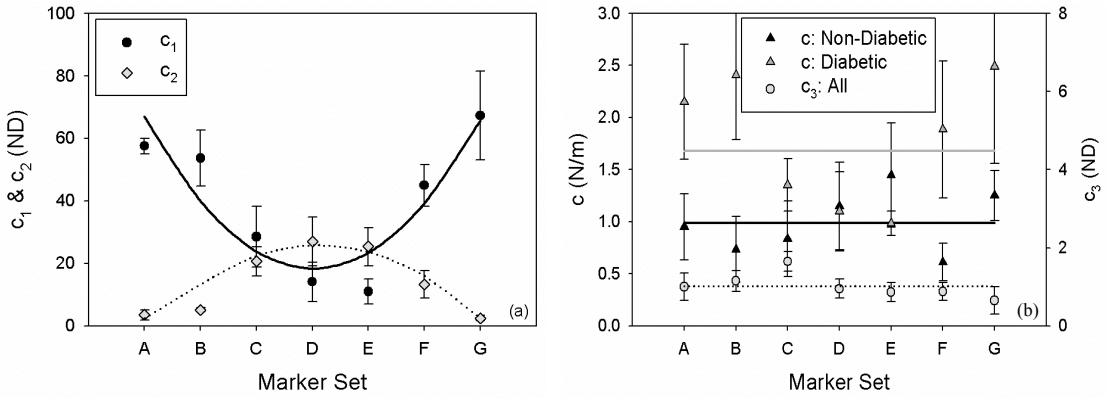

Figure 5.3. Material parameter values averaged with respect to marker set over seven experiments. These parameters include the overall stiffness parameter, c, circumferential stiffness, c_1, meridional stiffness, c_2, and c_3. Notice that as one moves radially from the pole (set D) towards the equator (sets A and G) **(a)** c_1 (solid) and c_2 (empty/dotted) increase and decrease, respectively (as clearly shown by their best-fit curves), with their ratio being nearly unity around the pole (indicating isotropy) but increasing nonlinearly proximal to the equator (indicating a regionally dependent anisotropy with the circumferential direction being preferred) and **(b)** c (solid) and c_3 (empty/dotted) are nearly constant as indicated by their non-statistical deviation from their set-based mean line (except for set C). Error bars represent ± standard error.

Stress Analysis. Pressure-loading of the lens capsule was simulated by endowing a flat (stress-free) quarter circle with the calculated material parameters and inflating to a "native" pressure of about 5 mmHg (determined experimentally – Figure 5.4).

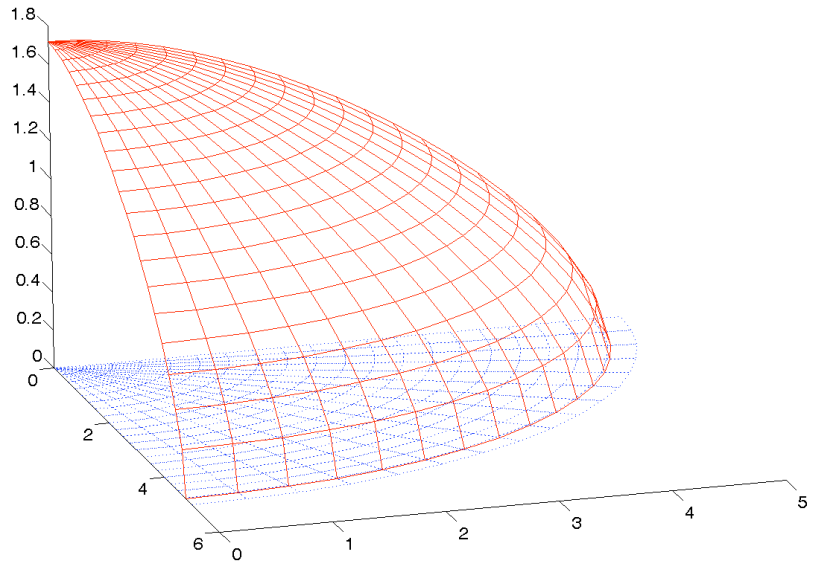

Figure 5.4. Schematic of our forward FEA. Plot shows elements and nodal positions of the computational lens capsule in a stress-free (flat) configuration and distended to a physiologically relevant pressure of 5 mmHg (approximate pressure that the lens exerts on the capsule).

Accounting for the measured nonlinear, regionally anisotropic material behavior and reported regional variations in thickness (ranging from 12 μm at the pole to 22 μm at the mid-periphery of 55 year old human anterior lens capsules; Fisher and Pettet, 1972) resulted in a predicted native stress field that was nearly uniform and equibiaxial except near the equator (Figure 5.5) where results are dominated by boundary conditions that are not well known. In particular, the biaxial stresses were on the order of 0.04 MPa. A CCC was also modeled within the assumption of hyperelasticity, thus we introduced the hole in the nearly flat quarter circle prior to inflation (i.e., modeling the effect of the lens). This resulted in a marked increase in the circumferential stress and a marked decrease in the meridional stress, especially near the edge of the CCC (Figure 5.5). In

particular, the meridional stress was zero at the edge of the CCC as required by the traction-free boundary condition.

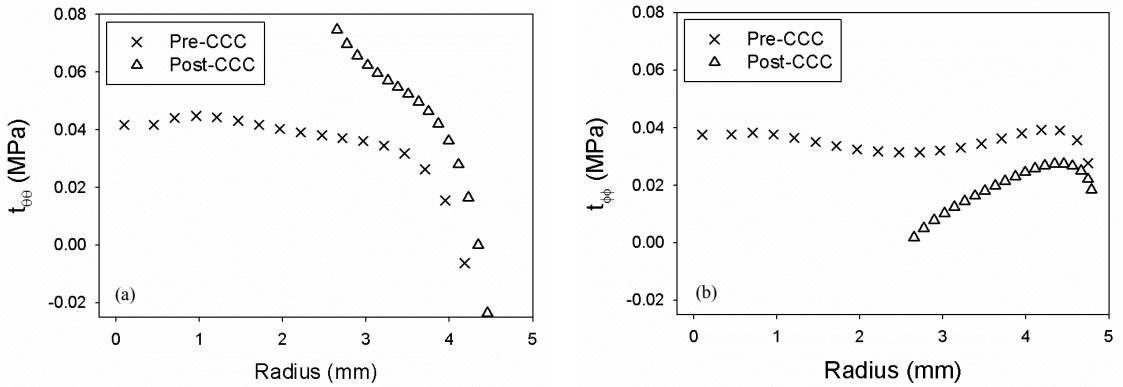

Figure 5.5. Predicted stress distribution in both the **(a)** circumferential and **(b)** meridional directions before and after computationally introducing a CCC of radius 2.5 mm into our forward FEM model of the human anterior lens capsule. Notice that the stresses are largest at the edge of the CCC and taper off radially towards the equator. This result showing that a CCC imparts large gradients into the lens capsule is qualitatively similar to that expected based on changes in strain induced in our prior CCC experiments (not shown).

Discussion

Analytical and computational biomechanical modeling of the lens has primarily been used to quantify the tractions involved during accommodation and to examine contributions of individual constituents. For example, early modeling of the accommodative apparatus employed simplified 2D geometries and constituent properties to determine those tractions that ensure mechanical equilibrium in the accommodated and disaccommodated states (e.g., Koretz and Handleman, 1982; Wyatt, 1988). More recently, finite element methods have been used to predict motions of the lens (e.g., altered anterior/posterior curvature and polar displacement) and corresponding

alterations in optical power (Schachar and Bax, 2001; Burd et al. 2002). All such models have assumed the lens nucleus, cortex, and capsule to be isotropic, homogeneous, and linearly elastic with material parameter values determined by Fisher (1969) or Krag and colleagues (Krag et al. 1997b; Krag and Andreassen, 2003a, 2003b).

Fisher (1969) isolated (including epithelial denudation) and clamped the capsule at its periphery between two glass chambers filled with saline. Pressurizing the lower chamber distended the capsule and associated deformations were calculated based on volume changes of saline in the upper chamber; hence, despite imposing biaxial loads within the capsule, only 1D (pressure-volume) data averaged over all regions and directions was obtained. Further, despite a demonstrated nonlinear material behavior over finite strains, the upper part of the exponential-like curve was modeled using a result from linear elasticity. His data (N=30; ages: 1-80 years) showed a decrease in both elastic modulus (6.0 to 2.0 MPa) and ultimate stress (2.3 to 0.7 MPa) of the anterior capsule with age. In contrast, Krag and colleagues (Krag and Andreassen 1996; Krag et al. 1997a, 1997b; Krag and Andreassen, 2003a, 2003b) studied the mechanical behavior of intact circumferential rings of human lens capsule in uniaxial tension (N=92; ages: 1-98 years); these annular specimens were approximately 100 μm wide and excised from the mid-region of both the anterior and posterior capsule. Similar to Fisher, they showed a nonlinear elastic behavior over finite strains, but approximated the data as bilinear rather than ignoring the first region of the curve. Their results for the anterior lens capsule in the "low modulus" region of the stress-strain curve (0-10% strain), which may have more physiological and clinical relevance, demonstrated an increase in elastic

modulus with age (0.4 to 1.5 MPa) whereas the "high modulus" region (based on ultimate strain) showed a linear decrease with age (~33 to 5 MPa). This latter result agrees qualitatively with findings of Fisher, as did the reported decrease in ultimate stress of the anterior capsule with age (17.5 to 1.5 MPa). Moreover, Krag and colleagues found the stress-strain behavior to be similar for the anterior and posterior capsules throughout life and that there was no significant difference between the left and right eye from the same donor. These are important findings. Finally, Bailey et al. (1993) similarly reported uniaxial stress-strain data as a function of the degree of glycosylation cross-links formed by incubating porcine lens capsules in a 133 mM glucose solution. As expected, the lens capsule became progressively stiffer and less extensible with increasing cross-links, which likely reflects that which occurs in diabetes and aging. Overall, these many studies provide important qualitative insight into some characteristics of the mechanical behavior of the lens capsule. Nonetheless, assumptions of isotropy and (implicitly) regional homogeneity, the use of 1D testing, and quantification using a linearized framework are not sufficient for quantifying fully the regionally varying, anisotropic, nonlinear, multiaxial behaviors that exist in vivo.

Similar to the aforementioned findings, our biaxial results also revealed a nonlinear behavior over finite strains and a stiffening effect due to diabetes. In addition, however, both the pressure-strain curves and the sub-domain parameter estimation suggested that the circumferential direction is increasingly stiffer than the meridional direction as one moves closer to the equator. Although there are no results to which these can be compared, we found a similar regional anisotropy in porcine anterior lens

capsules (David et al. 2007). Moreover, in an extensive parametric study using finite elements, Ryan and Humphrey (1999) showed that regional variations in anisotropy can help homogenize the stress field in otherwise complex saccular aneurysms. Specifically, it was found that for aneurysms having a small neck to height ratio, an increasing meridional stiffness towards the base tends to homogenize the stresses, whereas for a large neck to height ratio, an increasing circumferential stiffness towards the base tends to homogenize the stresses. These results were deemed reasonable teleologically for such variations would allow the lesion to grow toward a spherical shape, which is optimal for resisting a distension pressure, and would facilitate a stable growth; most intracranial aneurysms are stable, thus supporting this idea. Interestingly, the shape of the anterior lens capsule is comparable to a large neck to height ratio, thus the present findings are qualitatively consistent with prior finite element predictions for a very different collagenous biomembrane. Finally, we emphasize that the ratio of material parameters considered herein is defined point-wise, thus known regional variations in thickness of the capsule cannot explain our results on regional variations in anisotropy.

Comparison of the material parameters for capsules obtained from diabetic versus non-diabetic donors illustrated similar values for the ratio c_1/c_2, indicating that the regional anisotropy is maintained in the presence of glucose cross-links, but comparison of the overall stiffness parameter, c, revealed the diabetic-derived capsules to be statistically stiffer than the non-diabetic (ANOVA, $p<0.09$). This finding suggests that of the 4 material parameters in our model that describe the mechanical behavior of the lens capsule, the overall stiffness parameter, c, governs inter-capsular differences (further

comparisons of porcine versus human and porcine cultured in high glucose versus control media corroborated this finding; Pedrigi et al. 2007b). This finding may be useful in future experiments where biaxial testing of the lens capsule is not an option (e.g., capsules following cataract surgery), and uniaxial mechanical data will need to be related to biaxial data, which is feasible if only 1 parameter, c, is needed.

Direct quantitative comparisons of our results to those in the literature are limited by differences in both the testing (i.e., uniaxial vs. biaxial) and data analysis (i.e., linear vs. nonlinear elasticity). Nonetheless, our results are general enough to be used in additional analytical simulations of previous mechanical tests. Because we only tested to 20% biaxial strains, not to failure, it was best to compare such simulations to data of Krag and Andreassen (2003a) for 'low-modulus' behavior (10% uniaxial strain), which is within the strain range of accommodative function. Note, therefore, that Krag used 1st Piola-Kirchhoff stress (force per original area) rather than Cauchy stress (force per current area) and linearized strain, thus we converted our results accordingly. Moreover, their samples were taken from the mid-location of the capsule, thus we based our simulations on results from the appropriate region of the capsule. For non-diabetic capsules at 10% strain, we predict a 1st Piola-Kirchhoff stress of 0.28 MPa, which compared favorably to approximately 0.20 MPa reported by Krag. This slight discrepancy may reflect a stiffer behavior that is intrinsic to biaxial versus uniaxial loading. Alternatively, there is some subjectivity in identifying an appropriate stress-free configuration in excised tissues, which could have affected Krag's findings, particularly in the 'low-modulus' region. Another difference between our experiments and prior

studies is that we did not remove the epithelium prior to testing (although Krag et al. (1997b) did not explicitly comment on its removal in human studies, it was removed in an earlier study of the porcine capsule – see Krag and Andreassen, 1996). It seems unlikely, however, that a monolayer of native lens epithelial cells, which are non-contractile and of a symmetric cobblestone morphology, could have influenced greatly the regionally varying mechanical behavior found in our studies, but this is an open issue.

Our finite element calculations appear to be the first to include the relevant (geometric and material) nonlinearities and regional anisotropy. As noted above, we found that the normal distribution of biaxial stress was nearly uniform and equibiaxial, except near the equator. This predicted "boundary layer" effect should not be over-interpreted, however, for there is a pressing need for more experimental data on the tractions in the equatorial region. Rather, we should focus on far field stresses and strains, which are relatively insensitive to the boundary conditions and most relevant to the optical axis. We suggest that this "preferred" or "homeostatic" state of stress is teleologically reasonable based on findings for other tissues and that mechano-transduction mechanisms could be engaged if stress is perturbed from the preferred values (Humphrey, 2002). Clearly, cataract surgery will significantly perturb the stress field in the capsule. In particular, a remaining capsulorhexis ensures that the stress field cannot return to uniform and equibiaxial because the traction-free condition at the edge requires the meridional stress to remain zero there (cf. Figure 5.5, noting that subsequent removal of the lens will likely reduce stresses to near zero everywhere). Indeed, studies

by Hayashi et al. (2002) and Tehrani et al. (2003) suggest that contraction of the capsule by remnant LECs around an IOL likely creates a non-equibiaxial stress field due to the permanent capsulorhexis. We suggest that this persistent non-equibiaxial stress field may be a long-term stimulus that causes continued errant behavior by LECs well after cataract surgery. Whereas our current FEM model can only provide estimates for the altered mechanical environment experienced acutely by LECs due to cataract surgery, future studies should account for associated growth and remodeling of the lens capsule in response to this initial (and continuing) insult. Indeed, such studies will be needed to design future prosthetic IOLs that allow accommodation (see Haefliger et al. 1987; Sakka et al. 1996; Norrby et al. 2006). Interestingly, studies that have successfully allowed accommodation in an animal model through an injectable artificial lens seem to be continually plagued by a rapid and severe onset of PCO, possibly because this non-equibiaxial stress field is maintained by the capsulorhexis. A nominal example of this is summarized in the remarks concluding several years of research on these IOLs by Nishi and Nishi (1998), who simply stated that "prevention of this opacification (PCO) is an essential issue to be solved in lens refilling."

In summary, this paper represents a logical and necessary extension of prior work – uniaxial tests that revealed characteristic material properties and linearized finite element analyses that estimated stresses. Our biaxial mechanical testing methods and material model allow more natural predictions of in vivo capsular behavior; nonetheless, it is but another step toward our ultimate goal of understanding fully the biomechanics and mechanobiology of the lens capsule. Future experiments and computations should

focus on the evolution of properties and stress/strain as the LECs may respond to disease processes or clinical interventions by trying to recover a tensional homeostasis and normal cell function.

CHAPTER VI

REDISTRIBUTION OF STRAIN AND CURVATURE IN THE PORCINE ANTERIOR LENS CAPSULE FOLLOWING A CONTINUOUS CIRCULAR CAPSULORHEXIS*

Overview

Cataract surgery is the most commonly performed surgical procedure in the U.S. Basically, it consists of three parts: introduction of a hole into the lens capsule, removal of the clouded lens through this access hole, and insertion of an artificial lens. We hypothesize that errant behavior by the residual epithelial cells of the lens capsule following surgery are due, in part, to surgically-induced changes of the native stress and strain fields in the lens capsule. Because the capsular bag can be regarded mechanically as a membrane, here we study changes in curvature and strains due to the most common means of introducing the initial access hole: a continuous circular capsulorhexis (CCC). We show that a modest sized CCC increases circumferential strains and decreases meridional strains by up to ~20% and that curvatures change by up to ~13%, particularly near the edge of the CCC. We submit that such changes induce mechanobiological responses that are responsible, in part, for some of the long-term complications following cataract surgery.

---

*This article was published in Journal of Biomechanics, Vol. 39, M.R. Heistand, R.M. Pedrigi, J. Dziezyc, and J.D. Humphrey, Redistribution of strain and curvature in the porcine anterior capsule following a continuous circular capsulorhexis, pp. 1537-1542, Copyright Elsevier, 2005.

Introduction

At about 1.3 million procedures per year, cataract surgery is the most common surgical procedure in the United States. Unfortunately, a significant complication of this otherwise very successful procedure is posterior capsule opacification (PCO), which has occurred in up to 50% of all patients within 3-5 years following surgery (Spalton, 1999). PCO results from epithelial cells migrating from the bow region of the lens capsule to the central region of the posterior lens capsule, where they transdifferentiate, proliferate, synthesize matrix proteins, or contract as in a wound healing response (Marcantonio and Vrensen, 1999; Wormstone et al. 2002). Specifically, the epithelial cells tend to become more like myofibroblasts, having significant α-actin. Moreover, these cells primarily produce type IV collagen and laminin before cataract surgery but produce types I, III, V, and VI collagen, matrix metalloproteinase-2 (MMP-2) and MMP-9, tissue inhibitors of metalloproteinases (TIMPs), and osteopontin after surgery (Saika et al. 2003a). Finally, in addition to the increased proliferation, which may be stimulated by the cytokine TGF-β, there is an increased apoptosis. Each of these aspects of the cell biology of PCO corresponds, therefore, to either a typical wound healing response or a growth and remodeling response due to a mechano-stimulus. Indeed, Ohata et al. (2001) show that lens epithelial cells are mechanosensitive, that is, they belong to the family of cells known as mechanocytes.

We hypothesized in 2000 that PCO following cataract surgery results, in part, from mechanotransduction mechanisms causing the epithelial cells to transition from their normal to errant behavior. That is, we suggested that surgery causes regional

changes in stress or strain from normal values and thereby stimulates the epithelial cells to alter their gene expression and induce PCO. To investigate this hypothesis, we must know how the various aspects of cataract surgery perturb the stress and strain fields from normalcy.

There are typically three basic steps in cataract surgery. The first step is a partial anterior capsulotomy, whereby a portion of the anterior lens capsule is removed so that the clouded lens can be accessed. The second step entails a process called phacoemulsification, in which ultrasound is used to break the clouded lens into pieces, which are then aspirated through the hole in the lens capsule. The third step involves the skillful insertion of a synthetic, prosthetic device into the capsular bag to restore focus and thus sight. All three of these steps require extensive manipulation of the lens capsule, which in turn alters the native stress and strain fields. Of these three steps, our focus here is the redistribution of strain and changes in curvature due to a continuous circular capsulorhexis (CCC).

A CCC is the most common technique for gaining access to the lens, in which a circular tear is made via a continuous circumferential tearing of the lens capsule. This method is preferred because it provides a strong circular edge, resistant to radial tearing during insertion of the IOL. In addition, this technique allows for the creation of a hole with a diameter smaller than the prosthetic lens optic, which has been shown by Hollick et al. (1999) to decrease the occurrence of PCO.

Because the lens capsule is thin-walled with a large radius of curvature, it may be treated mechanically as a membrane, which in turn implies that curvatures influence

greatly the local stress field. In this paper, we report measurements of the changes in in-plane finite strain and curvature in the anterior lens capsule of porcine eyes following a continuous circular capsulorhexis performed by an experienced veterinary ophthalmologist.

Methods

Experimental Methods. Our basic test system, experimental procedures, and methods for strain analysis are similar to those discussed in Heistand et al. (2004). Briefly, we mount fresh, enucleated eyes in a moldable wax fixture, remove the cornea and iris, and then affix numerous closely placed, 40μm diameter fluorescent microspheres (markers) to the surface of the anterior lens capsule. After immersing the eye in a physiologic solution (Alcon BSS®) and warming it to 35°C, we then use blue light to excite the markers and a bi-plane video system (current resolution of ~7 μm) to monitor their 3-D positions both before and after creating the CCC.

Strain Calculation. Global reconstruction techniques can be used with the biplane video system to determine the 3-D position of the centroid of each marker as detailed in Heistand et al. (2004). Thereafter, a Delaunay triangularization technique (Matlab) was used to construct an array of lines connecting marker centroids, thus forming a mesh of triangles over the entire field of markers, with nodes at each marker centroid. The triangles are of similar size and shape, appropriate for calculating regional, in-plane components of the Green strain.

Briefly, the Green strain, **E**, which is exact for finite strains and independent of rigid body motions, is computed locally for each triplet via the deformation gradient, **F,** namely $\mathbf{E} = \frac{1}{2}(\mathbf{F}^T\mathbf{F}-\mathbf{I})$. The deformation gradient can be calculated directly for each marker triplet by finding how position vectors before the CCC (denoted by $\Delta\mathbf{X}$ and connecting vertices of the triplets) deform to position vectors after the CCC (denoted by $\Delta\mathbf{x}$). Because the marker triplets are close together and assuming no severe gradients in strain, we can assume a homogeneous deformation within each triangular region; thus, $\Delta\mathbf{x} \approx \mathbf{F}(\Delta\mathbf{X})$, which can easily be solved using matrix methods (Humphrey, 2002). The directional components of in-plane strain for each marker triplet are labeled as meridional and circumferential, where the origin of the localized strain region is prescribed to be at the centroid of each triplet. These components are tangent to the lens capsule at each centroid and perpendicular, with the meridional direction always pointing to the anterior pole of the lens capsule, which is defined anatomically by the Y-suture (Figure 6.1).

Finally, it is important to note that strains reported herein refer to the in situ, unloaded reference configuration, not a stress-free reference configuration. As shown in Heistand et al. (2005), the normal lens capsule is under a pre-strain of roughly 8% in the meridional direction and 13% in the circumferential direction. Herein, however, we compute only changes in strain from the native values; we do not compute the actual values of strain.

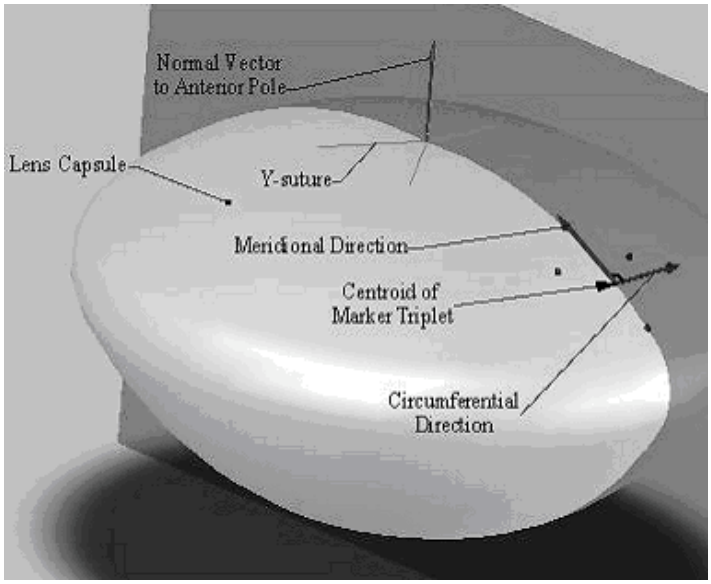

Figure 6.1. Schema of the lens capsule showing the directions for the different components of strain, which originate at the centroid of each marker triplet.

Curvature Calculation. Curvature is a measure of how an outward unit normal vector changes its orientation along a prescribed arc length. The curvatures of the anterior lens capsule can be calculated easily given a parameterized representation of its surface. As a first approach, we parameterized the surface by exploiting the suggestion that the anterior lens capsule is a hemi-ellipsoid (Fisher, 1969) and modeled it this way using the overall lens capsule geometry. We then refined our approach by finding the weighted, least-squares, best-fit parameters for an ellipsoid by minimizing the difference between measured and modeled surface positions. An ellipsoid can be defined parametrically by

$$\begin{bmatrix} x \\ y \\ z \end{bmatrix} = [\boldsymbol{R}_1][\boldsymbol{R}_2][\boldsymbol{R}_3] \begin{bmatrix} r_x \cos u \cos v \\ r_y \sin u \cos v \\ r_z \sin v \end{bmatrix} + \begin{bmatrix} x_c \\ y_c \\ z_c \end{bmatrix}, \tag{6.1}$$

where $-\pi \le u < \pi$ and $-\pi/2 \le v < \pi/2$ are auxiliary scalar parameters; $[x_c, y_c, z_c]^T$ are coordinates for the origin of the ellipsoid; r_x, r_y, and r_z are radii of the axes of the ellipsoid; and $[\mathbf{R}_1]$, $[\mathbf{R}_2]$, and $[\mathbf{R}_3]$ are plane rotation matrices given by

$$[\boldsymbol{R}_1]=\begin{bmatrix}\cos\theta_1 & \sin\theta_1 & 0\\ -\sin\theta_1 & \cos\theta_1 & 0\\ 0 & 0 & 0\end{bmatrix},\quad [\boldsymbol{R}_1]=\begin{bmatrix}\cos\theta_2 & 0 & \sin\theta_2\\ 0 & 1 & 0\\ -\sin\theta_2 & 0 & \cos\theta_2\end{bmatrix},\quad [\boldsymbol{R}_3]=\begin{bmatrix}1 & 0 & 0\\ 0 & \cos\theta_3 & \sin\theta_3\\ 0 & -\sin\theta_3 & \cos\theta_3\end{bmatrix}. \quad (6.2)$$

We seek to minimize the geometric distances between measured marker positions and the model ellipsoid, where the geometric distance is defined as the distance between a marker and its closest point on the ellipsoid (Gander, 1994). We can solve this optimization problem by finding values for the parameter set **s** that minimizes the quadratic function

$$Q = \sum_{i=1}^{m}\left[(x_i - x(u_i,v_i))^2 + (y_i - y(u_i,v_i))^2 + (z_i - z(u_i,v_i))^2\right] \quad (6.3)$$

for all markers ($i = 1 \ldots m$) where the coordinates of the ith marker are x_i, y_i, z_i, and the parameter set is $\mathbf{s} = \left[u_i \ldots u_m, v_i \ldots v_m, r_x, r_y, r_z, x_c, y_c, z_c, \theta_1, \theta_2, \theta_3\right]^T$. This is a non-linear problem, which must be solved iteratively, as, for example, using the Marquardt-Levenberg method.

Two difficulties arise in this approach. First, it is difficult to generate initial estimates of the parameter set **s**. This complication can be overcome, however, by first solving a simpler problem in which we develop a linear least squares solution to the algebraic representation of an ellipsoid. Although this solution does not provide the best geometrical fit to the data, it does provide good initial parameter estimates, $\hat{\mathbf{s}}$, of the parameter set **s**. The second complexity occurs because the geometry of the anterior lens

capsule closely resembles that of an oblate spheroid, in which the major and semi-major axes have nearly the same dimension. This can lead to numerical difficulties that often arise when fitting an ellipsoid to near-spherical data. Thus, we will use the technique developed by Turner et al. (1999) to avoid this problem; they derived an alternative parameterization for a best-fitting ellipsoid (in a geometrical, least-squares sense), and iteratively solved for the new parameter set **s*** using a nonlinear least squares method. Once the parameters of the equation for the ellipsoid are known, appropriate derivatives can be used to calculate the curvatures in different directions at various points on the ellipsoid. We are most interested in curvatures along parameterized lines on the surface of the ellipsoid that represent the major half-axis ($u = 0$) and the minor half-axis ($u = \pi/2$) of the anterior lens capsule (assumed to reside in the transverse and sagittal planes, respectively).

Presently, we simplified the ellipsoidal calculations by assuming certain symmetry conditions and geometry constraints. For instance, the major and minor axes of the lens capsule are nearly aligned with x and y axes of a laboratory coordinate system, respectively. Thus, the ellipsoid is assumed to have negligible rotation about any axis. Ultimately, we can calculate curvature in the x and y directions (major and minor axes of the lens capsule) from

$$\kappa_x = \frac{\dfrac{d^2z}{dx^2}}{\left(1+\left(\dfrac{dz}{dx}\right)^2\right)^{3/2}} \quad \text{and} \quad \kappa_y = \frac{\dfrac{d^2z}{dy^2}}{\left(1+\left(\dfrac{dz}{dy}\right)^2\right)^{3/2}}, \tag{6.4}$$

using a simplified ellipsoid or ellipsoid-like equation of the form $z = f(x,y)$.

Results

Figure 6.2 is a picture of the anterior surface of a lens capsule immediately following a continuous circular capsulorhexis, with a diameter of 5 mm, centered at the Y-suture of the lens. Although only partially visible in normal lighting, the 40-μm diameter fluorescent microspheres can be seen as the small white dots in the upper-right quadrant. Figure 6.3 is a digital image from the biplane video system, showing a smaller portion of the marker field remaining after the CCC; the microspheres have been excited with blue light.

Figure 6.4 shows changes in the meridional and circumferential strain fields from normalcy in a quadrant of the anterior lens capsule resulting from a CCC, approximately 5 mm in diameter; results were similar for all five specimens tested. For visual purposes, the strain fields were each plotted on an ellipsoid surface that represents the overall dimensions (in millimeters) of a typical, porcine anterior lens capsule. The *x*-direction is oriented along the transverse plane while the *y*-direction is oriented along the sagittal plane. The strain range is chosen between limits set by the minimum meridional strain and the maximum circumferential strain calculated for that particular specimen. It is evident that a high degree of strain redistribution occurs as a result of the CCC. We found that strain increases up to 20% in the circumferential direction and decreases nearly 20% in the meridional direction. Furthermore, the magnitude of the change in strain was always greater near the edge of the CCC and almost zero near the equator as expected. Both directional components of strain also appear slightly greater along the transverse plane than the sagittal plane.

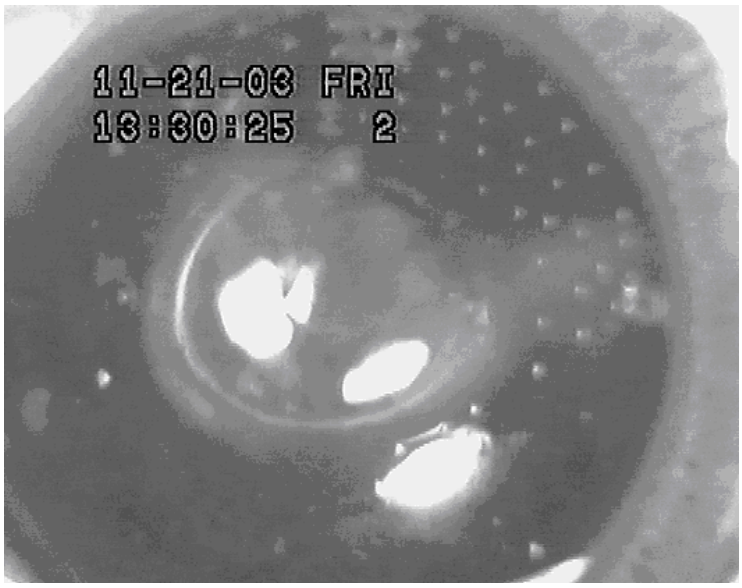

Figure 6.2. Anterior lens capsule with field of markers in top-right quadrant immediately after surgical introduction of CCC with 5 mm diameter. Note that this picture was imaged with a separate video system and VCR, not the experimental biplane video system, which provides better resolution and more contrast.

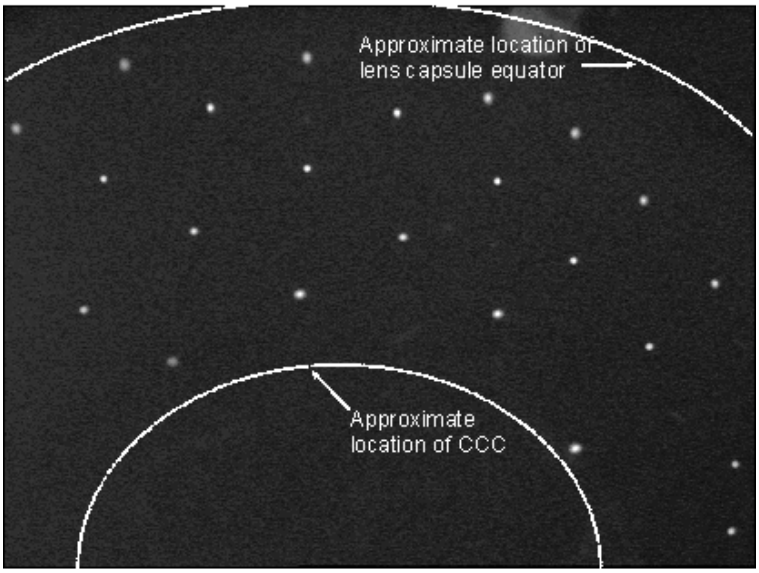

Figure 6.3. Section of anterior lens capsule imaged with the experimental biplane video system. Shown is a portion of marker field remaining after a CCC.

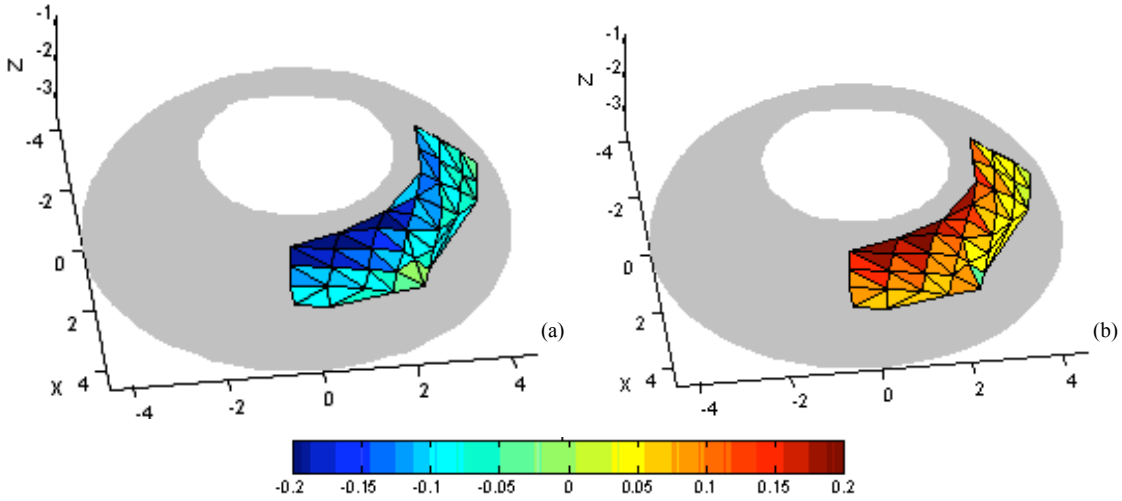

Figure 6.4. Changes in strain field from normalcy in quadrant of anterior lens capsule after introduction of CCC with 5 mm diameter (Number of nodes: 39, Number of elements: 59). **(a)** Strain redistribution in meridional direction. **(b)** Strain redistribution in circumferential direction.

Figure 6.5 is a plot of an ellipsoid-like surface fit to the coordinates of markers on the anterior surface of the lens capsule before the CCC; the equation of the quadric is shown along with associated parameter values. Unfortunately, the parameters have no physical meaning, and the equation is not written in parametric form. Nevertheless, we can still calculate curvature analytically, along the x and y directions, using the equations for κ_x and κ_y shown in the curvature calculation section. Figure 6.6 is a plot of the radius of curvature in the x and y direction of the quadric, which is an approximation of curvature in the major and minor axes of the anterior lens capsule, both before and after a 5 mm diameter CCC. The abscissa represents the distance along the meridional direction from the anterior pole to the equator.

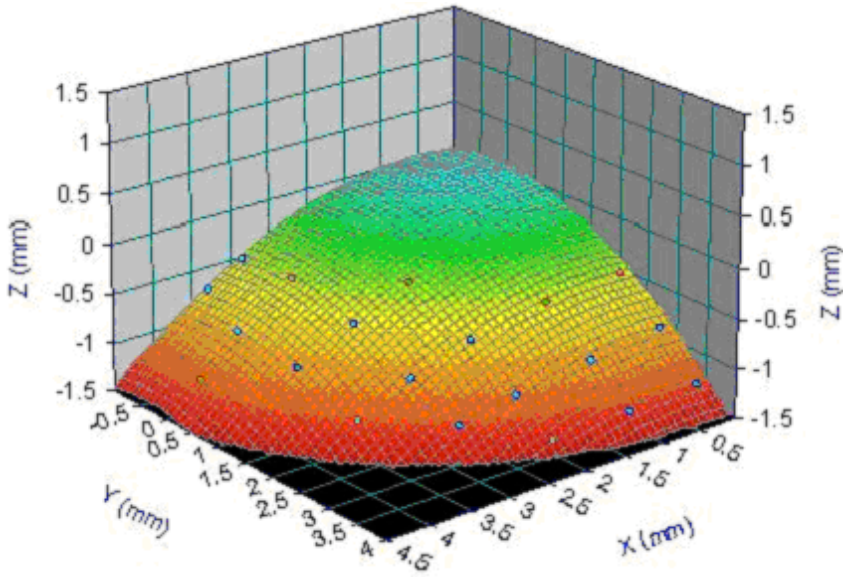

Figure 6.5. Plot showing section of an ellipsoid-like fit to marker coordinates before CCC. The quadric is represented by an equation of the form $z = a + bx + cy + dx^2 + ey^2 + fxy$, with parameters a = .0548, b = .0930, c = .0411, d = -.0939, e = -.0936, and f = -.0081, providing a surface-fit with a DF Adj r^2 = .9977.

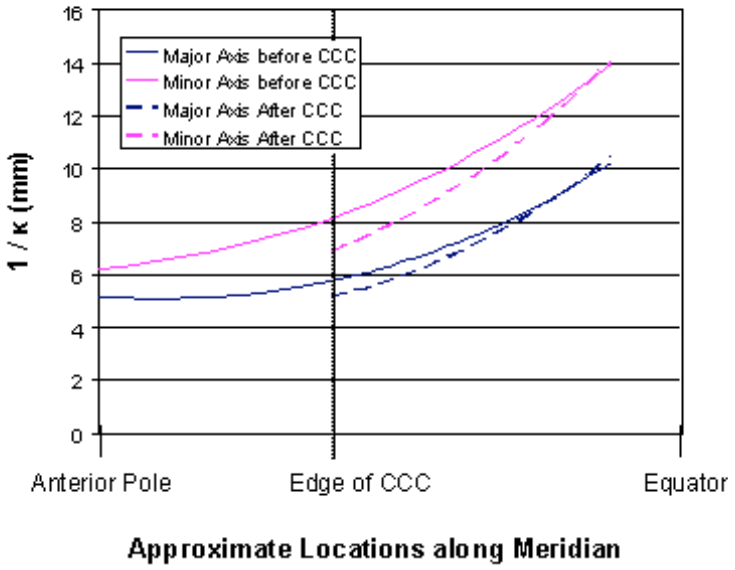

Figure 6.6. Estimates of the curvature along the major and minor axes of the anterior lens capsule, both before and after the CCC.

Discussion

The normal lens capsule consists primarily of type IV collagen, with admixed adhesion molecules and proteoglycans, woven in a fine 3-D network structure having polygonal-shaped interstices ~20 nm in diameter (Barnard et al. 1992). Given the thin-wall (on the order of 60 μm for the porcine anterior lens capsule) and large radius of curvature (~7 mm), these observations justify the use of a membrane assumption within a framework of continuum mechanics. It is well known in mechanics that introducing a hole in a material under load usually results in highly non-uniform stress and strain fields, including marked stress concentrations at the edge of the hole. Recently, however, we showed that the degree of material anisotropy (e.g., a circumferentially versus radially stiffer behavior) can dramatically affect the stress and strain distributions around a hole in a flat, pre-stressed, nonlinear membrane subjected to finite strains (David and Humphrey, 2004). Given the lack of a similar solution for a distended ellipsoidal membrane, there was a need for experimental measurements of the changes in finite strain and curvatures in the lens capsule following a CCC.

As expected, we found considerable redistribution of strain from the CCC in all specimens. These results seem reasonable from a mechanics point of view, as evident from the relatively smooth strain gradients and decreasing magnitude of strain from the edge of the CCC to the equator. Moreover, negative strains in the meridional direction (consistent with a retraction) and positive strains in the circumferential direction (consistent with expansion) are both consistent with the concept of pre-strain in the lens

capsule (i.e., the lens capsule is stretched in its in-situ state, thus the introduction of a tear or cut will cause retraction of the capsule).

It also appears that the CCC causes slight changes in curvature; this is expected in part because the CCC creates a traction-free boundary condition at the edge of the tear. More importantly, however, this suggests that the CCC allows the lens to change shape, perhaps tending to bulge-out near the CCC. Regardless, curvature should change most notably at the edge and should remain nearly the same close to the equator (as evident in Figure 6.6). Note, too, that Gauss-Codazzi relations combined with equilibrium equations from membrane theory reveal that, given axisymmetry, the meridional stress resultant is inversely related to the second principal curvature (which we have calculated as κ_x along the *x* axis and κ_y along the *y* axis). Therefore, as stress decreases in the meridional direction, after the CCC, curvature is expected to increase, thus qualitatively validating our curvature results.

Although the computed values of curvature seem reasonable, there is a need to parameterize the surface more rigorously and to calculate principal curvatures along the major and minor axes. This, along with equations derived from membrane theory, will allow us to calculate stress resultants in the lens capsule and quantify their changes as a consequence of the CCC.

In conclusion, it is interesting that Krag and Andreassen (2003) write that: “The posterior lens capsule is thinner than the anterior capsule. It loses its epithelial cells in fetal life and has not been shown to increase essentially in thickness with age, in contrast to the anterior capsule. Furthermore, the lamellar structure of the lens capsule disappears

earlier with age in the posterior lens capsule than in the anterior capsule and differences have been described in the relative proportion of macromolecular components such as heparan sulfate proteoglycan and fibronectin." Given that the epithelial cells on the anterior lens capsule tend to migrate to the posterior capsule following cataract surgery, it is intriguing to ask why the posterior capsule suddenly becomes a more "desirable" environment for these cells. Ultimately, there is a need to similarly evaluate how the native stress and strain fields in the anterior capsule change at the completion of the cataract surgery, after the artificial lens is inserted.

CHAPTER VII

ALTERED MECHANICAL BEHAVIOR OF THE ANTERIOR LENS CAPSULE AFTER CATARACT SURGERY

Overview

The native lens capsule of the eye is important biomechanically, and several studies have quantified its mechanical behavior and properties. Associated results have been used to develop computational models to understand better the process of accommodation, the primary function of the lens capsule. In addition, however, the lens capsule also plays a principle role after cataract surgery, a procedure that removes the native lens nucleus and cortex and implants a prosthetic intraocular lens. This prosthesis alters dramatically the mechanical environment of the lens capsule, and thereby modulates the errant lens epithelial cell (LEC) response that leads to capsular contraction and deposition of non-native matrix proteins. Although much has been done to understand biological alterations within the lens capsule after cataract surgery, little attention has been directed towards quantifying the altered mechanics. We performed uniaxial mechanical tests on cultured porcine and human cadaver specimens excised from anterior lens capsules that had undergone cataract surgery. We show for the first time that specimens closer to the capsulorhexis exhibited a stiffer behavior than those closer to the equator. These data promise to aid in the development of computational models of the post-surgical lens capsule and its interaction with implanted intraocular lenses.

Introduction

The lens capsule can be considered as having two primary functions: it stores mechanical energy that is released during the normal process of accommodation, which allows the elastic capsule to mold the underlying lens nucleus and cortex into a more quasi-spherical shape and thereby alter focus from distant to near objects; it also plays a paramount role during cataract surgery, which is a corrective procedure that becomes nearly inevitable with age, thus, motivating the need to consider this capsule 'function.' Cataract surgery introduces a continuous circular capsulorhexis (CCC) into the anterior lens capsule, breaks up and aspirates the lens nucleus and cortex, and implants a prosthetic intraocular lens (IOL). The lens capsule, therefore, houses the IOL and maintains its position along the optical axis. These two functions can be related through the need to incorporate an accommodative feature into IOL designs, a mechanism that will almost certainly include the native accommodative apparatus (i.e., ciliary body and lens capsule) and require an understanding of these functions from the perspective of mechanics.

Several studies of the mechanics of the lens capsule and the accommodative mechanism have been reported. Fisher (1969) excised the anterior portion of native human lens capsules and performed pressure-volume tests that revealed a nonlinear elastic mechanical behavior over finite strains. Later, Krag et al. (1997b) and Krag and Andreassen (2003a) performed uniaxial extension tests on excised annular specimens from the middle regions of both the anterior and the posterior portions of the human lens capsule. Again, the capsule exhibited a nonlinear elastic behavior, which was described

using a bi-linear model. Further, they demonstrated increased stiffening with age, and that the anterior and posterior capsules had a very similar behavior with the posterior less stiff due to its lesser thickness. Finally, Pedrigi et al. (2007a) performed inflation tests on the in situ anterior human lens capsule, and, beyond that which had already been established, demonstrated a regional anisotropy with increasing stiffness in the circumferential compared to the meridional direction (shown to be principal directions) moving from the pole towards the equator. The data were fit using a nonlinear Fung hyperelastic membrane model.

Using such data, often in combination with data on the geometry and mechanical properties of the underlying lens nucleus and cortex (see Brown, 1973 and Fisher, 1971), several computational models of the lens have been developed. These models have primarily explored the mechanism of accommodation and correspondingly quantified the altered geometry and tractions involved during this process (see Schachar and Bax, 2001; Burd et al. 2002; Hermans et al. 2006, 2008). In addition to understanding accommodation, a nonlinear finite element analysis performed by Pedrigi et al. (2007b; see also David and Humphrey, 2007) allowed calculation of the native stresses in the anterior capsule, due to the pressure from the underlying lens nucleus and cortex, as a function of radial position. They show that, despite regional variations in both mechanical properties and thickness (see Fisher and Pettet, 1972), the stress field in the native capsule is nearly homogeneous and equibiaxial. This finding strongly suggests that the resident lens epithelial cells (LECs) prefer a target state of stress, which is perturbed significantly due to cataract surgery.

Because of dramatic differences in the geometries of the native lens nucleus and cortex compared to a prosthetic IOL, the lens capsule is subjected to a nearly stress-free state immediately after cataract surgery. We hypothesize that it is primarily this mechanical perturbation that modulates the known errant behavior of the resident LECs after cataract surgery, which is characterized by a transdifferentiation into a wound-healing myofibroblast-like phenotype, proliferation, and migration to normally acellular regions of the capsule (i.e., the posterior capsule). Acutely, this phenotypic change leads to a contraction of the capsule around the implanted IOL (Hayashi, 2002; Tehrani, 2003), but in the years following the surgical procedure the cells synthesize matrix proteins that can ultimately lead to the most common complication of cataract surgery, posterior capsule opacification (PCO). The delayed development of PCO, which occurs over a period much longer than the inflammatory response to the surgical procedure, likely persists due to the inability of the LECs to restore their native stress field. Following surgery this hypothesis motivates the need to quantify the alterations in capsular stress and to study the associated mechanobiological responses to understand better the etiology of PCO. More fundamentally, however, PCO may simply be an adverse consequence of a cellular effort, which is seen to some degree in all persons who undergo cataract surgery, to alter the capsule matrix in an attempt to restore their homeostatic mechanical environment. Such dramatic alterations to the lens capsule will likely lead to an altered mechanical behavior and properties, quantification of which is essential for developing computational models of the post-surgical capsule to understand better its interaction with an implanted IOL.

We report here the first studies on the altered mechanical behavior of both cultured porcine and human anterior lens capsules after cataract surgery. Our results show that the lens capsule is much stiffer near the edge of the capsulorhexis, but away from this localized region the behavior is similar to that during normalcy.

Methods

Porcine Tissue Culture. Fresh whole globes were harvested from seven month old pigs at SiouxPreme Pork Products (Sioux Center, Iowa), and shipped overnight on iced saline; therefore, the tissue was received within 24 hours of harvest. Upon arrival, excess peri-scleral tissue was removed and whole globes were placed in a 10% povidone-iodine solution for 5 minutes, then transferred to individual containers filled with a 10% antibiotic-antimycotic media for transport to the ophthalmic surgery suite in the Texas A&M University Small Animal Clinic. Cataract surgery was performed on each experimental eye as follows: the cornea was removed, a 4 mm diameter CCC was introduced into the anterior lens capsule, phacoemulsification of the lens nucleus and cortex was performed, and an acrylic 1-piece IOL (MA30BA – Alcon, Inc.) was implanted into the remnant capsule. The whole globes were then transferred back to the Continuum Biomechanics Laboratory where the lens capsule was isolated from the eye and ten entomological pins were used to secure it around the equator to a silicon rubber substrate within a PMMA Petri dish. For controls, intact porcine lenses were isolated from the whole globe and placed free-floating in a PMMA Petri dish containing a silicon rubber substrate. All capsules were cultured in an incubator at 37°C with 5% CO_2 for

either one or two months. Cultures were maintained in Dulbecco's Modified Eagle Medium (DMEM) supplemented with 10% fetal bovine serum (FBS), 1% antibiotic-antimycotic, ascorbic acid, sodium bicarbonate, amino acids (proline, glycine, alanine), copper chloride, and insulin (all culture chemicals obtained from Sigma, St. Louis, MO unless otherwise specified).

Human Tissue. Enucleated human eyes were obtained from eye banks via overnight shipment in cold saline. In total, 23 specimens were tested from 17 eyes: 12 specimens were obtained from donors aged 45 to 82 years (experimental group – 78 ± 3, mean ± standard error) who had undergone cataract surgery, and 11 specimens were obtained from healthy donors aged 56 to 83 (control group – 71 ± 4). The ages between the experimental and control groups were not statistically different as determined by a *t*-test. All tissues underwent testing immediately upon receipt, which was an average 48 hours post-mortem.

Biomechanical Testing. For each lens capsule tested, two annular specimens were acquired using skin biopsy punches (Acuderm, Ft. Lauderdale, FL) -- one whose inner diameter was formed by the CCC (unless in the control group, wherein a biopsy punch was used to form an inner hole having a diameter comparable to the experimental group), and one immediately adjacent to the first (Figure 7.1). The cultured porcine capsules had a mean CCC diameter of 3.7 ± 0.5 mm; therefore, biopsy punches of 5 and 6 mm diameter were typically used to obtain inner and outer rings, respectively (for control capsules, the inner rings were formed with 4 mm diameter biopsy punches). The human post-surgical capsules had a mean CCC diameter of 4.8 ± 0.2 mm; therefore,

biopsy punches of 6 and 7 mm were typically used to obtain the two rings (for control capsules, the inner rings were formed with 5 mm diameter biopsy punches).

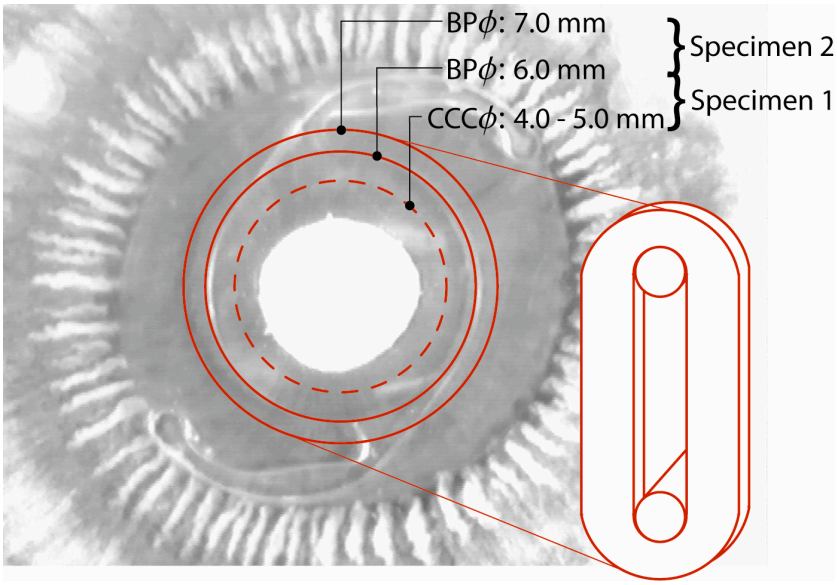

Figure 7.1. A digital photograph of the in situ human lens capsule with IOL implanted. A schematic diagram is placed over this image to illustrate the portions of the capsule where the annular specimens were obtained. Specimen 1 refers to that obtained nearest the CCC, and Specimen 2 is immediately adjacent to the first (denoted the peripheral specimen in text).

Each capsular ring was then mounted within a commercial uniaxial mechanical testing device (Myobath4 – World Precision Instruments, Sarasota, FL) by threading it through tungsten mounting feet that were attached to a micrometer drive, allowing for precise adjustment of tissue extension, and a force transducer, giving a precise measure of the load at a given extension. The mounted tissue was then submerged within a saline bath and kept at a physiologic temperature of 37°C. An initial stress-free length was estimated based on the measured inner diameter of the annular specimen; it was found, however, that the capsule shrank due to dehydration during excision, which was

accounted for post-experiment during data analysis (see below). In order to minimize viscoelastic effects, four cycles of preconditioning were performed to the maximum stretch of 1.25 (28% Green strain). Subsequently, the force transducer was sampled at every 0.04 increment of stretch (4% Green strain) for both the loading and unloading portions of the fifth cycle.

Calculation of Tension. Data were collected throughout the experiment with respect to an estimated stress-free length; therefore, a more precise value was determined during data analysis by incrementally increasing this length until the change in force between each increment of stretch increased from one stretch to the next (i.e., because the capsule exhibits nonlinear elasticity, the calculated slope of the stress-strain curve, interrogated at a particular stretch, should increase continually with increasing stretch). This post-experimental increase in the stress-free length caused corresponding increases in specimen length for a given stretch, which were also accounted for within the analysis. Also, the width of each specimen (roughly 0.5 mm) was larger than the maximum change in length of the inner portion of that specimen during the experiment; therefore, it was never loaded through entirely. To account for this, the loaded width during data analysis was calculated as the weighted average of the specimen width at each state of stretch through the entire experiment. Finally, tension was calculated by taking the mean force measured at each stretch divided by the mean loaded width of the specimen. This value was only calculated to a maximum stretch of 1.18 (20% Green strain).

Comparison to Biaxial Mechanical Model. We previously performed in situ biaxial mechanical tests on both native porcine (Heistand et al. 2005) and native human (Pedrigi et al. 2007b) anterior lens capsules, from which four material parameters for a 2-D Fung hyperelastic membrane model were calculated. Having quantified the mechanical complexities of this tissue in 2D (i.e., the regional anisotropy), we were then able to employ this model to predict the simpler 1D loading scenario defined by the uniaxial mechanical test. Therefore, we calculated the tension predicted by this model for each of these two tissue types, respectively, under loading conditions identical to that employed experimentally.

Results

Uniaxial mechanical behavior data for the cultured porcine anterior lens capsules, summarized in Figure 7.2, revealed that after cataract surgery a dramatic stiffening occurred, compared to native, within the region nearest the CCC (*t*-test, $p<0.001$). This stiffening appeared to progress as a function of time, at least during the first one-to-two months after the procedure. Further, the data illustrated that capsule behavior away from the CCC was not statistically different from 8-week control capsules as determined by a *t*-test. It can also be seen that simulations of the uniaxial extension based on the biaxial mechanical model predicted very well both the peripheral surgical capsule and the control capsule behaviors.

The post-surgical human capsules demonstrated a qualitatively similar behavior to the cultured porcine capsules; wherein, stiffening of the human anterior capsule was

observed nearest the CCC ($p<0.08$), but no changes in behavior were seen away from this localized region when compared to similar regions of native capsules as demonstrated by a *t*-test (Figure 7.3). We found that the biaxial mechanical model for the native human capsule also predicted reasonably well the experimentally determined behavior of the peripheral and native specimens in uniaxial extension; though the experimental responses were slightly more compliant at maximum stretches compared to the model.

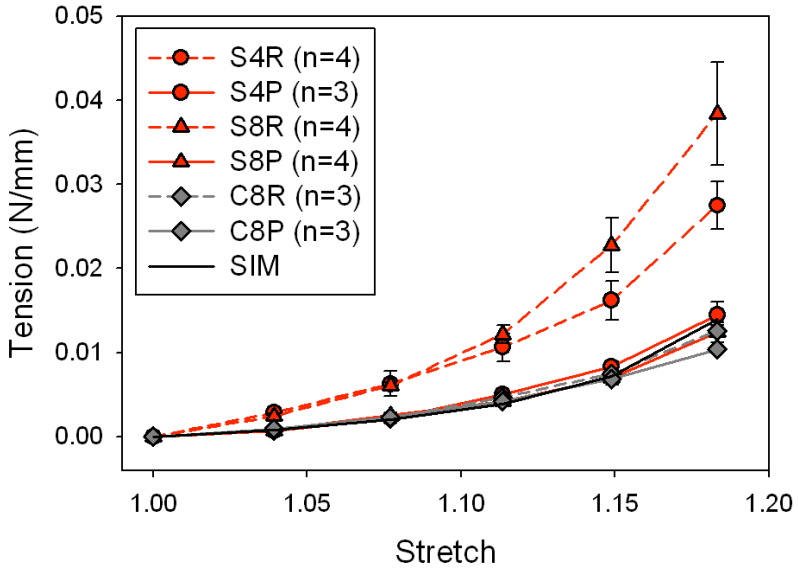

Figure 7.2. Comparison of the mechanical behavior of cultured porcine anterior capsules after cataract surgery (surgical – 'S') versus those left within the in situ configuration (control – 'C'). Two specimens were obtained from each capsule: one nearest the CCC and one adjacent to this towards the periphery. It can be seen that the specimens nearest the capsulorhexis (S4R & S8R) were stiffer than those at the periphery of the post-surgical tissue (S4P & S8P) and from the control capsules (C8R & C8P). Finally, the biaxial model (SIM) predicted well the behavior of both the peripheral and control capsules, which exhibited similar behavior.

Discussion

To our knowledge these data are the first to document changes in mechanical behavior of the lens capsule after cataract surgery. These changes are likely the consequence of an errant LEC behavior that ultimately leads to an altered capsular matrix, which is initially composed primarily of collagen type-IV and laminin (Barnard et al. 1992). Matrix alterations after surgery have been demonstrated by immunohistochemical studies.

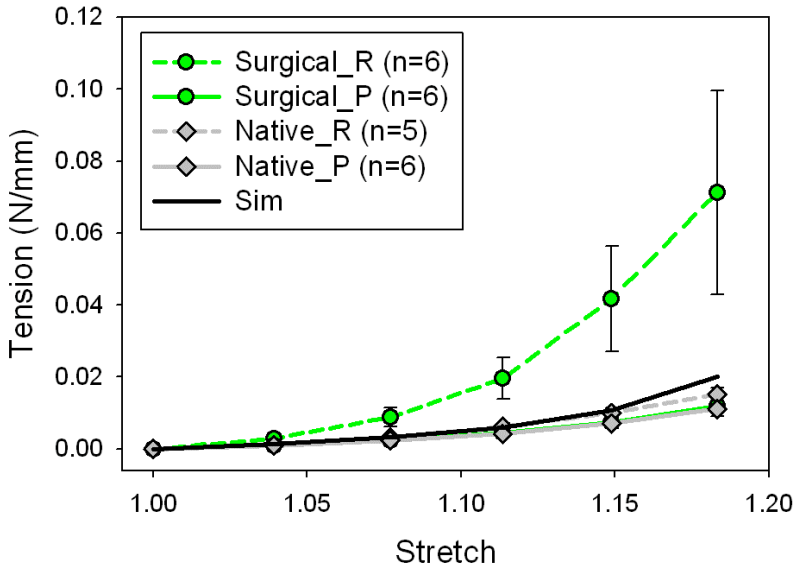

Figure 7.3. Uniaxial mechanical behavior of the human post-surgical and native anterior lens capsule. Similar to the cultured porcine capsules, the human post-surgical capsules were much stiffer than native nearest the CCC, but their behavior was not affected in the outer or peripheral region (P). Our biaxial model (SIM) for the human capsule predicts reasonably well the behavior of the native capsules, though slightly stiffer.

For example, Shigemitsu et al. (1999) obtained six human anterior capsule specimens, excised during invasive surgery for anterior capsule opacification (all patients had undergone cataract surgery within one year of the procedure), and

demonstrated the presence of the following several additional extracellular matrix proteins: fibronectin and collagen types I, III, V, and VI. Similar results were obtained by Hara et al. (1992), Namiki et al. (1993), and Saika et al. (1998). Further studies of different regions of the post-surgical anterior capsule by Marcantonio et al. (2000) illustrated a significant accumulation of multilayered, transdifferentiated LECs nearest the capsulorhexis edge, which were accompanied by a corresponding accumulation of extracellular matrix proteins. Conversely, the LECs in the remaining portions of the capsule away from this localized CCC edge maintained their native cobblestone morphology and monolayer organization (except for portions of the equator where the IOL haptics contacted). This finding provides direct histological evidence supporting our biomechanical results that show an increased stiffening of the lens capsule localized to the CCC edge, and maintenance of native behavior away from this location. In addition, the aforementioned histological studies suggest that this stiffening is due to LEC mediated deposition of matrix proteins not seen in the native capsule.

These previous studies also appear to corroborate our hypothesis that the altered mechanical environment introduced during cataract surgery modulates errant LEC matrix modifications. Beyond the aforementioned drastic reduction in capsular stress that results from removing the lens nucleus and cortex during surgery, we have shown that the presence of the CCC in the anterior capsule maintains a traction-free condition (in the radial direction) at the edge (Heistand et al. 2006). Ultimately, this prevents the LECs from restoring their homeostatic mechanical environment as they contract the remnant capsule down around the implanted IOL. Therefore, unlike surgery-induced

increases in cytokines and growth factors that return to baseline concentrations within months, the CCC indefinitely prevents the cells from restoring a normal mechanobiological environment. This could very well be the persistent stimulus for both continued matrix remodeling nearest the edge of the CCC, and the development of opacifications at various other locations in the capsule (e.g., Soemmering's ring at the equator, PCO, etc.) that characterize secondary complications in some patients.

Our data on the mechanical behavior of the cultured porcine lens capsules allowed calculation of the stiffness, which was 2.1- and 3.0-fold higher for the 4 and 8 week cultures compared to controls, respectively. This short-term (i.e., the first few months) change in mechanics following this procedure is corroborated qualitatively by previous studies quantifying the changing geometry of the capsule. Hayashi et al. (2002) showed that the remnant anterior and posterior portions of the lens capsule contract down and enclose the IOL within approximately 6 and 11 days, respectively. Tehrani et al. (2003) quantified the degree of contraction of the lens capsule through measurements of both the cross-sectional (equator-to-equator) and capsulorhexis diameters. Their results for a 6 month period showed that the lens capsule contracts significantly post-operatively, with a reduction in both the capsular and capsulorhexis diameters on the order of about 15% (from a mean of 10.53 to 9.01 mm and from 5.24 to 4.47 mm, respectively), with the majority of this contraction occurring within the first month. Although some of these metrics of capsular geometry appear to reach a steady state within this short period after surgery, continued LEC responses mentioned previously likely result in further alterations in capsular mechanics. This is demonstrated by

comparing the stiffness of our cultured porcine to human data. Estimations of time after cataract surgery for donors of the ocular tissue used in this study were provided by eye bank inquiries of the related family, which gave an average period of several years (a good representative of the long-term after surgery). Calculated stiffness of the human lens capsule was 4.1-fold higher than corresponding controls, which illustrates nicely, when compared to the aforementioned 3.0-fold increase of the two-month cultured porcine capsule stiffness, that capsular remodeling continues in the years following the procedure. It appears, however, that most of the remodeling occurs within the short-term after surgery, and subsequent long-term changes occur at a much slower rate.

In summary, the highly mechanical nature of the lens capsule demands an improved understanding of this tissue from the perspective of biomechanics. Yet, nearly all prior experimental and computational research has focused on the native capsule and understanding the mechanism of accommodation. A clear application of the present work is the development of accommodative IOLs, which necessitates the use of sophisticated mechanical models that can predict the interaction of the remnant capsule with the implant. Because cataract surgery causes dramatic alterations in the mechanics of the lens capsule, however, there is a pressing need to quantify before predictive models can be developed. We present here the first data on the altered mechanical behavior of the capsule, showing increased stiffening localized near the CCC that increases with time after surgery. Ideally, these data can be used to begin developing a computational model of the lens capsule that accounts for remodeling as a function of time after surgery.

CHAPTER VIII

NOVEL CULTURE DEVICE TO QUANTIFY THE TIME-COURSE OF CONTRACTILE LOADING OF THE LENS CAPSULE AFTER CATARACT SURGERY

Overview

Cataract surgery is a procedure that removes the lens nucleus and cortex, drastically reducing the stresses within the lens capsule. This mechanical perturbation is likely an underlying modulator of the errant lens epithelial cell (LEC) transdifferentiation that leads to a more contractile phenotype. It is well known that LEC contraction occurs after cataract surgery leading to a wrapping effect about the implant, and resultant changes in capsule geometry have been quantified previously. Nevertheless, little has been done to quantify the corresponding contractile loads involved during this process. We describe a novel experimental culture device that employs cantilever beams to transduce contractile loading within an attached isolated lens capsule as a function of time after cataract surgery. Our results show that maximal contractile forces are reached within a mean 27 days and have a magnitude of 5.8 mN, which corresponds to a final capsular stress of 14.1 kPa. These data are important for considering the mechanical stability of implants in vivo, and for the development of sophisticated biomechanical models of tissue growth and remodeling that may allow evaluation of implant efficacy as a function of time after surgery. This latter function may be important for the design of prosthetic accommodative intraocular lenses.

Introduction

Cataract surgery involves three primary steps following access to the aqueous chamber: introduction of a continuous circular capsulorhexis (CCC) into the anterior capsule, removal of the lens nucleus and cortex via phacoemulsification, and implantation of a prosthetic intraocular lens (IOL). Due to the permanent hole formed by the CCC and the dramatic differences in geometry between the native and prosthetic lenses, the lens capsule experiences a much different mechanical environment after cataract surgery. Specifically, the stress in the capsule is initially reduced to almost zero, and, unlike the nearly homogeneous equibiaxial stress field in the native capsule (Pedrigi et al. 2007b), the post-surgical capsule will have stress gradients due to the permanent CCC. We hypothesize that these mechanical alterations are an underlying modulator of the errant response by resident lens epithelial cells (LECs) after surgery, which is initiated by their transdifferentiation into a wound-healing, myofibroblast-like phenotype called epithelial-mesenchymal transition (EMT). One of the primary markers of EMT is alpha-smooth muscle actin (α-SMA), which enables for increased motility and contractility of the LECs (Kurosaka et al. 1995; Saika et al. 2003b; De Iongh et al. 2005). A foremost consequence of this latter capability is contraction of the remnant lens capsule down around the implanted IOL.

Contraction of the remnant capsular bag after cataract surgery is a well known phenomenon, with changing bag geometry being quantified by several investigators. Hayashi et al. (2002) show that anterior and posterior portions of the human lens capsule contract down and enclose the IOL within two weeks, which they hypothesize as the

mechanism that allows for its initial stabilization. Nishi et al. (2002) reported a similar study looking at the effect of IOL design on the speed of capsular contraction, and found that the capsule contracts completely in one month with one-piece acrylic lenses. Finally, Tehrani et al. (2003) implanted capsule measuring rings along with IOLs into patients during cataract surgery, and quantified the diameter of contraction at several times after the procedure. Their results showed that the capsule (as well as the CCC) contracted 15%, where the majority of this contraction occurred within the first month. Despite these studies illustrating significant contraction of the remnant capsular bag that clearly leads to deformations of the IOL, little has been done to quantify the cell-mediated contractile loads during this process. Therefore, this study introduces a novel device for quantifying contractile loads imposed endogenously onto membranous circular tissues, and reports some of the first data on the time-course of force, tension, and final stress exerted by contracting LECs within cultured porcine lens capsules after cataract surgery.

Methods

Porcine Tissue Preparation and Culture Protocol. Fresh whole globes were harvested from seven month old pigs at SiouxPreme Pork Products (Sioux Center, Iowa), and shipped overnight on iced saline; therefore, the tissue was received within 24 hours of animal extraction. Upon arrival, excess peri-scleral tissue was removed and whole globes were placed in a 10% povidone-iodine solution for 5 minutes, and then transferred to individual containers filled with a 10% antibiotic-antimycotic media for

transport to the ophthalmic surgery suite in the Texas A&M University Small Animal Clinic. Cataract surgery was performed on each experimental eye as follows: the cornea was removed, a 4 mm diameter CCC was introduced into the anterior lens capsule, and phacoemulsification of the lens nucleus and cortex was performed. Unlike extracapsular cataract surgeries, however, no IOL was implanted to eliminate its participation in bringing the contracting capsule into mechanical equilibrium (i.e., this study looks to quantify the absolute magnitude of contractile loads exerted on the capsule, which is done most easily without the presence of the ciliary body or an implant). The lens capsule was then isolated from the eye and six pieces of size 6-0 silk suture (Harvard Apparatus, Holliston, MA) were placed near its equator (within 1 mm), equidistant about the circumference of the capsule. The suture was held into place with a surgeons knot. The capsule was then transported back to the Continuum Biomechanics Laboratory, and sutured into the custom LEC force acquisition device (described below). The capsules were cultured within this device in an incubator at 37°C with 5% CO_2 for two months. Cultures were maintained in Dulbecco's Modified Eagle Medium (DMEM - Invitrogen) supplemented with 10% fetal bovine serum (FBS - Invitrogen), 1% antibiotic-antimycotic (Invitrogen), ascorbic acid, sodium bicarbonate, amino acids (proline, glycine, alanine), copper chloride, and insulin (all unlabeled culture chemicals obtained from Sigma, St. Louis, MO).

LEC Force Acquisition Device. Figure 8.1 is a CAD drawing of our experimental device, which was machined in-house from polycarbonate (McMaster-Carr, Inc.). Six 3.3 mm diameter rods were cut to a length of 125 mm, and shrink-fitted into through

holes in the top of the device. This assembly secured the rods at one end, forming six cantilever beams. The rest of the device was built to support this principle component as well as the attached tissue; secondary components include: the top portion that holds the beams and contains a 10 mm diameter hole for media exchange, the middle allows for additional height for purposes of containing entirely the cantilever beams, and the base contains the tissue and is the only component of the device that holds culture media.

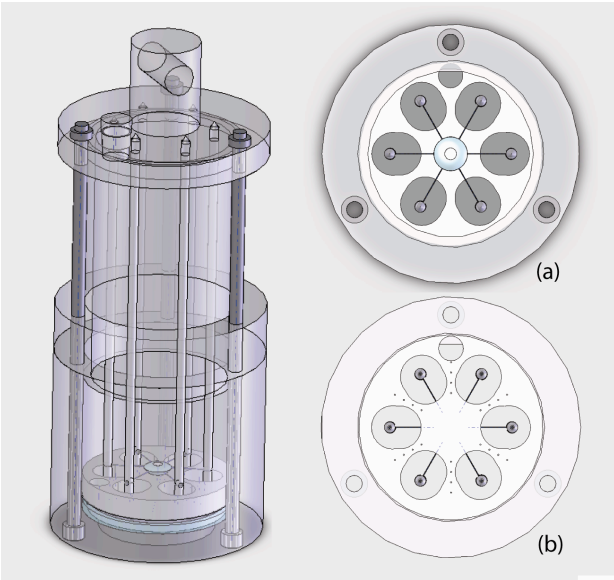

Figure 8.1. CAD model of our culture device, used to quantify contractile loads imposed onto the lens capsule after cataract surgery. Two orientations of the model are enlarged to the right; image **(a)** is looking down into the device from the top, and image **(b)** is looking up through the optic window at the base of the device. Note that the bottom orientation was the one used to acquire images of beam position (though hard to see) with respect to the small black markers along each beam well.

This base also includes an optic window (Edmund Optics, Barrington, NJ) sealed with Sylgard (Dow Corning Corp.), which allows imaging of the cantilever beams to determine their changing positions; it also holds a stationary reference piece (SRP) with

six wells that provide a reference to measure the position of the beam against. To ensure precise measurement of beam position, the beam and SRP have 0.5 mm diameter holes drilled superficially, filled with black enamel, and sealed with cyanoacrylate; therefore, upon imaging only the positions of these smaller points are acquired.

During assembly, a post-surgical lens capsule with attached sutures (preparation described above) is centered between the six cantilever beams. Each suture is threaded into one beam (through a small hole drilled 8 mm from its free end) so to attach the lens capsule at six points. A 0.5 mN weight is then tied to the free end of each suture to introduce a small axisymmetric preload and to center the tissue between the beams. Then, a small amount of cyanoacrylate (Adhesive Systems, Frankfort, IL) is used to secure the taught suture to each beam, after which the weights are cut away. Finally, the device is assembled by placing the top, middle, and base portions together and securing them with three 9.5 mm diameter stainless steel bolts that fit into aligned holes at each end. The base is then filled with 50 mL of culture media, and the device is placed in the incubator.

Data Acquisition and Analysis. The device was taken from the culture chamber twice a week and suspended over a Javelin CCD camera to image the ends of each of the six beams through the optical window at the base. The camera was outfitted with a macro lens (FD 100 mm – Cannon, Inc.) that provided a resolution of ~20 μm/pixel; this resolution only allowed one beam to be imaged with respect to the SRP per frame. Once images of all six beams were collected for a given culture period, a custom LabVIEW program was used to obtain their positions with respect to a local coordinate system.

These data were then imported to a custom Matlab program that performed several functions. Foremost, the positions of each beam were related to a global coordinate system that allowed calculation of their displacements relative to a common origin for all beams. Displacements were calculated as the difference between the distances of a beam from the origin at a particular time compared to that at time zero (note that the device was imaged before placing preloaded tissue onto it; therefore, the reference positions are with respect to a completely unloaded configuration). Forces were then calculated by simply multiplying this displacement by a beam stiffness, determined via calibration of each beam (see below). Because the displacements of each beam were small and the capsule could be considered static during the time needed to collect data on a given day, it was prudent to calculate the overall centroid of the tissue (versus using an arbitrary point, such as the center of the device); of course, the forces summed over all six beams equal to zero due to static equilibrium. A nonlinear regression was employed to find iteratively a new global origin of the tissue at each time point to ensure equilibrium. Based on this new origin, all displacements and corresponding forces were recalculated. Finally, we estimated that our error in measuring beam position was within 10 μm (less than 0.5 pixel), which correlates to a maximum possible force error of 0.3 mN (although mean errors across all time points are likely smaller).

Upon completion of the two-month culture, the tissue was imaged while attached to the beams to allow for a digital measurement of each of the suture lengths (Figure 8.2), which became an input to the aforementioned Matlab code that calculated the changing capsule diameter. From this measurement, tension was then calculated as the

force obtained from a displaced beam divided by one-sixth the circumference of the capsule. Finally the capsule was removed from the sutures, placed in a Petri dish, and thickness was measured using the displacement of a calibrated microscope vertical stage translator (100 nm resolution) focusing between an ink mark placed on the Petri dish and tissue, respectively. This measurement was used to calculate a final stress for the tissue.

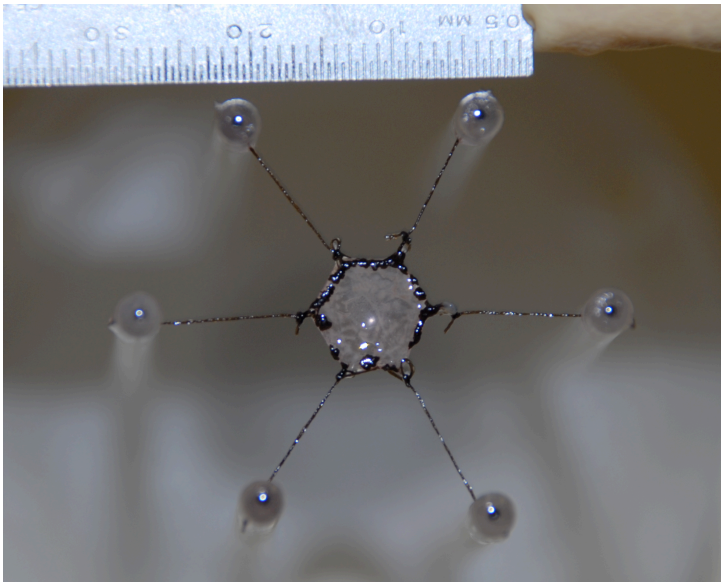

Figure 8.2. Photograph of one of our cultured capsules immediately after removal from culture on day 56, but still attached to the device beams and top. Notice the capsule, which is natively circular, contracted into the shape of a hexagon with the vertices being the points of suture attachment. Finally, the scale at the top of the image allows us to digitally measure the suture lengths and back-calculate the diameter of the capsule (approximated by the six points of suture attachment) at each time.

Calibration and Creep Tests. Prior to every experiment, each beam of the device was calibrated in air through a loading and unloading cycle from 0 to 10 mN. The beam exhibited a linear elastic behavior with a mean stiffness of 17.6 ± 0.4 mN/mm (mean ±

standard error), from which the elastic modulus was calculated as 2432.43 ± 6.87 MPa using the following equation from beam theory:

$$E = \frac{1}{2}\left(\frac{Pa^2}{I_{ZZ}\delta}\right)\left[L - \frac{a}{3}\right], \tag{8.1}$$

where E is elastic modulus, P is load, I_{zz} is second moment of area, d is beam displacement, L is beam length, and a is the distance from the inner portion of the device top (point of fixation) to the point of loading near the free end of the beam. Because the beams were loaded at physiologic temperatures, a calibration in a heated bath determined the beams to be 3.7% more compliant at 37°C than at 20°C, which was accounted for in our data analysis software.

To account for possible viscoelastic behavior exhibited by the beams in culture, creep tests were performed in a separate experimental setup; the beams were held horizontal and loaded statically with various weights up to 10 mN. Images were acquired daily to measure beam displacement until steady state was reached (less than 6 days). Data from multiple experiments were combined, from which a representative creep-displacement versus force modulus of 0.01 mm/mN was calculated. This value was incorporated into the data analysis by subtracting the calculated beam displacement that was due to creep and recalculating the force.

Results

Herein we present data on four capsules cultured for two-months each, where an average is given for each metric with respect to the six beams for a particular tissue, and,

within the text below (i.e., excluding figures), these beam-averaged values are also averaged with respect to each other; therefore, the plus/minus standard error signifies the degree of inter-capsular differences. The mean beam displacement between imaging sessions (every 2 to 4 days) was 32 ± 2 μm (until steady state was reached), and the overall displacement through the two-month culture was a mean 388 ± 20 μm. Figure 8.3 shows calculated forces of capsular contraction, obtained from these displacements, as a function of culture time; the average over the four capsules at the end of culture was 5.8 ± 0.3 mN.

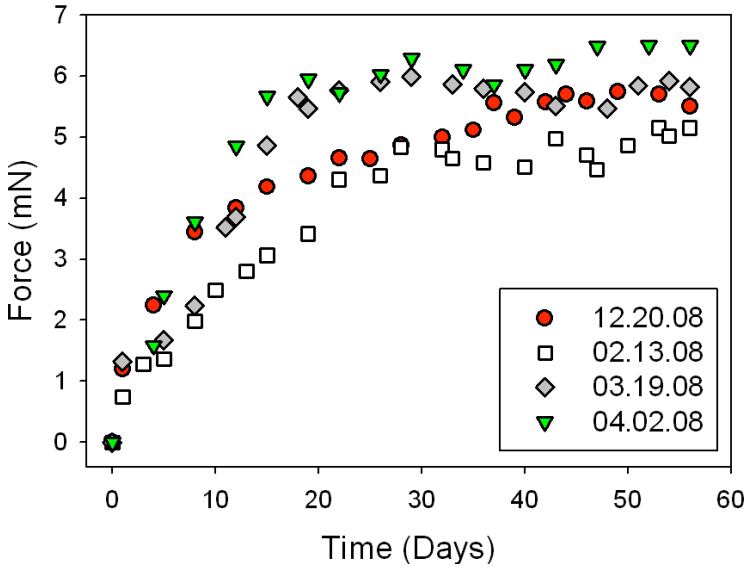

Figure 8.3. Forces (mN) of lens capsule contraction as a function of time (days) after cataract surgery. These data are obtained from the average beam displacements for each device (identified by the culture start date). Notice that forces reach a steady state in an average 27 days for all cultures.

The mean starting diameter of our cultured capsules was 8.80 ± 0.20 mm, which compares well to the native isolated capsule diameter of about 9.75 mm and illustrates

that the sutures were placed well within 1 mm of the equator; this provided a similar geometry to native during culture. By the end of the culture period, the capsules had contracted an average of 0.78 ± 0.04 mm (with respect to diameter). Using this information together with the calculated forces, the average tension (i.e., force per deformed length) between the four different cultured capsules was 1.4 ± 0.1 mN/mm. Figure 8.4 illustrates the complete time-course for changes in tension after surgery.

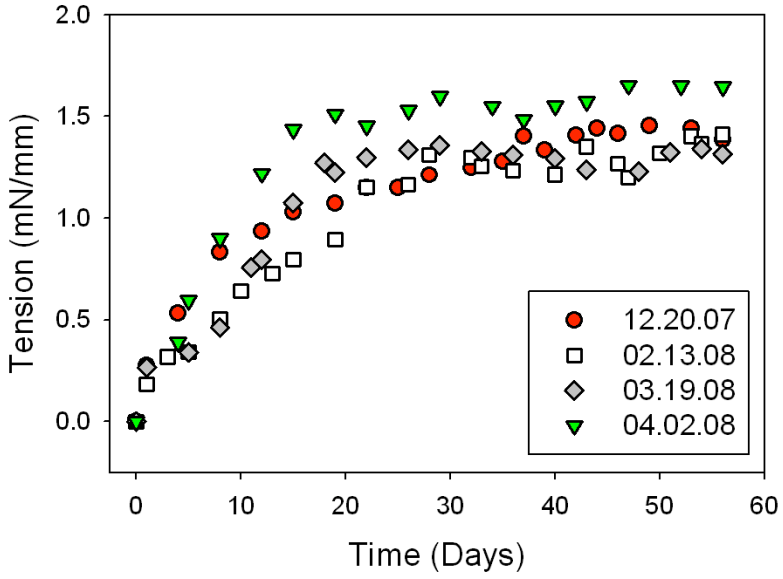

Figure 8.4. Tension, or membrane stress, (mN/mm) imposed onto the lens capsule as a function of time after cataract surgery. These data are calculated by taking the mean force over the six posts and dividing by one-sixth the circumference of the capsule at each time point.

Finally, the thickness of each capsule was measured at the end of culture proximal to the insertion point of the suture at the equator. The mean value for all capsules, anterior plus posterior, was 116 ± 8 μm, which is significantly thicker than our measured value for the

native capsule of 78 ± 5 μm. These values of thickness allowed calculation of a final stress in the capsule, the mean of which was 14.1 ± 1.3 kPa for all cultured capsules.

Discussion

Understanding the magnitude of contractile loads imposed on the remnant lens capsule by LECs is critical for assessing the efficacy and stability of IOL designs in vivo. Several studies have reported, both qualitatively and quantitatively, the deformation of various implants in vivo, and numerous studies have also reported the stiffness of isolated IOLs and capsule tension rings (CTRs). Interestingly, however, only one other study, to our knowledge, has quantified the contractile loads imposed on the capsular bag by LECs.

Guthoff et al. (1990) implanted one-piece silicon lenses in the capsular bag of dogs, and measured the displacement of the haptics at five and eight months post-operatively. Prior to implantation, mechanical tests (electronic dynamometry) were performed on these IOLs to obtain a force-displacement curve for the haptics; this calibration allowed them to infer contractile forces from the measured haptic displacement in vivo. They reported a range of forces from 0.20 to 1.23 mN. There are several limitations of this study, however. First, the gap in time between surgery and the evaluation of haptic displacement was well beyond the period that most of the contraction is known to occur; thus, key time-courses of change after surgery remain lacking. Furthermore, the implant is not axisymmetric, which yields a more complicated loading scheme, and contractile loads were not normalized with respect to the finite area

over which they acted (i.e., neither tension nor stress was reported). Most importantly, attempting to quantify the contractile loads of the capsule in vivo is complicated further by lack of information on the role played by the attached zonules (and, thus, ciliary body) in bringing the contracting capsule into mechanical equilibrium. In fact, we hypothesize that the zonules play a substantial role in this regard.

We present the first data quantifying the magnitude of contractile loads imposed onto the lens capsule as a function of time after cataract surgery. Directly comparing our results to those of Gutoff et al. suggests that, indeed, the zonules play a considerable role in offsetting the mechanical loads imposed by the contracting capsule, as our calculated forces are considerably higher (though this direct comparison may be difficult to interpret because of differences in experimentally transducing the loads). If this is the case, then the zonules can be thought of as protecting the implant from much larger compressive loads than it would otherwise experience. A possible worst-case scenario that should be considered when designing IOLs or CTRs is that weakened zonules of the patient can rupture during cataract surgery (termed zonular dialysis or dehiscence), which may expose these implants to higher compressive loads. A study by Jacob et al. (2003) illustrates that zonular dialysis can occur for a multitude of reasons, including: high myopia, Marfan's syndrome, blunt trauma (possibly leading to traumatic cataract), and pseudoexfoliation syndrome, which may imply a regular incidence (see also: Conway et al. 2004; Drolsum et al. 2007; Georgopoulos et al. 2007). Further, in cases of preoperative or intraoperative zonular dehiscence, CTRs are used to maintain the shape of the capsule and prevent further zonular rupture (Gimbel et al. 1997; Bayraktar et al.

2001; Jacob et al. 2003; Georgopoulos et al. 2007); therefore, optimal CTR designs should account for maximal loading scenarios.

Our result for the mean final stress within the remodeled capsules of 14 kPa compares well to stresses of 12 kPa reported by Goffin et al. (2006), who cultured myofibroblasts on deformable micropatterned elastic membranes and quantified their contraction at focal adhesions. These values of stress are approximately two- to four-fold higher than those obtained from maximal contractions of normal fibroblasts (Balaban et al. 2001; Tan et al. 2003). This correlation suggests that the LECs transdifferentiate into a myofibroblast-like phenotype for purposes of contracting the post-surgical capsule in an attempt to reestablish their homeostatic stress state. We have previously reported that the human anterior lens capsule has a nearly homogeneous equibiaxial stress field, estimated to be around 100 kPa (Pedrigi et al. 2007b). We have since refined our estimate, and now believe the native stresses in humans to be closer to 35 kPa; similar results hold for the porcine capsule (unpublished). It appears from our data that the contracting LECs are unable to reestablish this native stress field, possibly due to limitations in contractility but also the permanent CCC, which we have shown introduces a consistent traction-free boundary condition at its edge (Heistand et al. 2006). Regardless of the cause, this continued mechanical perturbation from normal may well be the underlying modulator of the persistent errant LEC behavior that can lead to such complications as posterior capsule opacification (PCO) over periods of months to years.

In addition to quantifying maximal loading, our results illustrate the time-course of capsular contraction after cataract surgery; wherein, the contractile loads appear to reach steady state within one month. This compares favorably to the aforementioned studies by Nishi et al. (2002), Hayashi et al. (2002), and Tehrani et al. (2003), which show that much of the remodeling is completed within the first month as well. In general, meticulous quantification of tissue remodeling time-courses following surgical insults are important towards the development of mechanical models that incorporate adaptations, such as wound healing, and reflect the altered mechanics experienced by these tissues and implants. Ultimately such biomechanical models promise to enable predictions of implant function and stability as a function of time after surgery. Introduction of the important feature of accommodation into IOL designs, for example, will require such sophisticated biomechanical modeling to determine the changing efficacy of this feature as the capsular bag contracts down around the implant and begins to impart compressive loads onto it.

In summary, we present results for a time-course of increased contractile loading (force, tension, and final stress) with cultured porcine lens capsules after cataract surgery. These data are particularly important for understanding implant stability and modeling the efficacy of current and future AIOLs. It is likely that our calculated stress resultant for these cultured young porcine lens capsules reflects closely that which would be expected for an adolescent human lens capsule after cataract surgery, given the mechanical similarities that we have seen between the human and porcine lens capsules (compare Heistand et al. 2005 to Pedrigi et al. 2007b). It is well known, however, that

cell viability diminishes with age; therefore, similar studies of the post-surgical human lens capsule need to be performed to quantify these possible alterations in contractile loading as a function of patient age.

CHAPTER IX

SUMMARY AND RECOMMENDATIONS

This dissertation presents a novel experimental system to quantify in situ the regional biaxial mechanical behavior of the anterior lens capsule, from which mechanical properties and native stresses were calculated. The capsule exhibits a nonlinear elastic regionally anisotropic mechanical behavior with significant stiffening unfolding in diabetic persons (though the regional anisotropy is maintained). Despite these regional variations in capsule properties and thickness (see Fisher and Pettet, 1972), a nearly homogeneous equibiaxial stress state exists in the native anterior lens capsule. This finding strongly suggests that the resident lens epithelial cells (LECs) work to maintain a homeostatic stress state, which is perturbed dramatically during cataract surgery. Specifically, the stresses in the capsule, which primarily result from the pressure exerted by the underlying lens nucleus and cortex, are mostly removed with removal of the native lens and implantation of a prosthetic intraocular lens (IOL). Though much has been done to quantify the resulting altered matrix of the post-surgical capsule, very little work has quantified the associated alterations in mechanics; therefore, this deficiency was a second thrust of this dissertation. Stiffening of the capsule, compared to native, was found to occur only proximal to the capsulorhexis edge (permanent hole placed in the anterior capsule during cataract surgery) and away from this localized region the mechanical behavior was similar to native. Finally, a novel culture device quantified the degree of contractile loading as a function of time after cataract surgery. This allowed

calculation of a final stress state in the capsule, which was found to be much lesser than native.

These studies collectively represent quantification of much of the mechanics associated with the native and post-cataract surgery lens capsule. This information on the overall changes in mechanics is important for understanding LEC mechanobiological responses to cataract surgery, and sets the stage for more in-depth studies on the mechanism of their altered behavior. Further, these data can be used to develop a computational model of the lens capsule specifically for the purpose of aiding in the design of prosthetic lenses with an accommodative feature. These computational analyses should be constructed to model the time-course of capsule remodeling after surgery (reported within) and, therefore, have an adaptive feature that is capable of altering the associated mechanics (geometry, properties, and loads). Such models will provide a powerful predictor of implant efficacy (i.e., stability and effectiveness of the accommodative feature) as a function of time after surgery.

REFERENCES

Ahmed N, Thornalley PJ, Dawczynski J, Franke S, Strobel J, Stein G, Haik GM (2003) Methylglyoxal-derived hydroimidazolone advanced glycation end-products of human lens proteins. Invest Ophthalmol Vis Sci 44:5287-5292

Annes JP, Chen Y, Munger JS, Rifkin DB (2004) Integrin alphaVbeta6-mediated activation of latent TGF-beta requires the latent TGF-beta binding protein-1. J Cell Biol 165:723-734

Aronson D (2003) Cross-linking of glycated collagen in the pathogenesis of arterial and myocardial stiffening of aging and diabetes. J Hypertens 21:3-12

Bailey AJ, Sims TJ, Avery NC, Miles CA (1993) Chemistry of collagen cross-links: glucose-mediated covalent cross-linking of type-IV collagen in lens capsules. Biochem J 296:489-496

Balaban NQ, Schwarz US, Riveline D, Goichberg P, Tzur G, Sabanay I, Mahalu D, Safran S, Bershadsky A, Addadi L, Geiger B (2001) Force and focal adhesion assembly: a close relationship studied using elastic micropatterned substrates. Nat Cell Biol 3:466-472

Barnard K, Burgess SA, Carter DA, Woolley DM (1992) Three-dimensional structure of type IV collagen in the mammalian lens capsule. J Struct Biol 108:6-13

Bayraktar S, Altan T, Küçüksümer Y, Yilmaz OF (2001) Capsular tension ring implantation after capsulorhexis in phacoemulsification of cataracts associated with pseudoexfoliation syndrome. Intraoperative complications and early postoperative findings. J Cataract Refract Surg 27:1620-1628

Ben-Nun J (2006) The NuLens accommodating intraocular lens. Ophthalmol Clin North Am 19:129-134

Bhat SP (2001) The ocular lens epithelium. Biosci Rep 21:537-563

Bhowmick NA, Zent R, Ghiassi M, McDonnell M, Moses HL (2001) Integrin beta 1 signaling is necessary for transforming growth factor-beta activation of p38MAPK and epithelial plasticity. J Biol Chem 276:46707-46713

Bloemendal H, de Jong W, Jaenicke R, Lubsen NH, Slingsby C, Tardieu A (2004) Ageing and vision: structure, stability and function of lens crystallins. Prog Biophys Mol Biol 86:407-485

Boscia F, Grattagliano I, Vendemiale G, Micelli-Ferrari T, Altomare E (2000) Protein oxidation and lens opacity in humans. Invest Ophthalmol Vis Sci 41:2461-2465

Boyce JF, Bhermi GS, Spalton DJ, El-Osta AR (2002) Mathematical modeling of the forces between an intraocular lens and the capsule. J Cataract Refract Surg 28:1853-1859

Brown N (1973) The change in shape and internal form of the lens of the eye on accommodation. Exp Eye Res 15:441-459

Brown N (1974) The change in lens curvature with age. Exp Eye Res 19:175-183

Brown RA, Prajapati R, McGrouther DA, Yannas IV, Eastwood M (1998) Tensional homeostasis in dermal fibroblasts: mechanical responses to mechanical loading in three-dimensional substrates. J Cell Physiol 175:323-332

Burd HJ, Judge SJ, Cross JA (2002) Numerical modeling of the accommodating lens. Vision Res 42:2235-2251

Burd HJ, Judge SJ, Flavell MJ (1999) Mechanics of accommodation of the human eye. Vision Res 39:1591-1595

Candido R, Forbes JM, Thomas MC, Thallas V, Dean RG, Burns WC, Tikellis C, Ritchie RH, Twigg SM, Cooper ME, Burrell LM (2003) A breaker of advanced glycation end products attenuates diabetes-induced myocardial structural changes. Circ Res 92:704-706

Centers for Disease Control and Prevention (CDC) (2004) Prevalence of visual impairment and selected eye diseases among persons aged >=50 years with and without diabetes--United States, 2002. Morb Mortal Wkly Rep 53:1069-1071

Chamberlain CG, McAvoy JW (1989) Induction of lens fibre differentiation by acidic and basic fibroblast growth factor (FGF). Growth Factors 1:125-134

Chow RL, Roux GD, Roghani M, Palmer MA, Rifkin DB, Moscatelli DA, Lang RA (1995) FGF suppresses apoptosis and induces differentiation of fibre cells in the mouse lens. Development 121:4383-4393

Coleman DJ (1986) On the hydraulic suspension theory of accommodation. Trans Am Ophthalmol Soc 84:846-868

Coleman DJ, Fish SK (2001) Presbyopia, accommodation, and the mature catenary. Ophthalmology 108:1544-1551

Conway RM, Schlötzer-Schrehardt U, Küchle M, Naumann GO (2004) Pseudoexfoliation syndrome: pathological manifestations of relevance to intraocular surgery. Clin Experiment Ophthalmol 32:199-210

Cook CA, Koretz JF, Pfahnl A, Hyun J, Kaufman PL (1994) Aging of the human crystalline lens and anterior segment. Vision Res 34:2945-2954

Coulombre JL, Coulombre AJ (1963) Lens development: fiber elongation and lens orientation. Science 142:1489-1490

Cowin SC (1998) On mechanosensation in bone under microgravity. Bone 22:119S-125S

David G, Humphrey JD (2004) Redistribution of stress due to a circular hole in a nonlinear anisotropic membrane. Journal of Biomechanics 37:1197-1203

David G, Humphrey JD (2007) Finite element model of stresses in the anterior lens capsule of the eye. Comput Methods Biomech Biomed Engin 10:237-243

David G, Pedrigi RM, Heistand MR, Humphrey JD (2007) Regional multiaxial mechanical properties of the porcine anterior lens capsule. J Biomech Eng 129:97-104

De Iongh RU, Wederell E, Lovicu FJ, McAvoy JW (2005) Transforming growth factor-beta-induced epithelial-mesenchymal transition in the lens: a model for cataract formation. Cells Tissues Organs 179:43-55

De Jong-Hesse Y, Kampmeier J, Lang GK, Lang GE (2005) Effect of extracellular matrix on proliferation and differentiation of porcine lens epithelial cells. Graefes Arch Clin Exp Ophthalmol 243:695-700

Delcourt C, Cristol JP, Tessier F, Leger CL, Michel F, Papoz L (2000) Risk factors for cortical, nuclear, and posterior subcapsular cataracts: the POLA study. Pathologies Oculaires Liees a l'Age. Am J Epidemiol 151:497-504

Dick HB, Dell S (2006) Single optic accommodative intraocular lenses. Ophthalmol Clin North Am 19:107-124

Drexler W, Baumgartner A, Findl O, Hitzenberger CK, Fercher AF (1997) Biometric investigation of changes in the anterior eye segment during accommodation. Vision Res 37:2789-2800

Drolsum L, Ringvold A, Nicolaissen B (2007) Cataract and glaucoma surgery in pseudoexfoliation syndrome: a review. Acta Ophthalmol Scand 85:810-821

Dubbelman M, Van der Heijde GL, Weeber HA (2001) The thickness of the aging human lens obtained from corrected Scheimpflug images. Optom Vis Sci 78:411-416

Dubbelman M, Van der Heijde GL, Weeber HA (2005) Change in shape of the aging human crystalline lens with accommodation. Vision Res 45:117-132

Dubbelman M, Van der Heijde GL, Weeber HA, Vrensen GF (2003) Changes in the internal structure of the human crystalline lens with age and accommodation. Vision Res 43:2363-2375

Emery J (1999) Capsular opacification after cataract surgery. Current Opinion in Opthalmology 10:73-80

Fagerholm PP, Philipson BT, Lindstrom B (1981) Normal human lens - the distribution of protein. Exp Eye Res 33:615-620

Farnsworth PN, Mauriello JA, Burke-Gadomski P, Kulyk T, Cinotti AA (1976) Surface ultrastructure of the human lens capsule and zonular attachments. Invest Ophthalmol 15:36-40

Farnsworth PN, Shyne SE (1979) Anterior zonular shifts with age. Exp Eye Res 28:291-297

Fisher RF (1969) Elastic constants of the human lens capsule. J Physiol 201:1-19

Fisher RF (1971) The elastic constants of the human lens. J Physiol 212:147-180

Fisher RF (1973) Presbyopia and the changes with age in the human crystalline lens. J Physiol 228:765-779

Fisher RF, Pettet BE (1972) The postnatal growth of the capsule of the human crystalline lens. J. Anat 112:207-214

Franke S, Dawczynski J, Strobel J, Niwa T, Stahl P, Stein G (2003) Increased levels of advanced glycation end products in human cataractous lenses. J Cataract Refract Surg 29:998-1004

Fung YC (1990) Biomechanics: mechanical properties of living tissue. Springer, Berlin Heidelberg New York

Gander W, Golub GH, Strebel R (1994) Least squares fitting of circles and ellipses. BIT 34:556-577

Georgopoulos GT, Papaconstantinou D, Georgalas I, Koutsandrea CN, Margetis I, Moschos MM (2007) Management of large traumatic zonular dialysis with phacoemulsification and IOL implantation using the capsular tension ring. Acta Ophthalmol Scand 85:653-657

Giblin FJ (2000) Glutathione: a vital lens antioxidant. J Ocul Pharmacol Ther. 16:121-135

Gimbel HV, Neuhann T (1990) Development, advantages, and methods of the continuous circular capsulorhexis technique. J Cataract Refract Surg 16:31-37

Glasser A, Campbell MC (1998) Presbyopia and the optical changes in the human crystalline lens with age. Vision Res 38:209-229

Glasser A, Campbell MC (1999) Biometric, optical and physical changes in the isolated human crystalline lens with age in relation to presbyopia. Vision Res 39:1991-2015

Goffin JM, Pittet P, Csucs G, Lussi JW, Meister JJ, Hinz B (2006) Focal adhesion size controls tension-dependent recruitment of alpha-smooth muscle actin to stress fibers. J Cell Biol 172:259-268

Guthoff R, Abramo F, Draeger J, Chumbley LC, Lang GK, Neumann W (1990) Forces on intraocular lens haptics induced by capsular fibrosis. An experimental study. Graefes Arch Clin Exp Ophthalmol 228:363-368

Haefliger E, Parel JM, Fantes F, Norton EW, Anderson DR, Forster RK, Hernandez E, Feuer WJ (1987) Accommodation of an endocapsular silicone lens (Phaco-Ersatz) in the nonhuman primate. Ophthalmology 94:471-477

Haloui Z, Jeanny JC, Jonet L, Courtois Y, Laurent M (1988) Immunochemical analysis of extracellular matrix during embryonic lens development of the Cat Fraser mouse. Exp Eye Res 46:463-474

Hammond C (2001) The epidemiology of cataract. Optometry Today 8:24-29

Hara T, Azuma N, Chiba K, Ueda Y, Hara T (1992) Anterior capsular opacification after endocapsular cataract surgery. Ophthalmic Surg 23:94-98

Harris AK, D Stopak, P Wild (1981) Fibroblast traction as a mechanism for collagen morphogenesis. Nature 290:249-251

Hayashi H, Hayashi K, Nakao F, Hayashi F (2002) Elapsed time for capsular apposition to intraocular lens after cataract surgery. Ophthalmology 109:1427-1431

Heatley CJ, Spalton DJ, Boyce JF, Marshall J (2004) A mathematical model of factors that influence the performance of accommodative intraocular lenses. Ophthalmic Physiol Opt 24:111-118

Heistand MR, Pedrigi RM, Delange SL, Dziezyc J, Humphrey JD (2005) Multiaxial mechanical behavior of the porcine anterior lens capsule. Biomech Model Mechanobiol 4:168-177

Heistand MR, Pedrigi RM, Dziezyc J, Humphrey JD (2006) Redistribution of strain and curvature in the porcine anterior lens capsule following a continuous circular capsulorhexis. J Biomech 39:1537-1542

Hermans EA, Dubbelman M, Van der Heijde GL, Heethaar RM (2006) Estimating the external force acting on the human eye lens during accommodation by finite element modelling. Vision Res 46:3642-50

Hermans EA, Dubbelman M, Van der Heijde GL, Heethaar RM (2008) Change in the accommodative force on the lens of the human eye with age. Vision Res 48:119-1126

Heys KR, Cram SL, Truscott RJ (2004) Massive increase in the stiffness of the human lens nucleus with age: the basis for presbyopia? Mol Vis 10:956-963

Hollick EJ, Spalton DJ, Meacock WR (1999) The effect of capsulorhexis size on posterior capsular opacification: one-year results of a randomized prospective trial. Am J Ophthalmology 128:271-284

Huang H, Kamm RD, Lee RT (2004) Cell mechanics and mechanotransduction: pathways, probes, and physiology. Am J Physiol Cell Physiol 287:C1-C11

Humphrey JD (1998) Review: Computer methods in membrane biomechanics. Comput Methods Biomech Biomed Engin 1:171-210

Humphrey JD (2002) Cardiovascular solid mechanics: cells, tissues, and organs. Springer, Berlin Heidelberg New York

Humphrey JD, Rajagopal KR (2003) A constrained mixture model for arterial adaptations to a sustained step change in blood flow. Biomech Model Mechanobiol 2:109-126

Jacob S, Agarwal A, Agarwal S, Patel N, Lal V (2003) Efficacy of a capsular tension ring for phacoemulsification in eyes with zonular dialysis. J Cataract Refract Surg 29:315-321

Jones CE, Atchison DA, Meder R, Pope JM (2005) Refractive index distribution and optical properties of the isolated human lens measured using magnetic resonance imaging (MRI). Vision Res 45:2352-2366

Judge SJ, Burd HJ (2002) Modelling the mechanics of accommodation and presbyopia. Ophthalmic Physiol Opt 22:397-400

Kaufman P, Alm A (2003) Adler's physiology of the eye: clinical application. Mosby Company, Saint-Louis

Klein BE, Klein R, Moss SE (1985) Prevalence of cataracts in a population-based study of persons with diabetes mellitus. Ophthalmology 92:1191-1196

Koch DD, Kohnen T (1997) A retrospective comparison of techniques to prevent secondary cataract formation following posterior chamber intraocular lens implantation in infants and children. Trans Am Ophthalmol Soc 95:351-360

Koopmans SA, Terwee T, Barkhof J, Haitjema HJ, Kooijman AC (2003) Polymer refilling of presbyopic human lenses in vitro restores the ability to undergo accommodative changes. Invest Ophthalmol Vis Sci 44:250-257

Koopmans SA, Terwee T, Glasser A, Wendt M, Vilupuru AS, van Kooten TG, Norrby S, Haitjema HJ, Kooijman AC (2006) Accommodative lens refilling in rhesus monkeys. Invest Ophthalmol Vis Sci 47:2976-2984

Koretz JF, Handelman GH (1982) Model of the accommodative mechanism in the human eye. Vision Res 22:917-927

Koretz JF, Kaufman PL, Neider MW, Goeckner PA (1989) Accommodation and presbyopia in the human eye--aging of the anterior segment. Vision Res 29:1685-1692

Koretz JE, Strenk SA, Strenk LM, Semmlow JL (2004) Scheimpflug and high-resolution magnetic resonance imaging of the anterior segment: a comparative study. J Opt Soc Am A Opt Image Sci Vis 21:346-354

Krag S, Andreassen TT (1996) Biomechanical measurements of the porcine lens capsule. Exp Eye Res 62:253-260

Krag S, Andreassen TT (1998) Effect of freezing on lens capsule mechanical behavior. Ophthalmic Res 30:280-285

Krag S, Andreassen TT (2003a) Mechanical properties of the human lens capsule. Prog Retin Eye Res 22:749-767

Krag S, Andreassen TT (2003b) Mechanical properties of the human posterior lens capsule. Invest Ophthalmol Vis Sci 44:691-696

Krag S, Danielsen CC, Andreassen TT (1997a) Thermal and mechanical stability of the lens capsule. Curr Eye Res 17:470-477

Krag S, Olsen T, Andreassen TT (1997b) Biomechanical characteristics of the human anterior lens capsule in relation to age. Invest Ophthalmol Vis Sci 38:357-363

Kurosaka D, Kato K, Nagamoto T, Negishi K (1995) Growth factors influence contractility and alpha-smooth muscle actin expression in bovine lens epithelial cells. Invest Ophthalmol Vis Sci 36:1701-1708

Kurz S, Krummenauer F, Hacker P, Pfeiffer N, Dick HB (2005) Capsular bag shrinkage after implantation of a capsular bending or capsular tension ring. J Cataract Refract Surg 31:1915-1920

Layton BE, Sastry AM (2004) A mechanical model for collagen fibril load sharing in peripheral nerve of diabetic and nondiabetic rats. J Biomech Eng 126:803-814

Leaming DV (2004) Practice styles and preferences of ASCRS members--2003 survey. J Cataract Refract Surg 30:892-900

Lee YI, Kwon YJ, Joo CK (2004) Integrin-linked kinase function is required for transforming growth factor beta-mediated epithelial to mesenchymal transition. Biochem Biophys Res Commun 316:997-1001

Linnola RJ (1997) Sandwich theory: bioactivity-based explanation for posterior capsule opacification. J Cat Refract Surg 23:1539-1542

Lou MF (2003) Redox regulation in the lens. Prog Retin Eye Res 22:657-682

Lovicu FJ, McAvoy JW (2005) Growth factor regulation of lens development. Dev Biol 280:1-14

Manns F, Fernandez V, Zipper S, Sandadi S, Hamaoui M, Ho A, Parel JM (2004) Radius of curvature and asphericity of the anterior and posterior surface of human cadaver crystalline lenses. Exp Eye Res 78:39-51

Marcantonio JM, Rakic JM, Vrensen GF, Duncan G (2000) Lens cell populations studied in human donor capsular bags with implanted intraocular lenses. Invest Ophthalmol Vis Sci 41:1130-1141

Marcantonio J, Vrensen GFJM (1999) Cell biology of posterior capsulater opacification. Eye 13:484-488

Martin H, Guthoff R, Terwee T, Schmitz KP (2005) Comparison of the accommodation theories of Coleman and of Helmholtz by finite element simulations. Vision Res 45:2910-2915

McAvoy JW, Chamberlain CG, de Iongh RU, Hales AM, Lovicu FJ (1999) Lens development. Eye 13:425-437

McGinty SJ, Truscott RJ (2006) Presbyopia: the first stage of nuclear cataract? Ophthalmic Res 38:137-148

Menapace R, Findl O, Kriechbaum K, Leydolt-Koeppl C (2006) Accommodating intraocular lenses: a critical review of present and future concepts. Graefes Arch Clin Exp Ophthalmol 245:473-489

Millward-Sadler SJ, Salter DM (2004) Integrin-dependent signal cascades in chondrocyte mechanotransduction. Ann Biomed Eng 32:435-446

Moffat BA, Atchison DA, Pope JM (2002) Age-related changes in refractive index distribution and power of the human lens as measured by magnetic resonance micro-imaging in vitro. Vision Res 42:1683-1693

Mosmann T (1983) Rapid colorimetric assay for cellular growth and survival: application to proliferation and cytotoxicity assays. J Immunol Methods 65:55-63

Nagamoto T, Eguchi G, Beebe DC (2000) Alpha-smooth muscle actin expression in cultured lens epithelial cells. Invest Ophthalmol Vis Sci 41:1122-1129

Nagaraj RH, Shamsi FA, Huber B, Pischetsrieder M (1999) Immunochemical detection of oxalate monoalkylamide, an ascorbate-derived Maillard reaction product in the human lens. FEBS Lett 453:327-330

Nagata T, Minakata A, Watanabe I (1998) Adhesiveness of acrysof to a collagen film. J Cat Refract Surg 24:367-370

Namiki M, Tagami Y, Morino I, Kano M, Sugiura T (1993) Findings from slit lamp and histological examination of the anterior capsule in patients with severe anterior capsular shrinkage and opacities after implantation of intraocular lenses [in Japenese] [English abstract]. Nippon Ganka Gakkai Zasshi 97:716-720

Nishi O, Nakai Y, Mizumoto Y, Yamada Y (1997) Capsule opacification after refilling the capsule with an inflatable endocapsular balloon. J Cat Refract Surg 23:1548-1555

Nishi O, Nishi K (1998) Accommodation amplitude after lens refilling with injectable silicone by sealing the capsule with a plug in primates. Arch Ophthalmol 116:1358-1361

Nishi O, Nishi K, Akura J (2002) Speed of capsular bend formation at the optic edge of acrylic, silicone, and poly(methyl methacrylate) lenses. J Cataract Refract Surg 28:431-437

Nishi O, Nishi K, Menapace R, Akura J (2001) Capsular bending ring to prevent posterior capsule opacification: 2 year follow-up. J Cat Refract Surg 27:1359-1365

Nishi O, Nishi K, Wickstrom K (2000) Preventing lens epithelial cell migration using intraocular lenses with sharp rectangular edges. J Cat Refract Surg 26:1543-1549

Norrby S, Koopmans S, Terwee T (2006) Artificial crystalline lens. Ophthalmol Clin North Am 19:143-146

Oharazawa H, Ibaraki N, Lin LR, Reddy VN (1999) The effects of extracellular matrix on cell attachment, proliferation and migration in a human lens epithelial cell line. Exp Eye Res 69:603-610

Ohata H, Tanaka K, Maeyama N, Yamamoto M, Momose K (2001) Visualization of elementary mechanosensitive Ca^{2+} spots, in bovine lens epithelial cells. J Physiol 532: 31-42

O'Neill WD, Doyle JM (1968) A thin shell deformation analysis of the human lens. Vision Res 8:193-206

Oner FH, Gunenc U, Ferliel ST (2000) Posterior capsule opacification after phacoemulsification: foldable acrylic versus poly(methyl methacrylate) intraocular lenses. J Cataract Refract Surg 26:722-726

Pandey SK, Apple DJ, Werner L, Maloof AJ, Milverton EJ (2004) Posterior capsule opacification: a review of the aetiopathogenesis, experimental and clinical studies and factors for prevention. Indian J Ophthalmol 52:99-112

Parmigiani C, McAvoy J (1984) Localisation of laminin and fibronectin during rat lens morphogenesis. Differentiation 28:53-61

Parmigiani CM, McAvoy JW (1989) A morphometric analysis of the development of the rat lens capsule. Curr Eye Res 8:1271-1277

Parmigiani CM, McAvoy JW (1991) The roles of laminin and fibronectin in the development of the lens capsule. Curr Eye Res 10:501-511

Parsons C, Jones DS, Gorman SP (2005) The intraocular lens: challenges in the prevention and therapy of infectious endophthalmitis and posterior capsular opacification. Expert Rev Med Devices 2:161-173

Pau H, Kranz J (1991) The increasing sclerosis of the human lens with age and its relevance to accommodation and presbyopia. Graefes Arch Clin Exp Ophthalmol 229:294-296

Pedrigi RM, David G, Dziezyc J, Humphrey JD (2007a) Regional mechanical properties and stress analysis of the human anterior lens capsule. Vision Res 47:1781-1789

Pedrigi RM, Staff E, David G, Glenn S, Humphrey JD (2007b) Altered multiaxial mechanical properties of the porcine anterior lens capsule cultured in high glucose. J Biomech Eng 129:121-125

Pokupec R, Kalauz M, Turk N, Turk Z (2003) Advanced glycation endproducts in human diabetic and non-diabetic cataractous lenses. Graefes Arch Clin Exp Ophthalmol 241:378-384

Raina UK, Mehta DK, Monga S, Arora R (2004) Functional outcomes of acrylic intraocular lenses in pediatric cataract surgery. J Cataract Refract Surg 30:1082-1091

Rizvi AA (2004) Type 2 diabetes: epidemiologic trends, evolving pathogenetic concepts, and recent changes in therapeutic approach. South Med J 97:1079-1087

Robinson ML, Overbeek PA, Verran DJ, Grizzle WE, Stockard CR, Friesel R, Maciag T, Thompson JA (1995) Extracellular FGF-1 acts as a lens differentiation factor in transgenic mice. Development 121:505-514

Ryan JM, Humphrey JD (1999) Finite element based predictions of preferred material symmetries in saccular aneurysms. Ann Biomed Eng 27:641-647

Saika S, Kawashima Y, Miyamoto T, Okada Y, Tanaka SI, Ohmi S, Minamide A, Yamanaka O, Ohnishi Y, Ooshima A, Yamanaka A (1998) Immunolocalization of prolyl 4-hydroxylase subunits, alpha-smooth muscle actin, and extracellular matrix components in human lens capsules with lens implants. Exp Eye Res 66:283-294

Saika S, Miyamoto T, Ishida I, Obnishi Y, Ooshima A (2003a) Osteopontin: a component of matrix in capsular opacification and subcapsular cataract. IOVS 44:1622-1628

Saika S, Miyamoto T, Tanaka T, Ishida I, Ohnishi Y, Ooshima A (2001) Latent TGFbeta binding protein-1 and fibrillin-1 in human capsular opacification and in cultured lens epithelial cells. Br J Ophthalmol 85:1362-1366

Saika S, Miyamoto T, Tanaka S, Tanaka T, Ishida I, Ohnishi Y, Ooshima A, Ishiwata T, Asano G, Chikama T, Shiraishi A, Liu CY, Kao CW, Kao WW (2003b) Response of lens epithelial cells to injury: role of lumican in epithelial-mesenchymal transition. Invest Ophthalmol Vis Sci 44:2094-2102

Sakka Y, Hara T, Yamada Y, Hara T, Hayashi F (1996) Accommodation in primate eyes after implantation of refilled endocapsular balloon. Am J Ophthalmol 121:210-212

Sato T, Roy S (2002) Effect of high glucose on fibronectin expression and cell proliferation in trabecular meshwork cells. Invest Ophthalmol Vis Sci 43:170-175

Saxby L, Rosen E, Boulton M (1998) Lens epithelial cell proliferation, migration, and metaplasia following capsulorhexis. Br J Ophthalmol 82:945-952

Schachar RA (2004a) Central surface curvatures of postmortem- extracted intact human crystalline lenses: implications for understanding the mechanism of accommodation. Ophthalmology 111:1699-1704

Schachar RA (2004b) Qualitative effect of zonular tension on freshly extracted intact human crystalline lenses: implications for the mechanism of accommodation. Invest Ophthalmol Vis Sci 45:2691-2695

Schachar RA, Bax AJ (2001) Mechanism of human accommodation as analyzed by nonlinear finite element analysis. Compr Ther 27:122-132

Schachar RA, Tello C, Cudmore DP, Liebmann JM, Black TD, Ritch R (1996) In vivo increase of the human lens equatorial diameter during accommodation. Am J Physiol 271:R670-R676

Seland JH (1992) The lens capsule and zonulae. Acta Ophthalmol Suppl 205:7-12

Seshaiyer P, Humphrey JD (2003) A sub-domain inverse finite element characterization of hyperelastic membranes including soft tissues. J Biomech Eng 125:363-371

Shigemitsu T, Ishiguro K, Shimizu Y, Horiguchi M, Kasahara M, Arakaki S (1999) Immunocytochemical features of lens after cataract tissue--signalling molecules (growth factors, cytokines, other signalling molecules), cytoskeleton proteins, cellular and extracellular matrix proteins. Int Ophthalmol 23:137-144

Smith GN Jr, Linsenmayer TF, Newsome DA (1976) Synthesis of type II collagen in vitro by embryonic chick neural retina tissue. Proc Natl Acad Sci USA 73:4420-4423

Spalton DJ (1999) Posterior capsular opacification after cataract surgery. Eye 13:489-492

Spector A (1995) Oxidative stress-induced cataract: mechanism of action. FASEB J 9:1173-1182

Sponer U, Pieh S, Soleiman A, Skorpik C (2005) Up-regulation of alphavbeta6 integrin, a potent TGF-beta1 activator, and posterior capsule opacification. J Cataract Refract Surg 31:595-606

Stitt AW (2001) Advanced glycation: an important pathological event in diabetic and age related ocular disease. Br J Ophthalmol 85:746-753

Streeten BW (1977) The zonular insertion: a scanning electron microscopic study. Invest Ophthalmol Vis Sci 16:364-375

Strenk SA, Semmlow JL, Strenk LM, Munoz P, Gronlund-Jacob J, DeMarco JK (1999) Age-related changes in human ciliary muscle and lens: a magnetic resonance imaging study. Invest Ophthalmol Vis Sci 40:1162-1169

Strenk SA, Strenk LM, Koretz JF (2005) The mechanism of presbyopia. Prog Retin Eye Res 24:379-393

Strenk SA, Strenk LM, Semmlow JL, DeMarco JK (2004) Magnetic resonance imaging study of the effects of age and accommodation on the human lens cross-sectional area. Invest Ophthalmol Vis Sci 45:539-545

Sweeney MH, Truscott RJ (1998) An impediment to glutathione diffusion in older normal human lenses: a possible precondition for nuclear cataract. Exp Eye Res 67:587-595

Tan JL, Tien J, Pirone DM, Gray DS, Bhadriraju K, Chen CS (2003) Cells lying on a bed of microneedles: an approach to isolate mechanical force. Proc Natl Acad Sci USA 100:1484-1489

Tehrani M, Dick HB, Krummenauer F, Pfirrmann G, Boyle T, Stoffelns BM (2003) Capsule measuring ring to predict capsular bag diameter and follow its course after foldable intraocular lens implantation. J Cataract Refract Surg 29:2127-2134

Truscott RJ (2000) Age-related nuclear cataract: a lens transport problem. Ophthalmic Res 32:185-94

Truscott RJ (2005) Age-related nuclear cataract-oxidation is the key. Exp Eye Res 80:709-725

Turner DA, Anderson IJ, Mason JC (1999) An algorithm for fitting an ellipsoid to data. University of Huddersfield Thesis, Huddersfield, UK

Weale RA (2000) Myopia and its mechanisms. Lancet 356:2194

Werner L, Pandey SK, Escobar-Gomez M, Visessook N, Peng Q, Apple DJ (2000) Anterior capsule opacification: a histopathological study comparing different IOL styles. Ophthalmology 107:463-471

Wormstone IM (2002) Posterior capsule opacification: a cell biological perspective. Exp Eye Res 74:337-347

Wyatt HJ (1988) Some aspects of the mechanics of accommodation. Vision Res 28:75-86

Zarina S, Zhao HR, Abraham EC (2000) Advanced glycation end products in human senile and diabetic cataractous lenses. Mol Cell Biochem 210:29-34

Zuk A, Hay ED (1994) Expression of beta 1 integrins changes during transformation of avian lens epithelium to mesenchyme in collagen gels. Dev Dyn 201:378-393

VITA

Name:	Ryan Michael Pedrigi
Address:	Texas A&M University, Biomedical Engineering, 337 Zachry Engineering Center, College Station, TX 77840-3120
Email Address:	rpedrigi@tamu.edu
Education:	B.S., Mechanical Engineering, Kansas State University, 2003 Ph.D., Biomedical Engineering, Texas A&M University, 2008